



Eruptive stars spectroscopy

Cataclysmics, Symbiotics, Nova Supernovae



ARAS Eruptive Stars

Information Letter n° 26 #2016-05 15-07-2016

Observations of May-June 2016

News

Two novae in May :
LMC 2016 and Sco 2016

StHa 169 outburst in
May

Contents

Novae

Spectra of nova LMC 2016 and nova Sco 2016 obtained by
Terry Bohlsen

Supernovae

SN 2016 COJ in NGC 4125 by Etienne Bertrand

Symbiotics

AG Dra : "hot" outburst
CH Cyg : ongoing campaign
T CrB : "superactive state"
StHa 169 : outburst in May by David Boyd
Last minute : collimated outflow in BF Cygni

Notes

Analysis Techniques

Steve Shore

A note on stellar winds in symbiotic binaries

Augustin Skopal

Authors : F. Teyssier, S. Shore, A. Skopal, P. Somogyi, D. Boyd, P. Berardi,
T. Lester, U Sollecchia, T. Bohlsen, J. Montier, F. Campos, K. Graham, O.
Garde, P. Cazzato, E. Bertrand, L. Franco

"We acknowledge with thanks the variable star observations from the AAVSO International Database contributed by observers worldwide and used in this letter."

Kafka, S., 2015, Observations from the AAVSO International Database, <http://www.aavso.org>

Nova LMC 2016 = MASTER OT J051032.58-692130.4

NOVAE

Coordinates (2000.0)

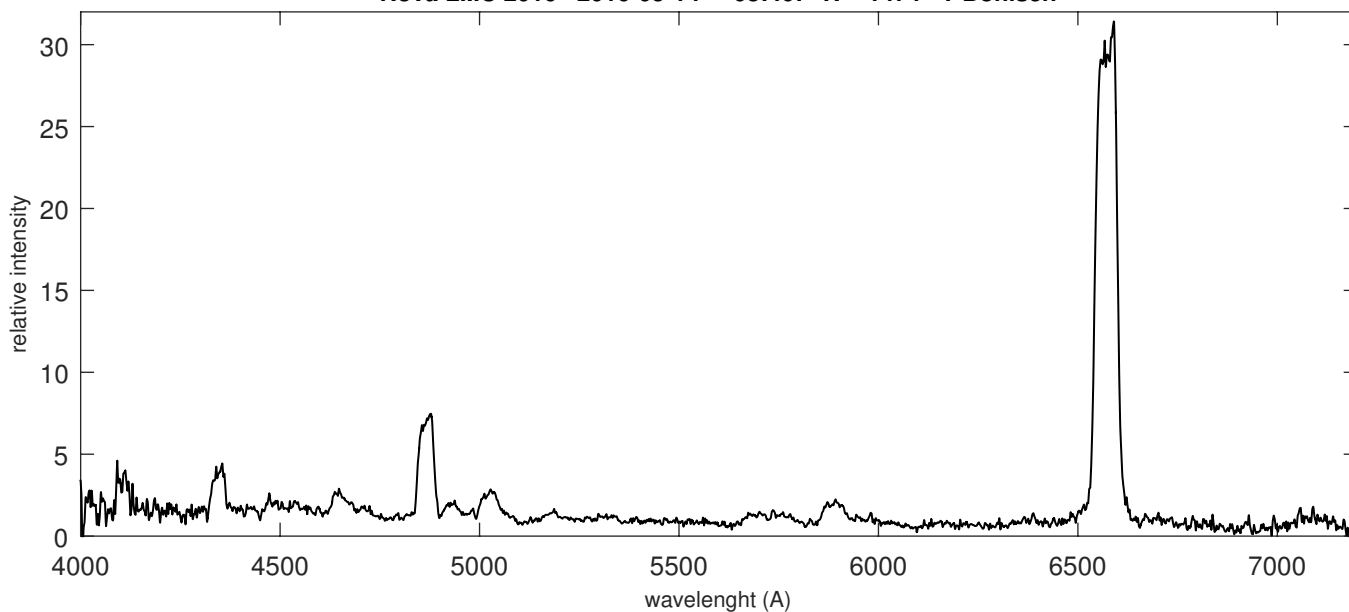
R.A.	05 10 32.6
Dec	-69 21 30.4
Mag	~ 12 at max

MASTER OT J051032.58-692130.4 discovery - 12m OT in LMC

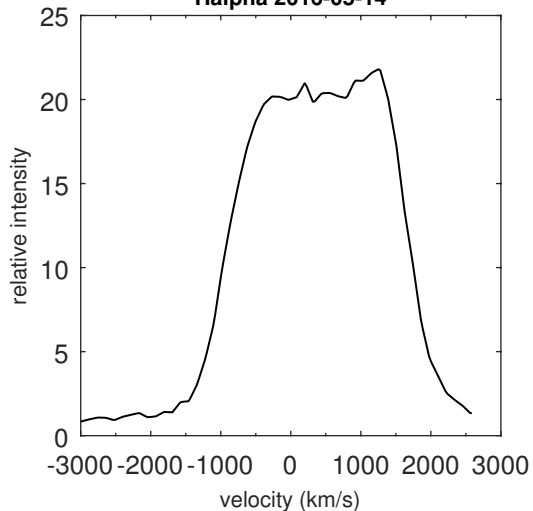
MASTER-SAAO auto-detection system (Lipunov et al., "MASTER Global Robotic Net", Advances in Astronomy, 2010, 349171) discovered OT source at (RA, Dec) = 05h 10m 32.58s -69d 21m 30.4s on 2016-05-10.72797 UT.
The OT unfiltered magnitude is 12.0m

(Astronomer's Telegram # 9039, 11 May 2016)

Nova LMC 2016 2016-05-14 08:40: R = 1474 T Bohlsen



Halpha 2016-05-14



Nova Sco 2016 = PNV J17381927-3725077

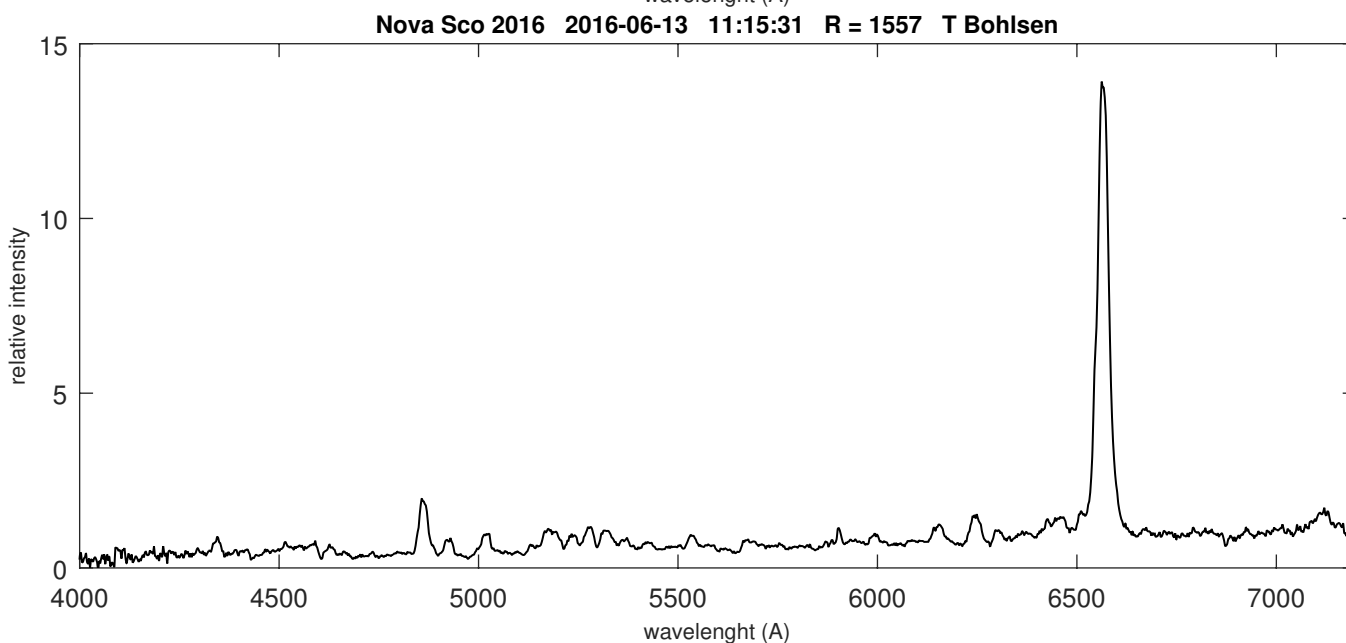
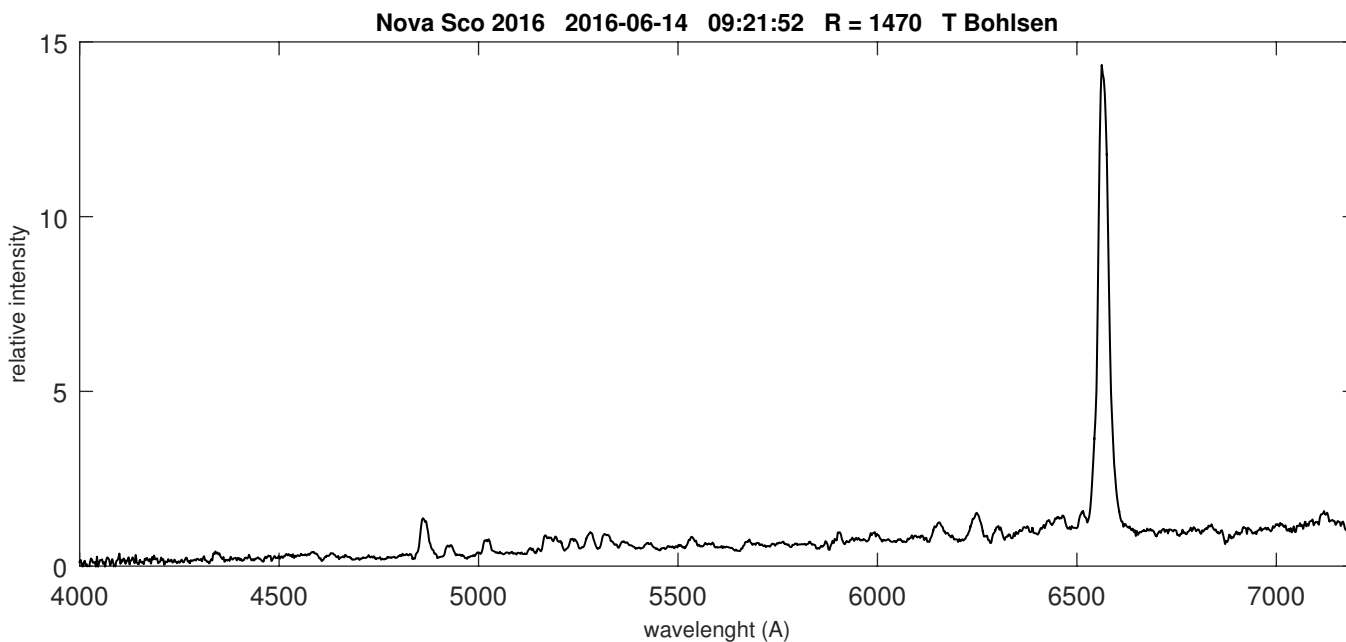
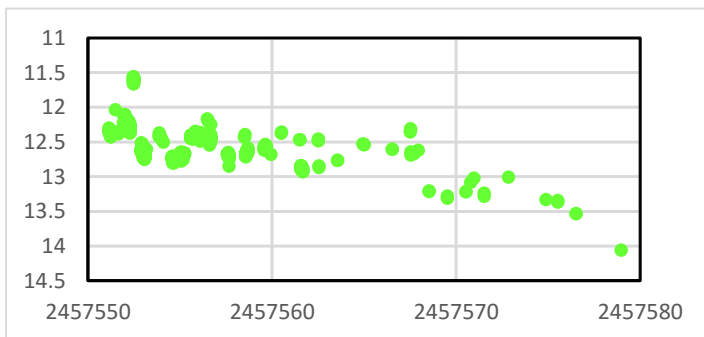
NOVAE

Coordinates (2000.0)	
R.A.	17 38 19.31
Dec	-37 25 08.7
Mag	

Discovered by: Hideo Nishimura (Kakegawa, Shizuoka-ken, Japan) at mag 12.4 (unfiltered CCD) the 2016 June 10.629 UT

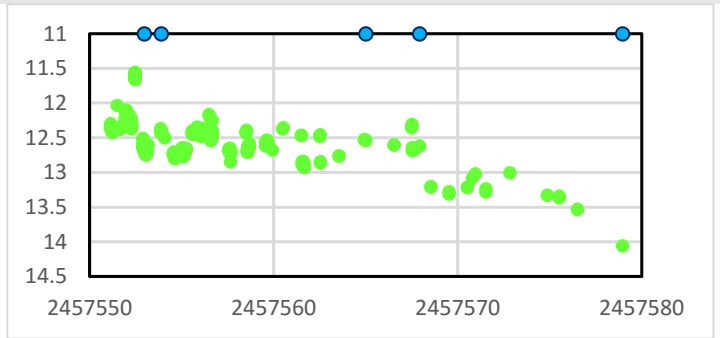
Spectroscopy obtained by K. Ayani (Bisei Astronomical Observatory, BAO) on 2016 Jun. 11.65 UT with the BAO 1.01-m telescope shows the star to be a nova in early stages.

Terry Bolhsen obtained a first spectrum of the nova with a LISA, 3 days after the discovery with a LISA

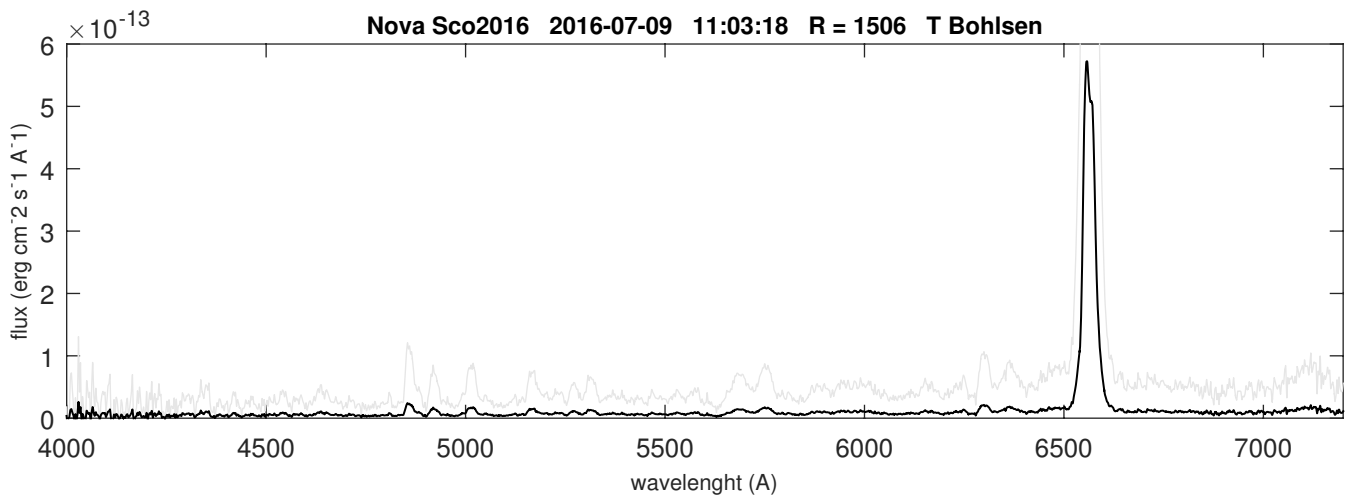
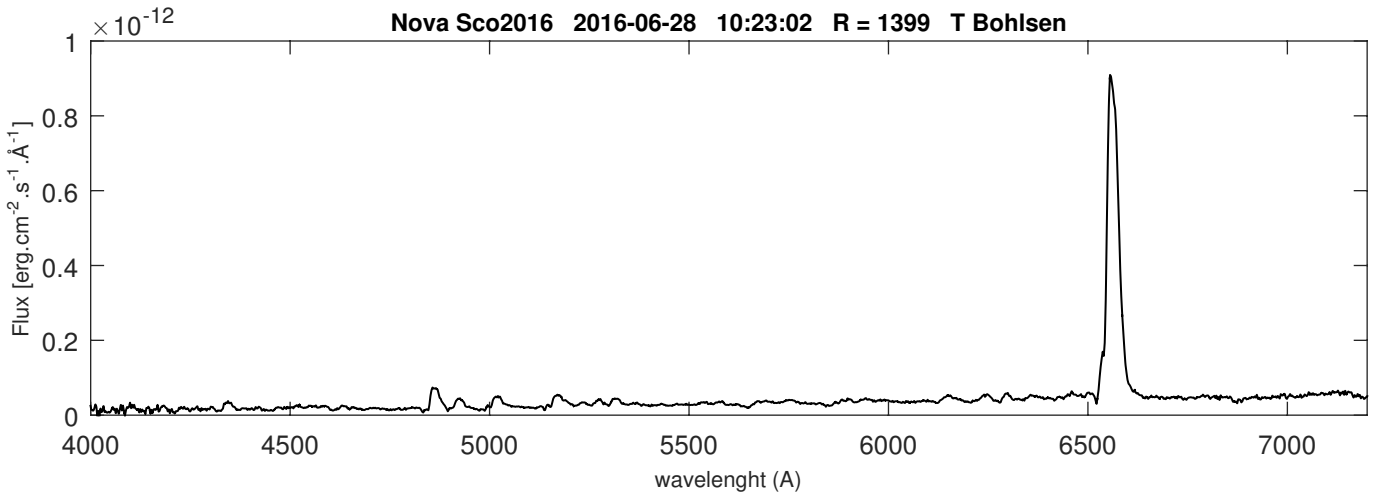
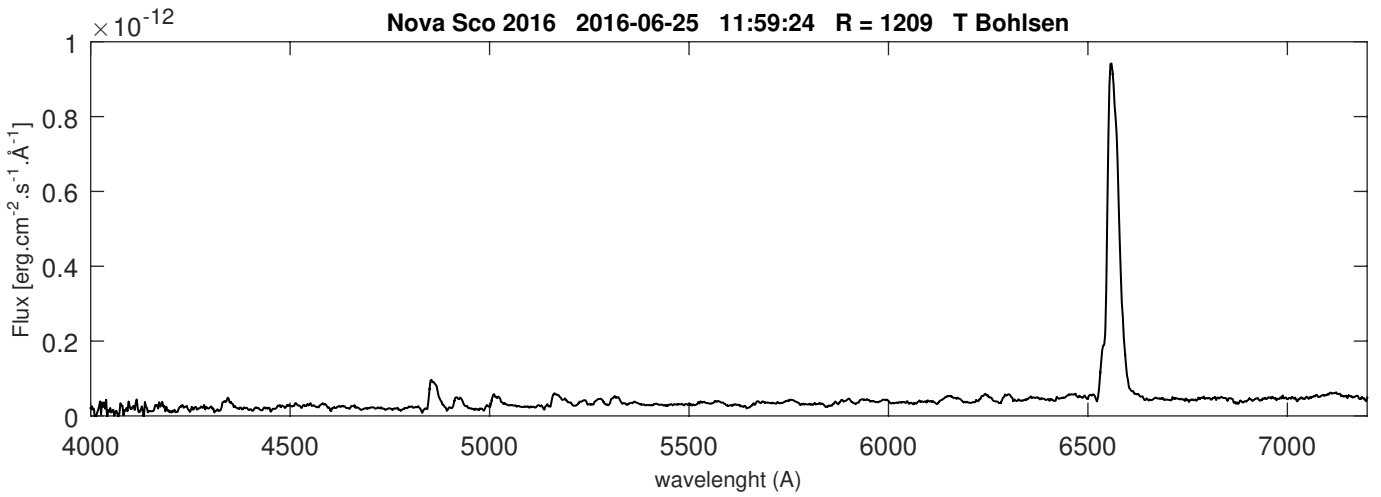


Nova Sco 2016 = PNV J17381927-3725077

NOVAE



AAVSO light curve (V) and Terry's spectra



SN 2016 COJ

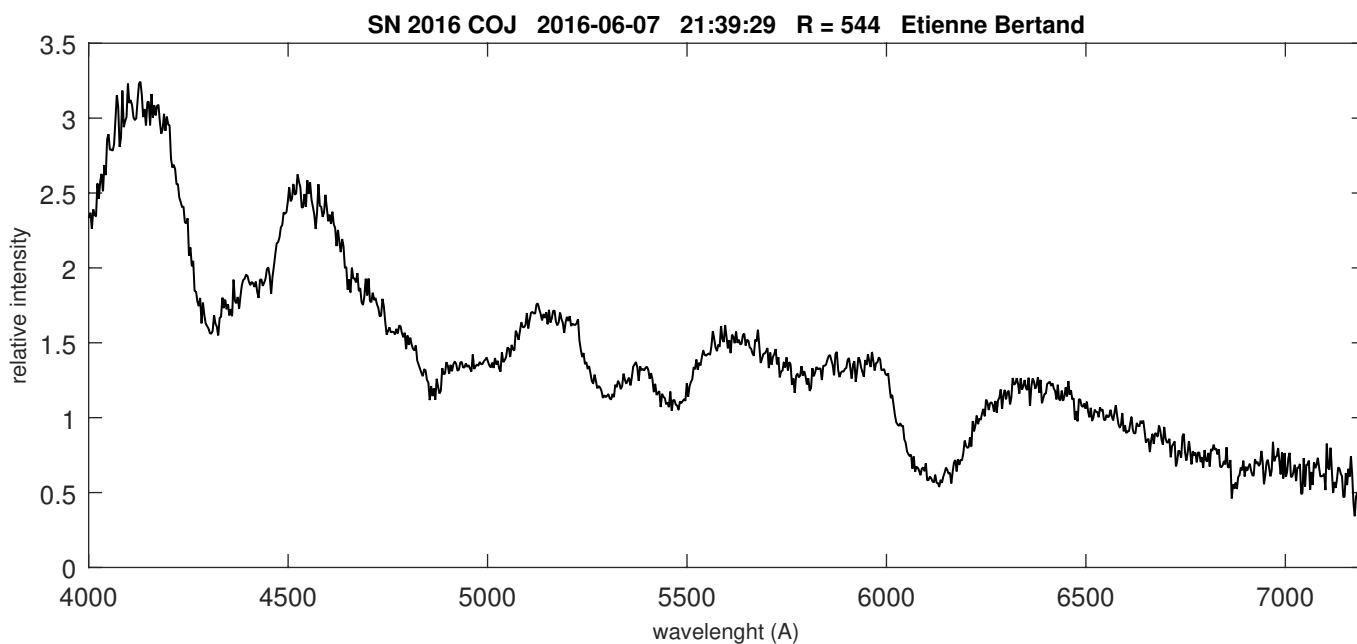
Coordinates (2000.0)

R.A.	05 10 32.6
Dec	-69 21 30.4
Mag	

A bright supernova discovered in NGC4125

The spectrum shows that SN2016coj is a Type Ia supernova. Cross-correlation with a library of supernova spectra using the "Supernova Identification" code (SNID; Blondin and Tonry 2007, Ap.J. 666, 1024) indicates a best match with normal Type Ia SN2002er at age -6 days, as well as a few other template around one week time before maximum light. Adopting the host redshift $z=0.00448$, the rest-frame photospheric velocity estimated from the minimum of the Si II 635.5-nm feature, is about 15400 ± 100 km/s. (ATel 9095) <http://www.astronomerstelegam.org/?read=9095>

Etienne Bertrand got several spectra of this bright SN



Etienne Bertrand describes his observations in :

<http://www.lescepheides.com/archives/2016/06/09/33938558.html>

CH Cygni : ongoing campaign upon the request of Augustin Skopal

AG Dra : returns to quiescence

T CrB : superactive phase

Observing : main targets

Ungoing campaign : **CH Cygni** for A Skopal (low resolution and H alpha profile at $R > 10000$)
Almost one spectrum a month. See also call for observations by Margarita

T CrB : high cadency coverage should be welcome until the next nova outburst (could take a few years)

AG Dra : returning to quiescence after Apr.-May Outburst

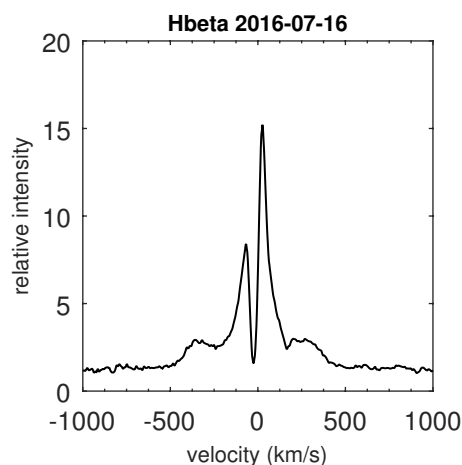
AG Peg in the morning sky after its historic symbiotic outburst in 2015

And also : **V443 Her, YY Her, CI Cyg, BF Cyg, V1016 Cyg, Z And, StHa 190**

BF Cyg : signature of highly collimated jets

"I have looked also to our spectra, and found that these bipolar outflow developed already in June". So, if possible, continue observation of BF Cyg.

A. Skopal



F. Teyssier
 $R = 11000$

See :
About the discovery of jets in BF Cyg, see Augustin Skopal's publication :
<http://adsabs.harvard.edu/abs/2013A%26A...551L..10S>

Symbiotics in ARAS Data Base Update : 10-07-2016

S S C - - O - - B - - Y S

#	Name	AD (2000)	DE (2000)	Nb. Of spectra	First spectrum	Last spectrum	Days Since Last Spectrum
1	EG And	0 44 37.1	40 40 45.7	44	12/08/2010	24/02/2016	138
2	AX Per	1 36 22.7	54 15 2.5	98	04/10/2011	31/03/2016	102
3	V471 Per	1 58 49.7	52 53 48.4	3	06/08/2013	04/02/2016	158
4	o Ceti	2 19 20.7	-2 58 39.5	6	28/11/2015	20/02/2016	142
5	BD Cam	3 42 9.3	63 13 0.5	15	08/11/2011	06/03/2016	127
6	UV Aur	5 21 48.8	32 30 43.1	38	24/02/2011	07/03/2016	126
7	V1261 Ori	5 22 18.6	-8 39 58	5	16/01/2016	20/02/2016	142
8	StHA 55	5 46 42	6 43 48	2	17/01/2016	25/01/2016	168
9	ZZ CMi	7 24 13.9	8 53 51.7	32	29/09/2011	05/04/2016	97
10	BX Mon	7 25 24	-3 36 0	36	04/04/2011	12/03/2016	121
11	V694 Mon	7 25 51.2	-7 44 8	166	03/03/2011	21/04/2016	81
12	NQ Gem	7 31 54.5	24 30 12.5	41	01/04/2013	17/04/2016	85
13	GH Gem	7 4 4.9	12 2 12	3	10/03/2016	29/03/2016	104
14	CQ Dra	12 30 06	69 12 04	7	11/06/2015	02/07/2016	9
15	TX CVn	12 44 42	36 45 50.6	31	10/04/2011	02/07/2016	9
16	IV Vir	14 16 34.3	-21 45 50	3	28/02/2015	20/06/2016	21
17	T CrB	15 59 30.1	25 55 12.6	121	01/04/2012	06/07/2016	5
18	AG Dra	16 1 40.5	66 48 9.5	148	03/04/2013	05/07/2016	6
19	V503 Her	17 36 46	23 18 18	1	05/06/2013	05/06/2013	1132
20	RS Oph	17 50 13.2	-6 42 28.4	16	23/03/2011	16/09/2015	299
21	V934 Her	17 6 34.5	23 58 18.5	15	09/08/2013	09/06/2016	32
22	AS 270	18 05 33.7	-20 20 38	2	01/08/2013	02/08/2013	1074
23	AS 289	18 12 22	-11 40 13				
24	YY Her	18 14 34.3	20 59 20	18	25/05/2011	05/05/2016	67
25	FG Ser	18 15 6.2	0 18 57.6	3	26/06/2012	24/07/2014	718
26	StHa 149	18 18 55.9	27 26 12	3	05/08/2013	14/10/2015	271
27	V443 Her	18 22 8.4	23 27 20	26	18/05/2011	09/06/2016	32
28	FN Sgr	18 53 52.9	-18 59 42	4	10/08/2013	02/07/2014	740
29	V335 Vul	19 23 14.2	24 27 40.2				
30	BF Cyg	19 23 53.4	29 40 25.1	72	01/05/2011	11/05/2016	61
31	CH Cyg	19 24 33	50 14 29.1	349	21/04/2011	09/07/2016	2
32	V919 Sgr	19 3 46	-16 59 53.9	2	10/08/2013	10/08/2013	1066
33	V1413 Aql	19 3 51.6	16 28 31.7	5	10/08/2013	26/09/2015	289
34	HM Sge	9 41 57.1	16 44 39.9	7	20/07/2013	11/11/2015	243
35	QW Sge	19 45 49.6	18 36 50				
36	CI Cyg	19 50 11.8	35 41 3.2	111	25/08/2010	09/07/2016	2
37	StHA 169	19 51 28.9	46 23 6	2	12/05/2016	14/05/2016	58
38	V1016 Cyg	19 57 4.9	39 49 33.9	8	15/04/2015	18/06/2016	23
39	PU Vul	20 21 12	21 34 41.9	14	20/07/2013	23/11/2015	231
40	LT Del	20 35 57.3	20 11 34	1	28/11/2015	28/11/2015	226
41	ER Del	20 42 46.4	8 40 56.4	3	02/09/2011	05/11/2014	614
42	V1329 Cyg	20 51 1.1	35 34 51.2	4	08/08/2015	26/09/2015	289
43	V407 Cyg	21 2 13	45 46 30				
44	StHA 190	21 41 44.8	2 43 54.4	14	31/08/2011	08/11/2015	246
45	AG Peg	21 51 1.9	12 37 29.4	162	06/12/2009	09/07/2016	2
46	V627 Cas	22 57 41.2	58 49 14.9	12	06/08/2013	18/02/2016	144
47	Z And	23 33 39.5	48 49 5.4	58	30/10/2010	05/02/2016	157
48	R Aqr	23 43 49.4	-15 17 4.2	27	25/09/2010	25/01/2016	168
49	SU Lyn	06 42 55.1	+55 28 27.2	2	02/05/2016	04/05/2016	68

AAVSO V magnitude of Symbiotic (or suspected) stars				Updated		12/07/2016		
#	Name	AD (2000)	DE (2000)	V	JD	Date	OBS	Days
1	EG And	0 44 37.1	40 40 45.7	7.8	2457533.903	2016 May 25.4	DKS	48
2	AX Per	1 36 22.7	54 15 2.5	10.78	2457479.322	2016 Mar 31.8	BDG	102
3	V471 Per	1 58 49.7	52 53 48.4	12.98	2457469.517	2016 Mar 22.0	DKS	112
4	o Cet	2 19 20.7	-2 58 39.5	4.35	2457436.521	2016 Feb 18.0	SAH	145
5	BD Cam	3 42 9.3	63 13 0.5	5.16	2455566.614	2011 Jan 05.1	PSEB	2015
6	UV Aur	5 21 48.8	32 30 43.1	9.92	2457489.352	2016 Apr 10.8	MEV	92
7	V1261 Ori	5 22 18.6	-8 39 58	6.97	2457376.631	2015 Dec 20.1	SBL	205
8	StHa 55	5 46 42	6 43 48					
9	ZZ CMi	7 24 13.9	8 53 51.7	10.18	2456713.286	2014 Feb 24.7	HPIA	868
10	BX Mon	7 25 24	-3 36 0	9.96	2457484.265	2016 Apr 05.7	TIA	97
11	V694 Mon	7 25 51.2	-7 44 8	9.19	2457548.496	2016 Jun 08.9	HMB	33
12	NQ Gem	7 31 54.5	24 30 12.5	7.94	2457479.431	2016 Mar 31.9	BDG	102
13	GH Gem	7 4 4.9	12 2 12	12.82	2457522.541	2016 May 14.0	DKS	59
14	CQ Dra	12 30 06	69 12 04					
15	TX CVn	12 44 42	36 45 50.6	10.01	2457561.56	2016 Jun 22.0	DKS	20
16	IV Vir	14 16 34.3	-21 45 50					
17	T CrB	15 59 30.1	25 55 12.6	9.61	2457555.685	2016 Jun 16.1	SGEA	26
18	AG Dra	16 1 40.5	66 48 9.5	9.73	2457568.455	2016 Jun 28.9	MEV	13
19	V503 Her	17 36 46	23 18 18	12.33	2457530.609	2016 May 22.1	DKS	51
20	RS Oph	17 50 13.2	-6 42 28.4	11.28	2457540.887	2016 Jun 01.3	HBB	41
21	V934 Her	17 6 34.5	23 58 18.5	8.65	2454102.417	2007 Jan 01.9	GMZ	3479
22	AS 270	18 05 33.7	-20 20 38	13.32	2457548.508	2016 Jun 09.0	HKEB	33
23	AS 289	18 12 22	-11 40 13	13.17	2456355.011	2013 Mar 03.5	OCN	1226
24	YY Her	18 14 34.3	20 59 20	12.98	2457574.438	2016 Jul 04.9	MEV	7
25	FG Ser	18 15 6.2	0 18 57.6	12.01	2456783.432	2014 May 05.9	TIA	798
26	StHa 149	18 18 55.9	27 26 12	12.15	2456844.496	2014 Jul 05.9	GCO	737
27	V443 Her	18 22 8.4	23 27 20	11.67	2457329.311	2015 Nov 02.8	BCP	252
28	FN Sgr	18 53 52.9	-18 59 42	12.98	2457543.944	2016 Jun 04.4	OCN	38
29	V335 Vul	19 23 14.2	24 27 40.2	13.03	2456861.606	2014 Jul 23.1	OCN	720
30	BF Cyg	19 23 53.4	29 40 25.1	10.66	2457539.949	2016 May 31.4	DDJ	42
31	CH Cyg	19 24 33	50 14 29.1	7.66	2457578.707	2016 Jul 09.2	SGEA	3
32	V919 Sgr	19 3 46	-16 59 53.9	13.19	2457543.949	2016 Jun 04.4	OCN	38
33	V1413 Aql	19 3 51.6	16 28 31.7	11.75	2457538.957	2016 May 30.4	PYG	43
34	HM Sge	19 41 57.1	16 44 39.9	12.43	2457484.597	2016 Apr 06.0	TIA	97
35	QW Sge	19 45 49.6	18 36 50	12.72	2457530.507	2016 May 22.0	MEV	51
36	CI Cyg	19 50 11.8	35 41 3.2	10.7	2457576.903	2016 Jul 07.4	DKS	5
37	StHA 169	19 51 28.9	46 23 6	13.03	2457543.955	2016 Jun 04.4	OCN	38
38	V1016 Cyg	19 57 4.9	39 49 33.9	11.48	2457246.469	2015 Aug 11.9	LCLA	335
39	PU Vul	20 21 12	21 34 41.9	12.75	2457515.542	2016 May 07.0	TIA	66
40	LT Del	20 35 57.3	20 11 34	13.11	2457530.556	2016 May 22.0	MEV	51
41	ER Del	20 42 46.4	8 40 56.4	10.25	2457210.509	2015 Jul 07.0	LCLA	371
42	V1329 Cyg	20 51 1.1	35 34 51.2	13.48	2457549.941	2016 Jun 10.4	OCN	32
43	V407 Cyg	21 2 13	45 46 30	15.87	2457327.553	2015 Nov 01.0	OCN	254
44	StHA 190	21 41 44.8	2 43 54.4	10.59	2455855.553	2011 Oct 21.0	DKS	1726
45	AG Peg	21 51 1.9	12 37 29.4	8.52	2457554.985	2016 Jun 15.4	SGEA	27
46	V627 Cas	22 57 41.2	58 49 14.9	12.13	2457437.341	2016 Feb 18.8	BDG	144
47	Z And	23 33 39.5	48 49 5.4	9.88	2457532.878	2016 May 24.3	DKS	49
48	R Aqr	23 43 49.4	-15 17 4.2	10.32	2457419.537	2016 Feb 01.0	BJFB	162
49	SU Lyn	06 42 55.1	+55 28 27.2	8.62	2457511.473	2016 May 02.9	BDG	70

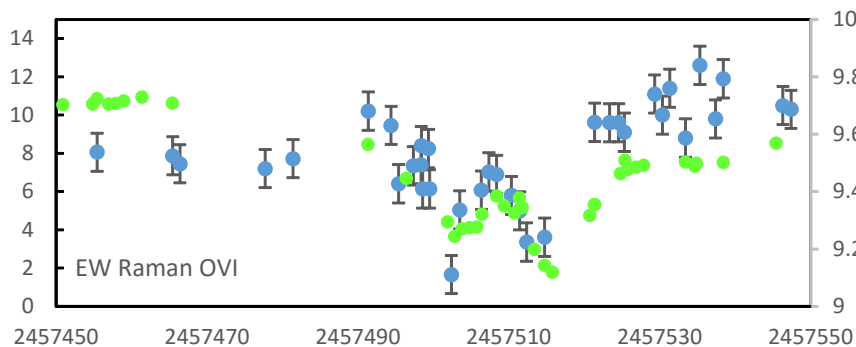
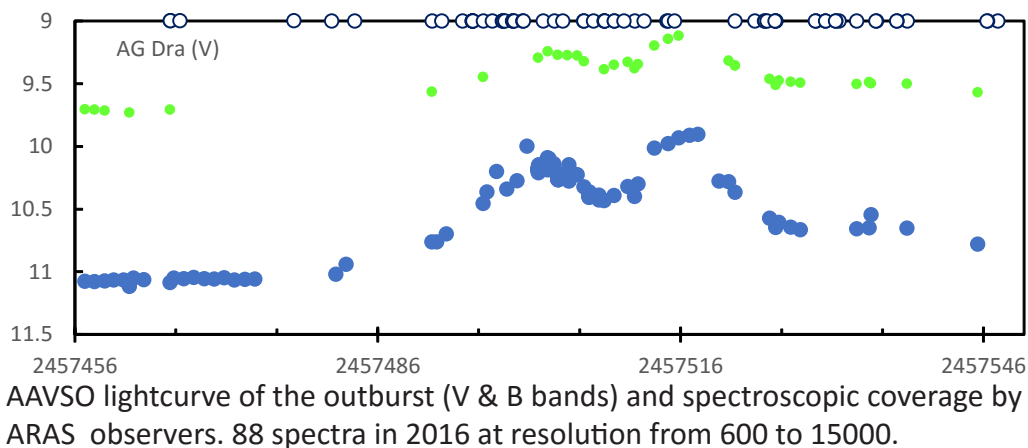
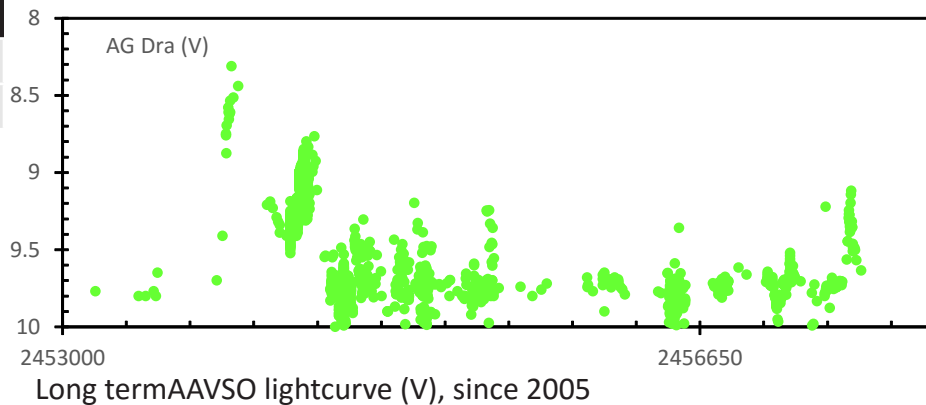
Daily (almost) update on :

<http://www.astronomie-amateur.fr/Actualite/AAVSO.htm>

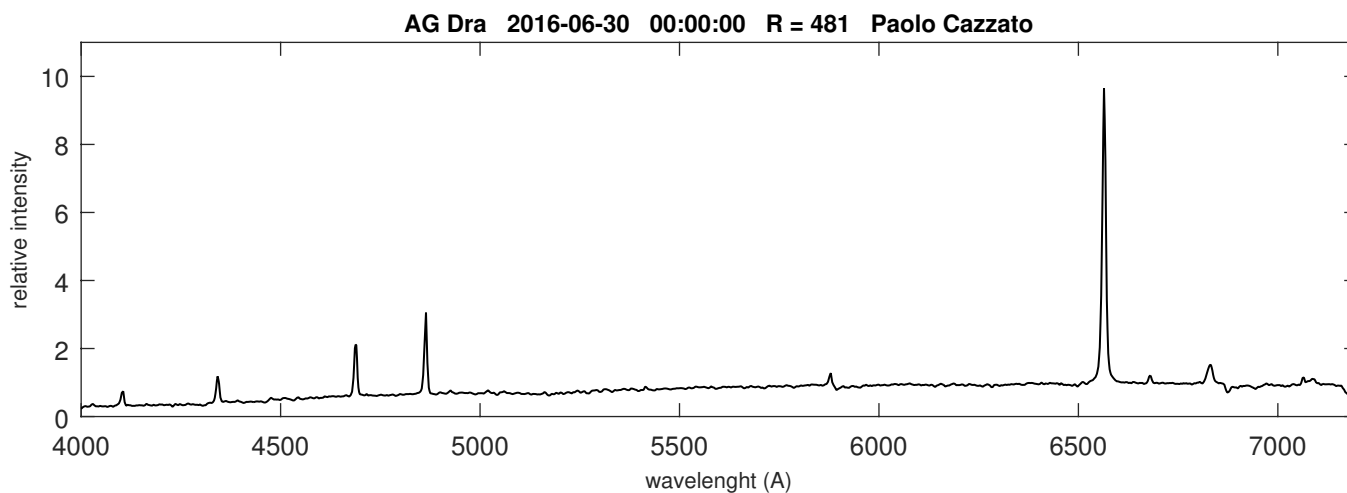
AG Dra

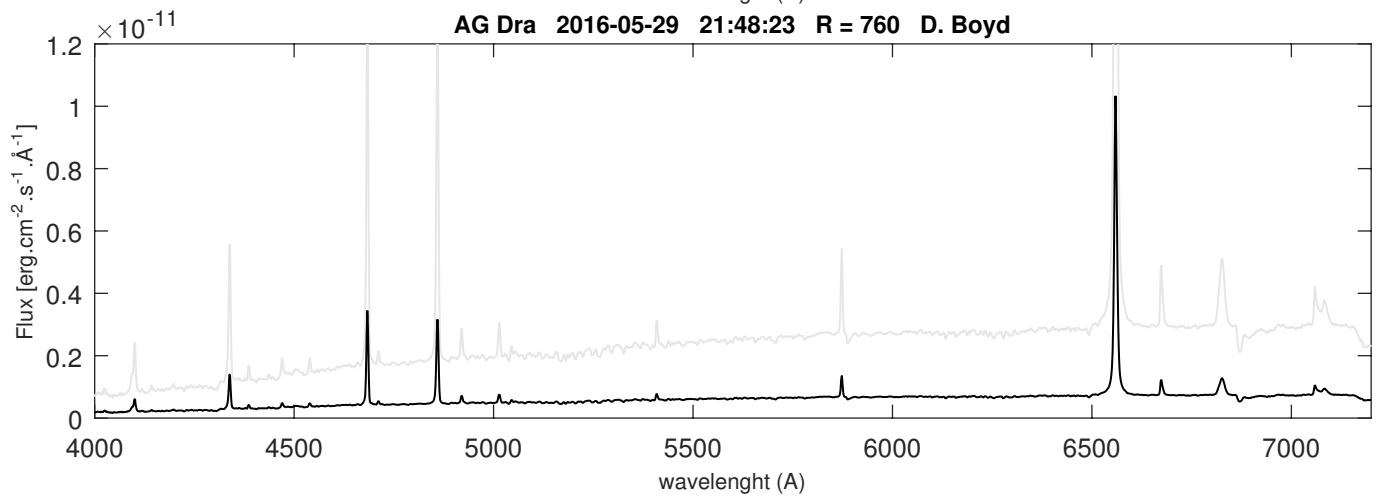
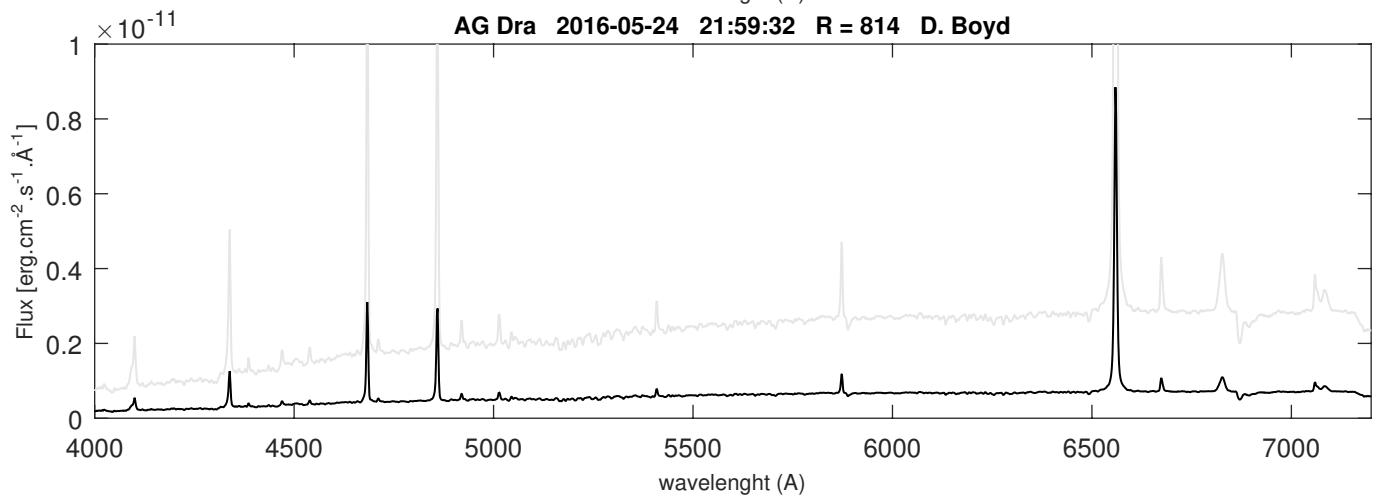
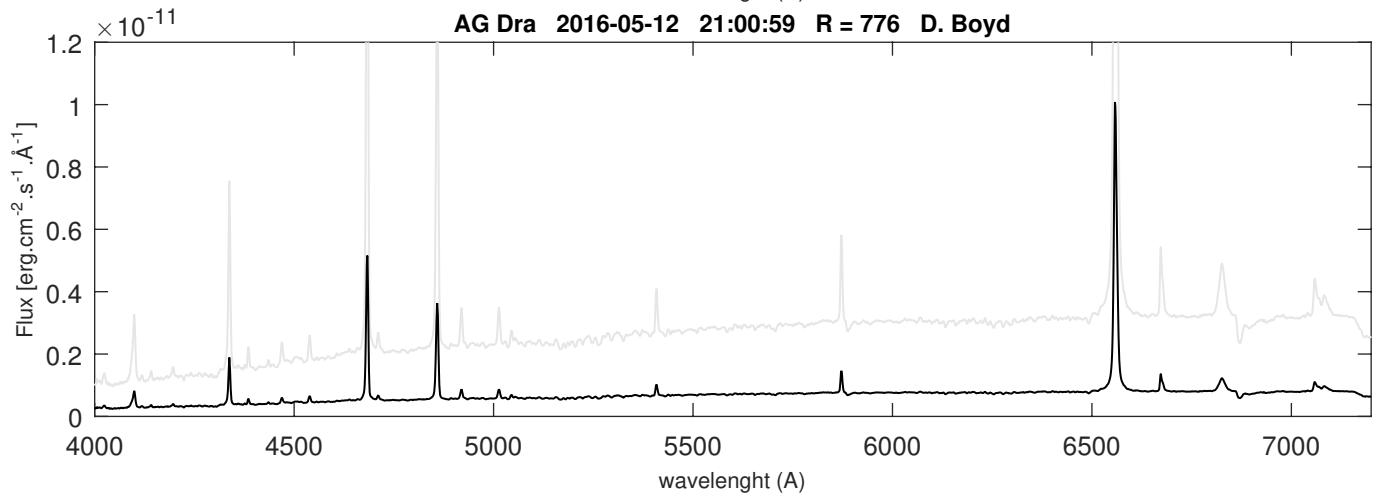
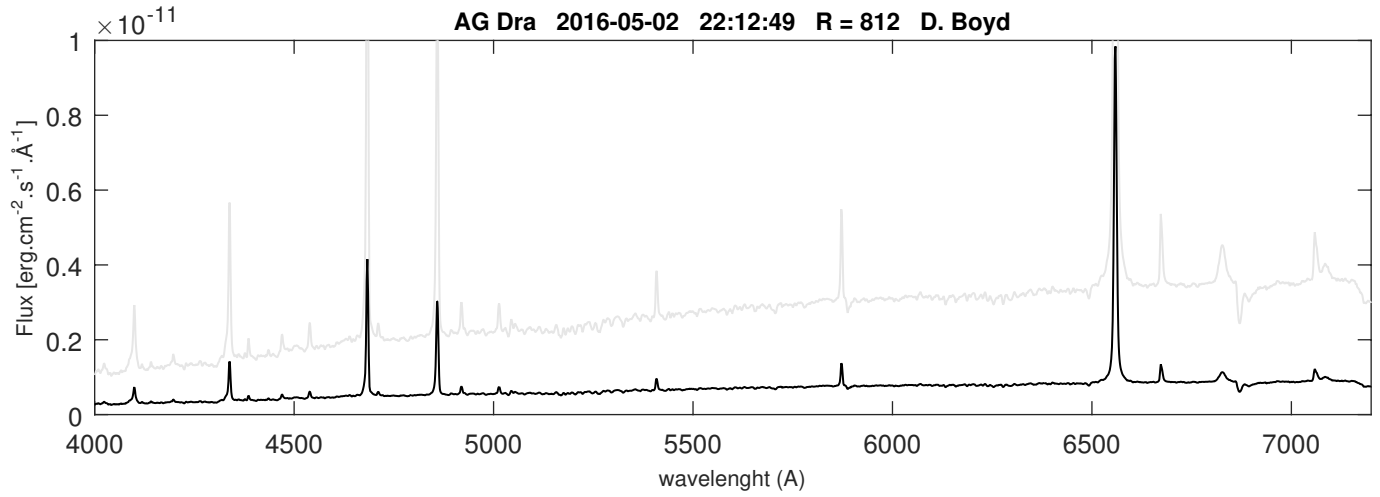
Coordinates (2000.0)	
R.A.	16 01 41.0
Dec	+66 48 10.1

Further observations of the outburst of AG Dra

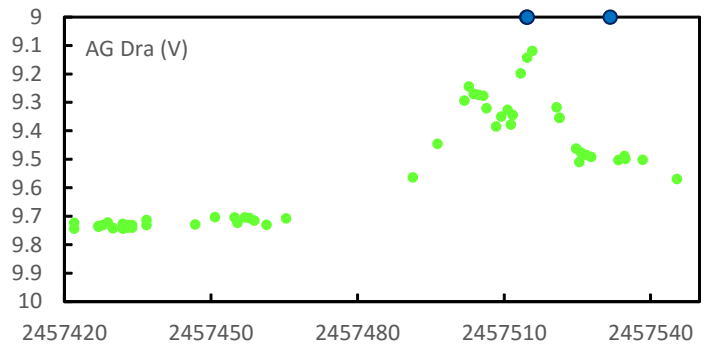


Raman OVI equivalent width (bleu dots) and V magnitude from AAVSO (green dots). The magnitude axe is inverted.

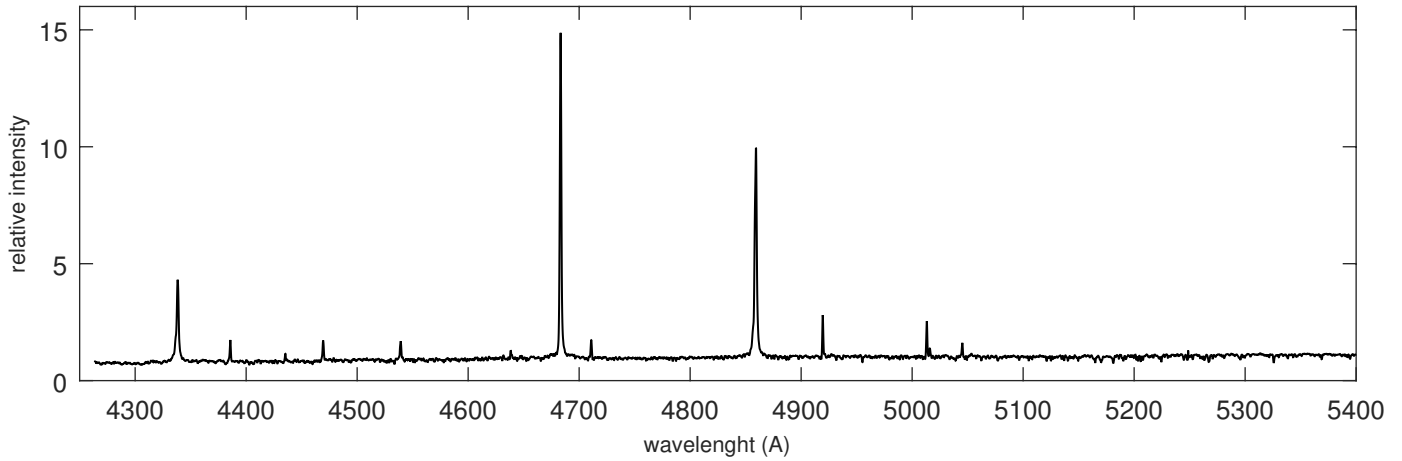




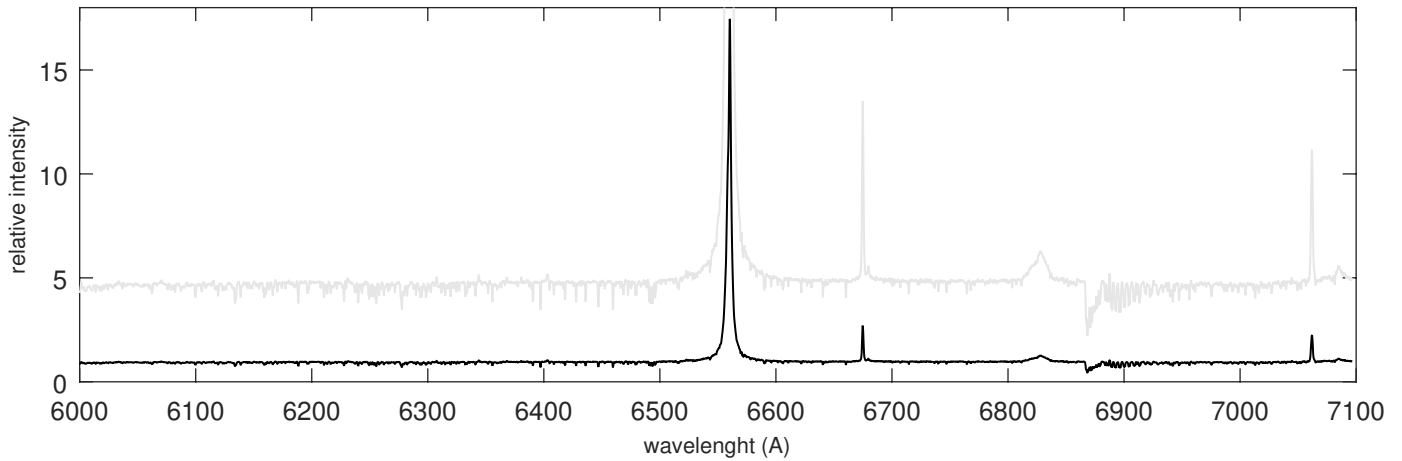
AG Dra



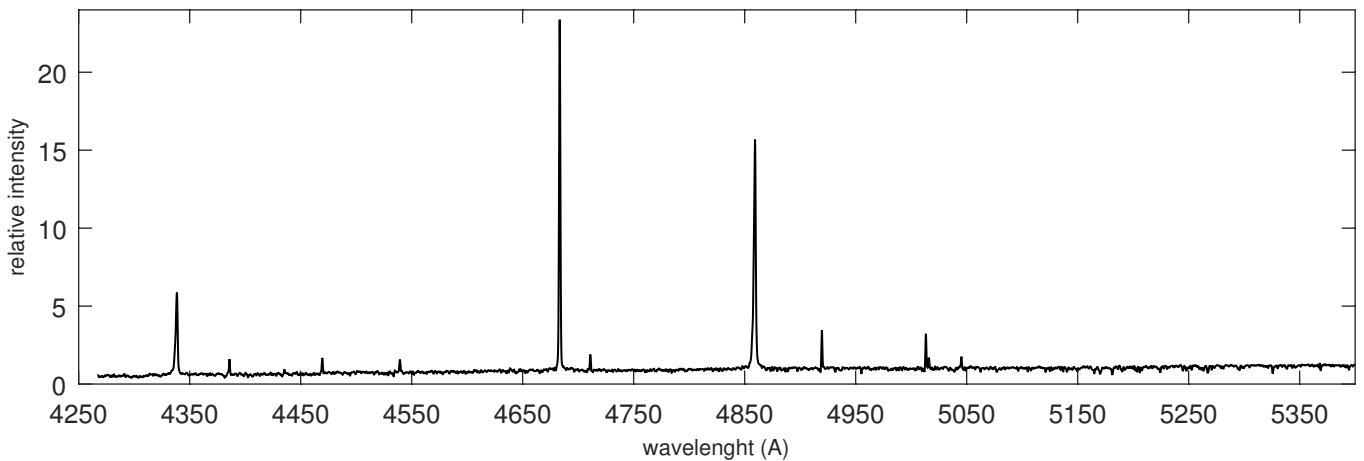
AG Dra 2016-05-06 02:01:21 R = 6500 T Lester



AG Dra 2016-05-06 06:00:13 R = 9000 T Lester

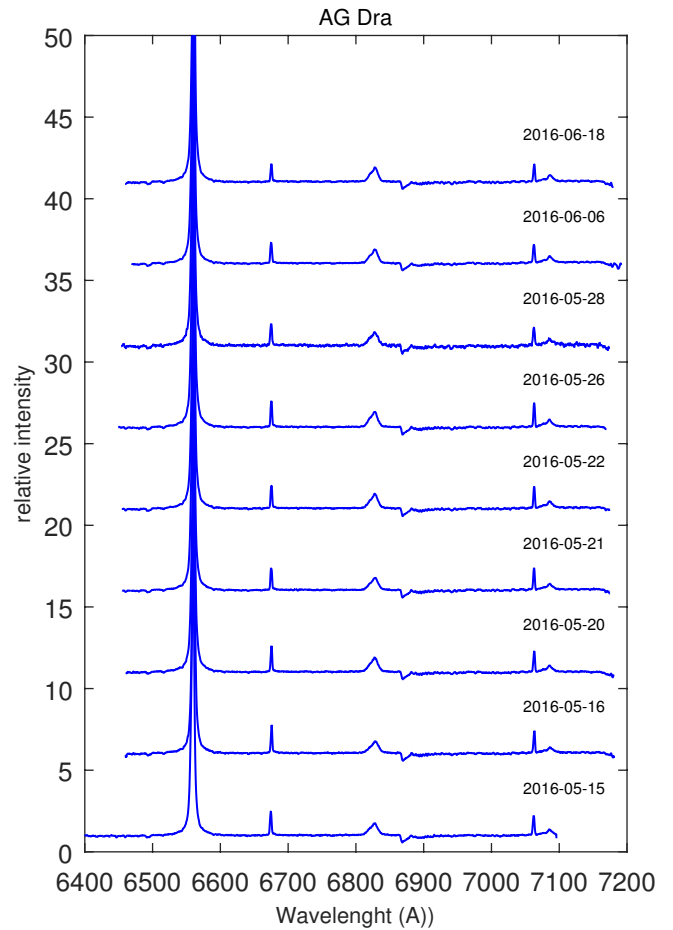
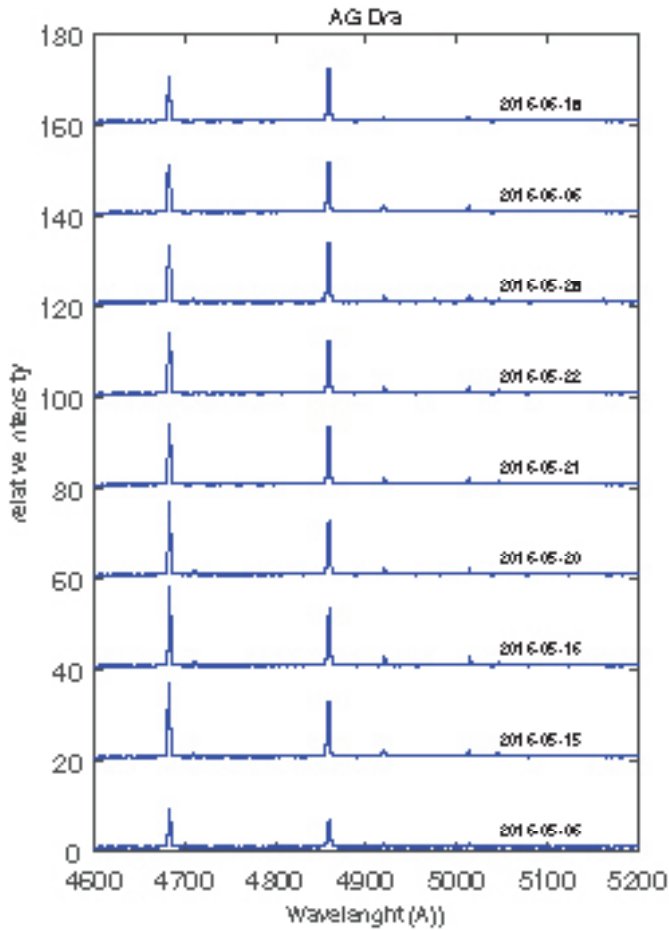
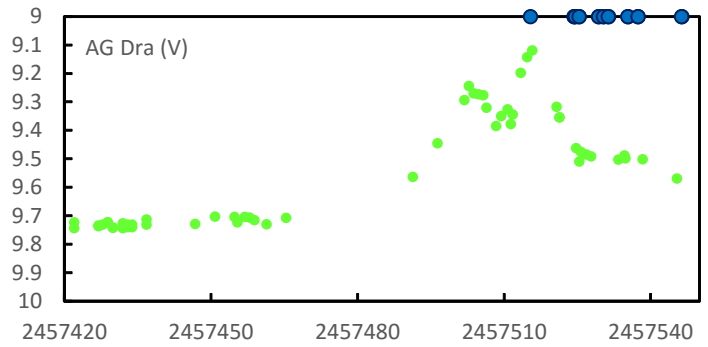


AG Dra 2016-05-23 04:00:28 R = 6400 T Lester

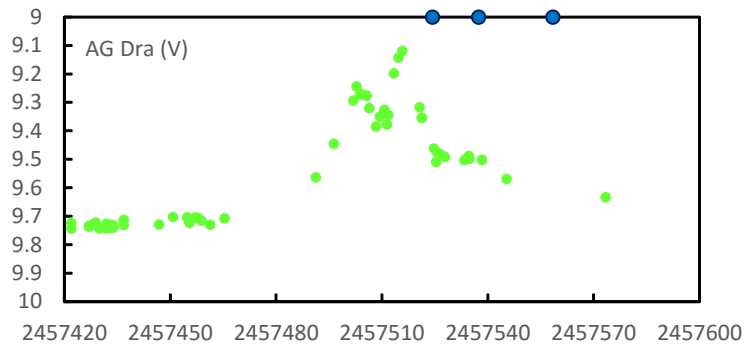


AG Dra H β and H α regions by P. Somogyi

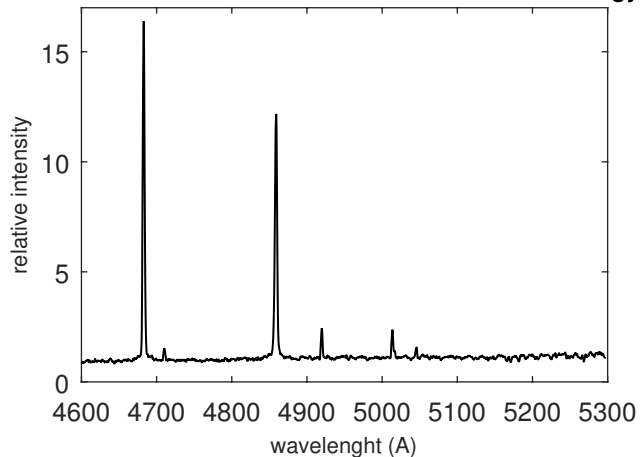
H α and H β region obtained by P. Somogyi with a Lhires III (600 In/mm, R = 2500)



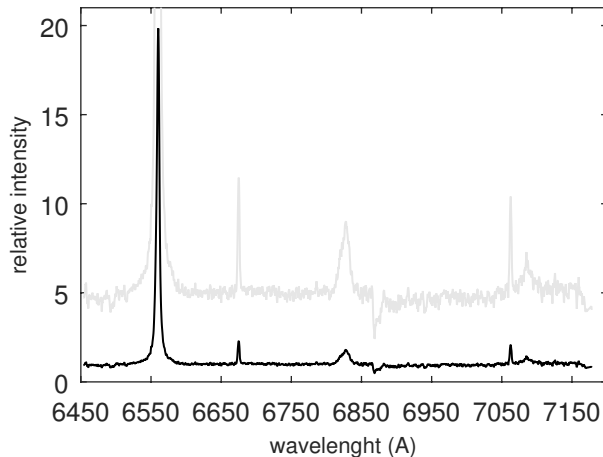
AG Dra



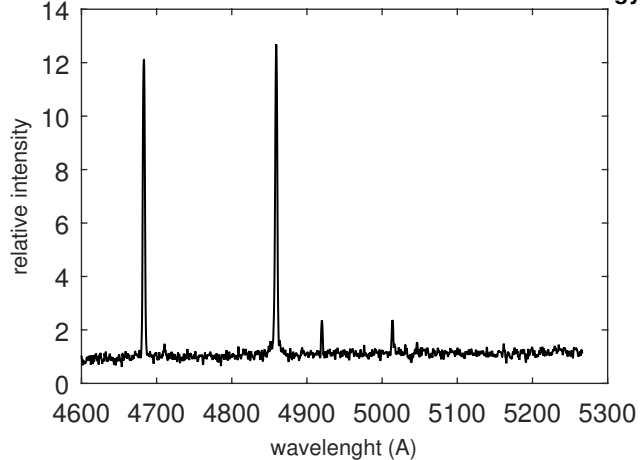
AG Dra 2016-05-15 19:23:36 R = 1735 P Somogyi



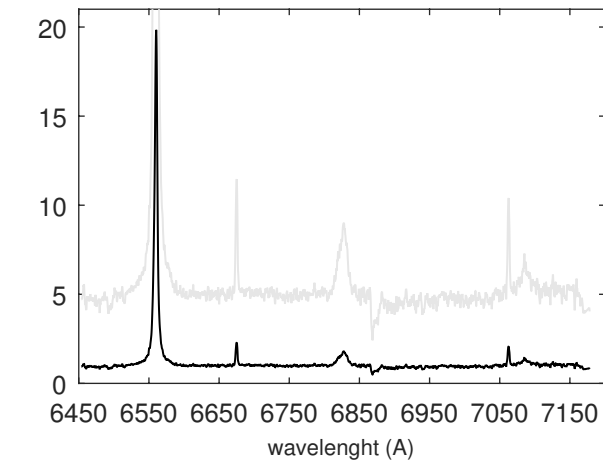
AG Dra 2016-05-28 21:26:55 R = 2503 P. Somog



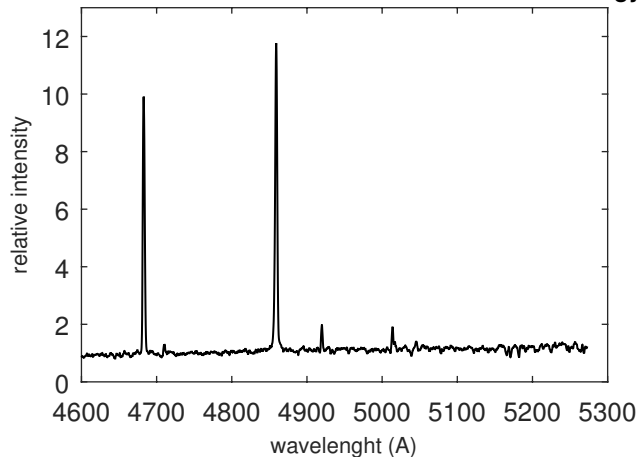
AG Dra 2016-05-28 21:59:09 R = 1899 P. Somogyi



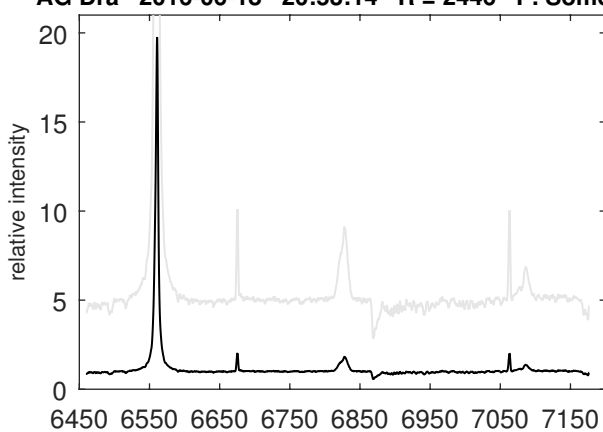
AG Dra 2016-05-28 21:26:55 R = 2503 P. Somogyi



AG Dra 2016-06-18 22:54:51 R = 1840 P. Somogyi



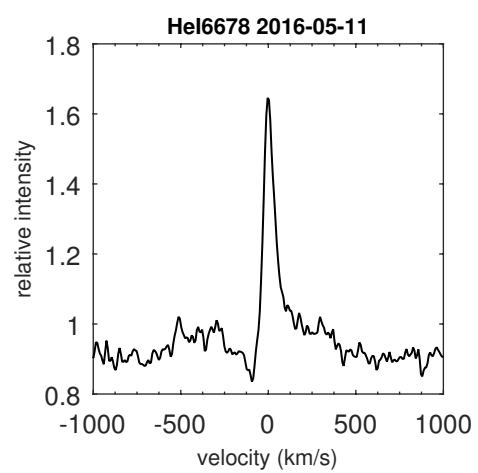
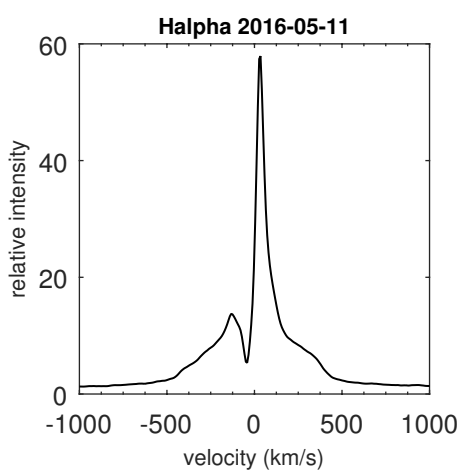
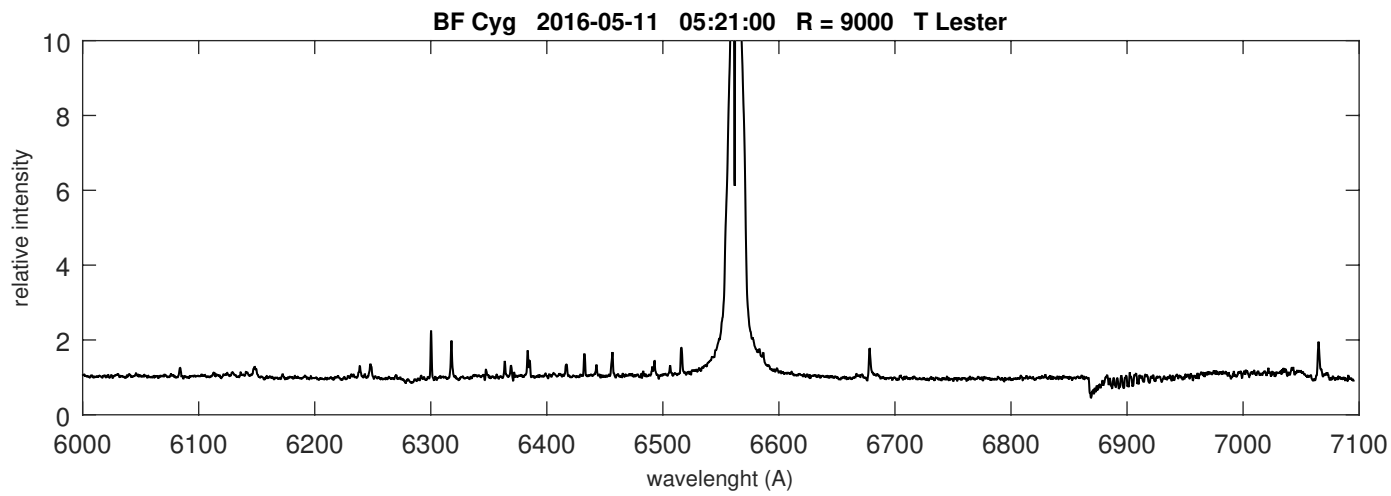
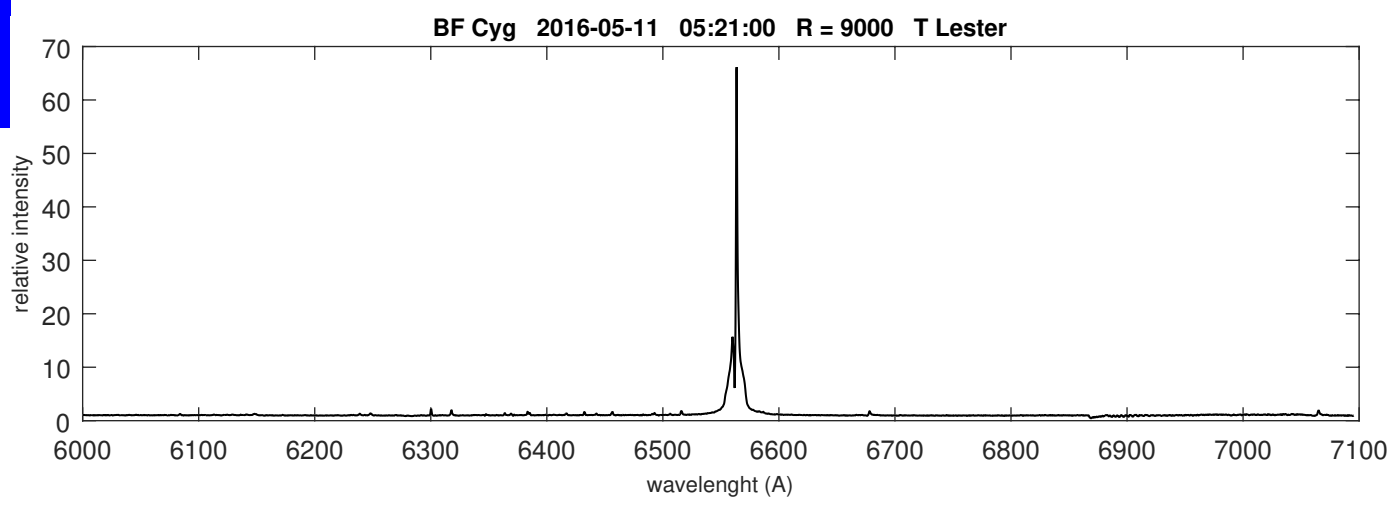
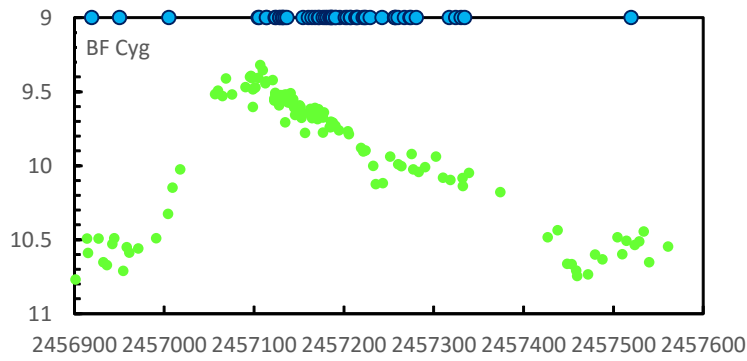
AG Dra 2016-06-18 20:53:14 R = 2446 P. Somog



BF Cyg

Coordinates (2000.0)	
R.A.	19 23 53.5
Dec	+29 40 29.2
Mag	9.2-10.8

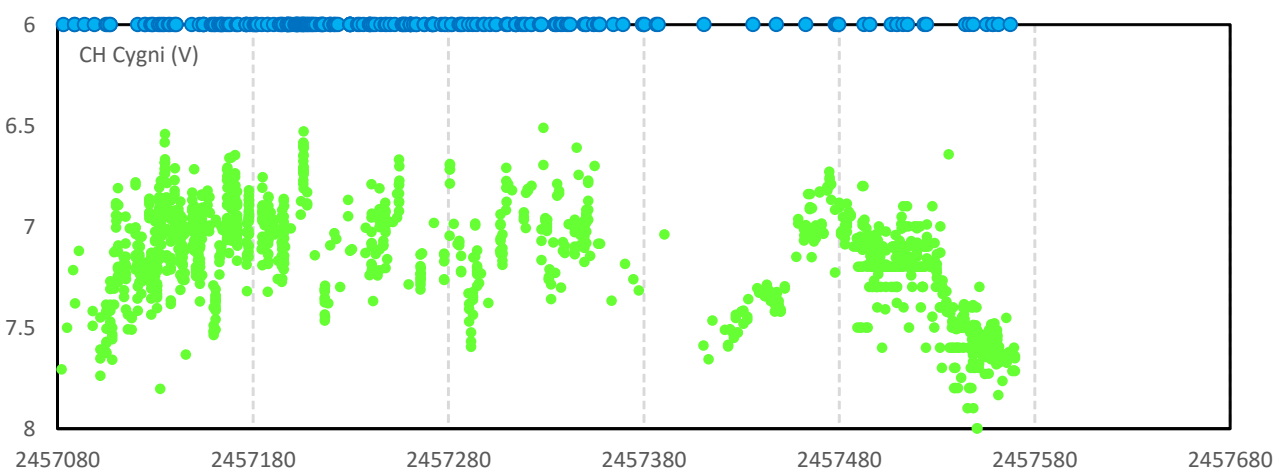
BF Cyg is now back to quiescence state after a long outburst



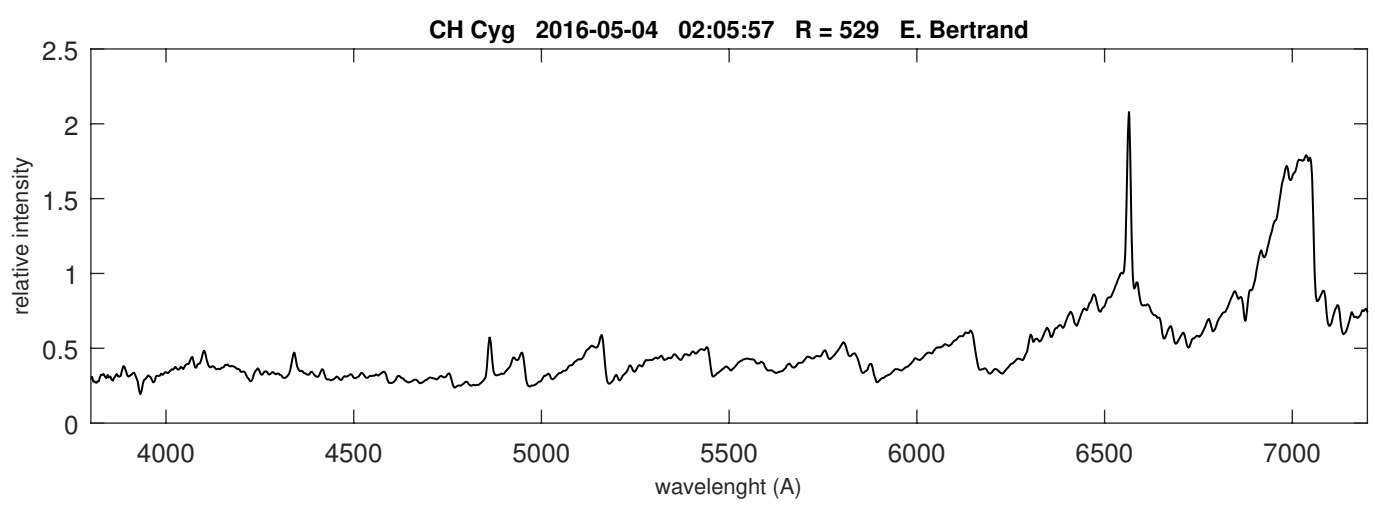
CH Cyg

Coordinates (2000.0)	
R.A.	19 24 33.1
Dec	+50 14 29.1
Mag	

Ongoing campaign upon the request of Augustin Skopal
At least one spectrum a month (high resolution and low resolution, with a correct atmospheric response)



AAVSO V lightcurve in 2015-2016 and ARAS spectra (blue dots)
CH Cygni is currently declining (V ~ 7.7 late June)



And also a message from Margarita Karovska

Dear Friends of CH Cyg,

Our friend seems to be dropping abruptly in B and V in the recent weeks which may indicate a significant change in the activity in the system (including a new jet).

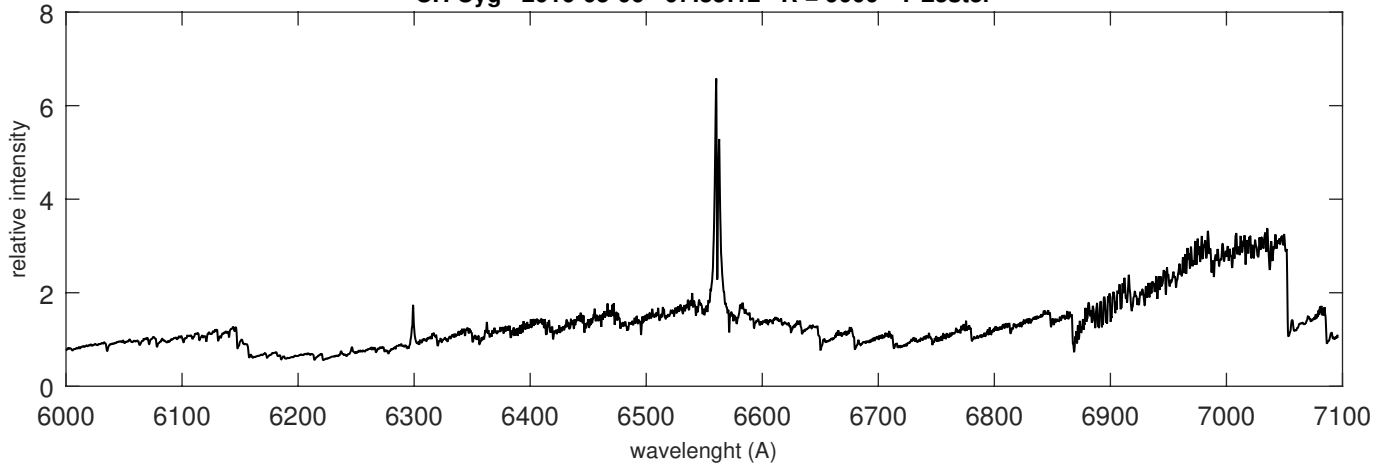
Do you have recent spectra of this system?

It would be very helpful if you could monitor it spectroscopically (at least once a week if it is possible). We are trying to understand what is causing this activity (as well as several similar events observed in the past decade or so).

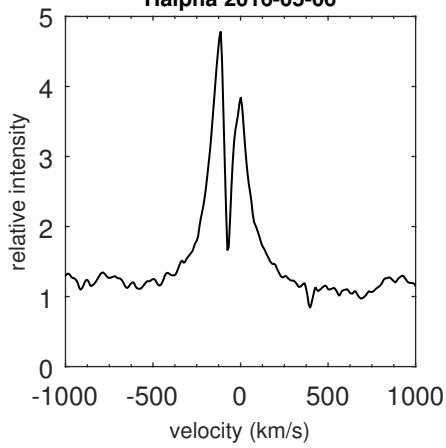
As before, H alpha, [O III] 5007A, (or any part of the spectrum) will be great!

CH Cyg

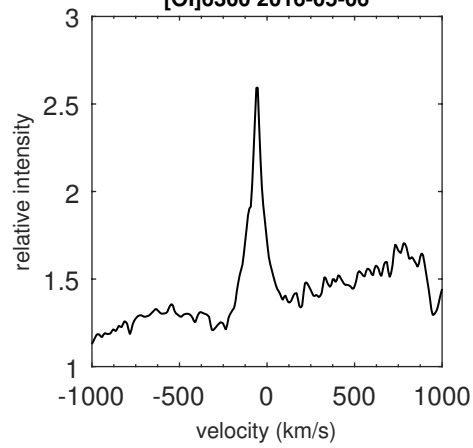
CH Cyg 2016-05-06 07:35:12 R = 9000 T Lester



Halpha 2016-05-06



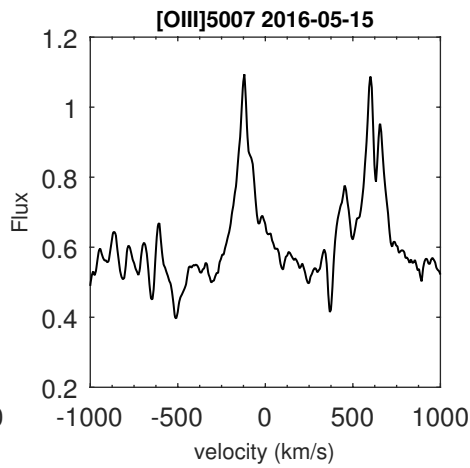
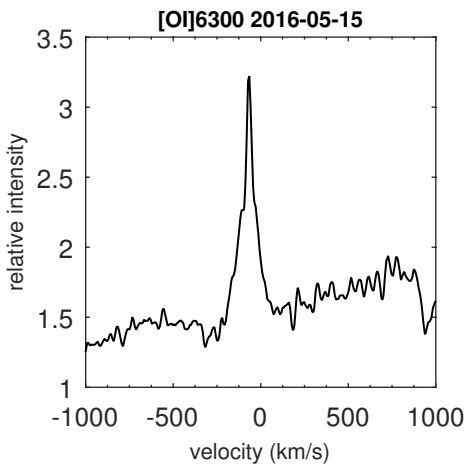
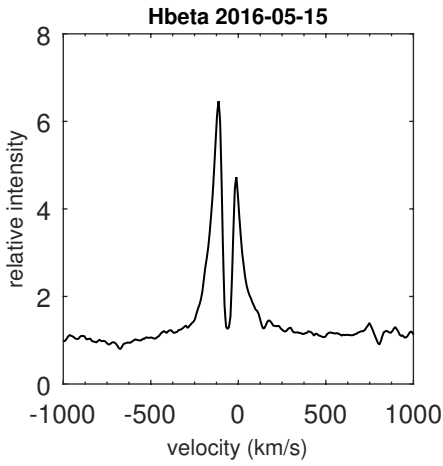
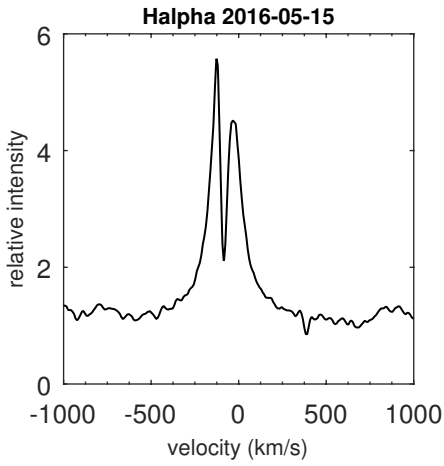
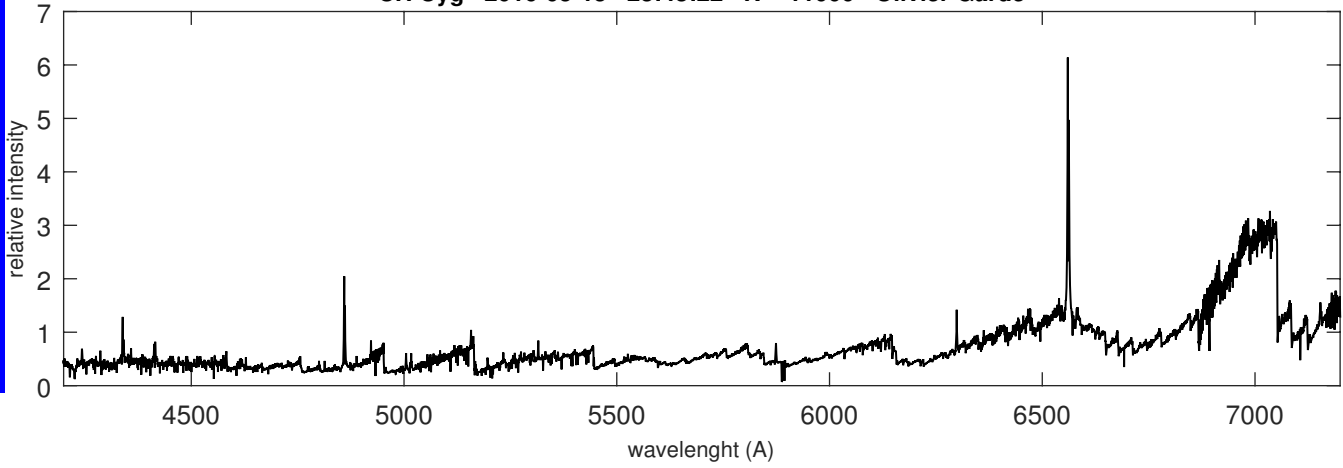
[O I]6300 2016-05-06



CH Cyg

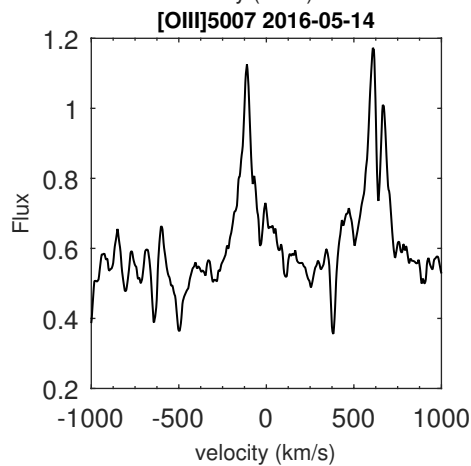
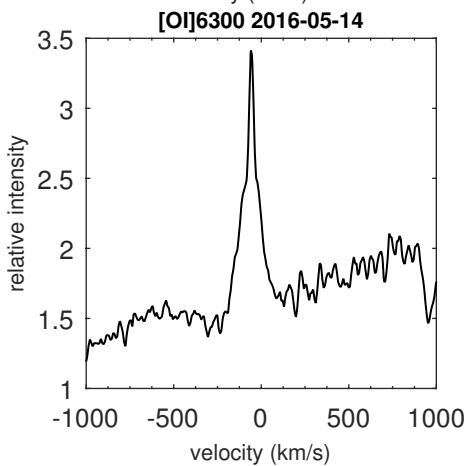
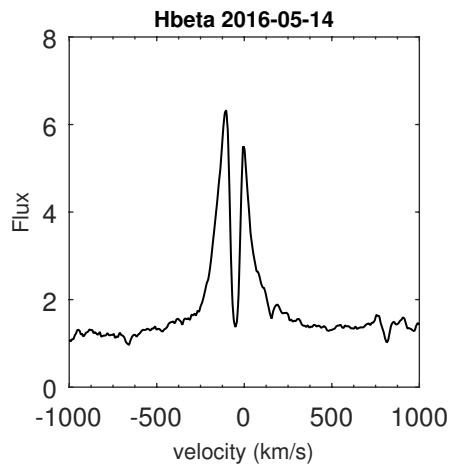
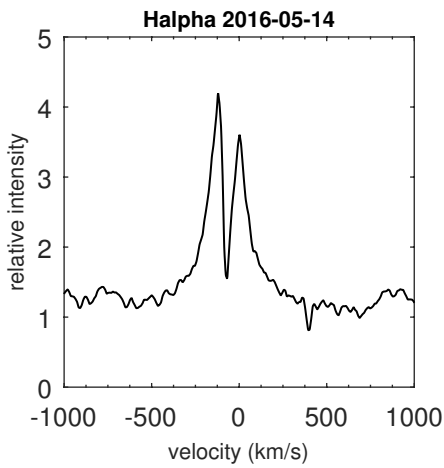
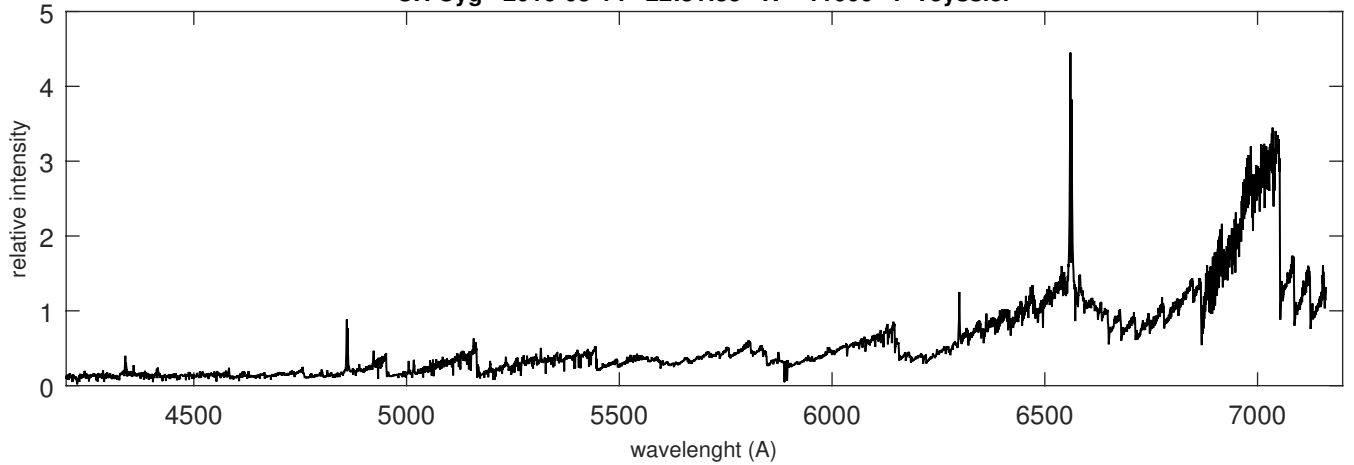
S
C
-
H
O
-
B
-
M
Y
S

CH Cyg 2016-05-15 23:43:22 R = 11000 Olivier Garde



CH Cyg

CH Cyg 2016-05-14 22:31:35 R = 11000 F Teyssier

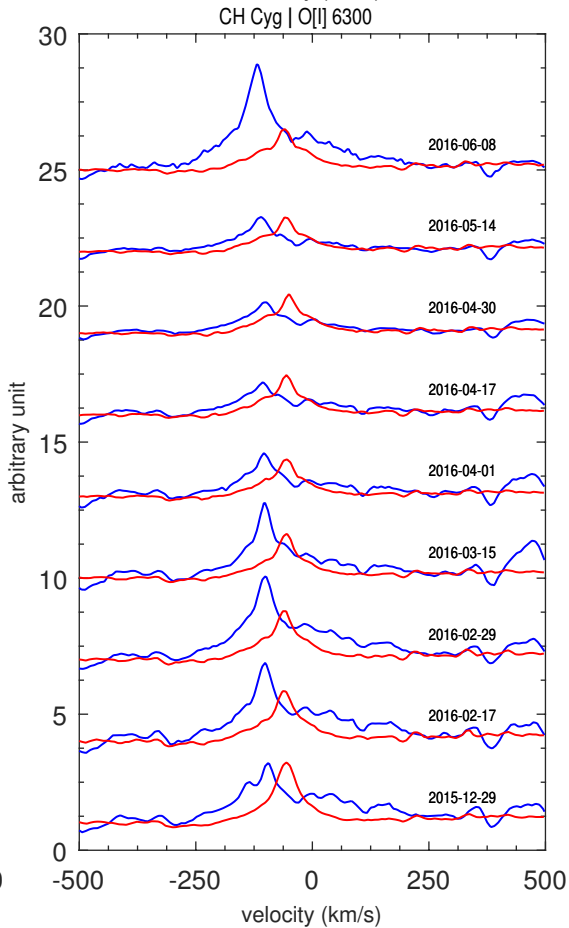
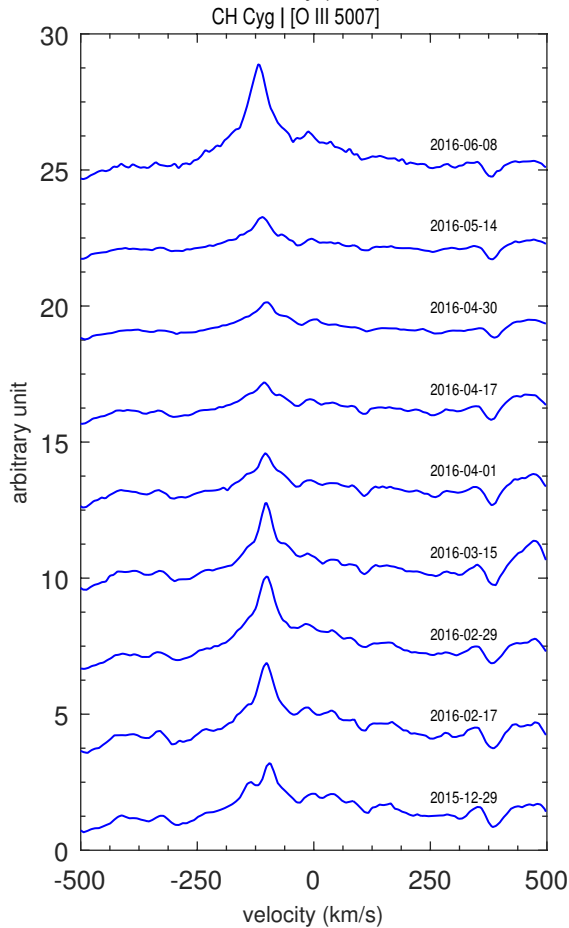
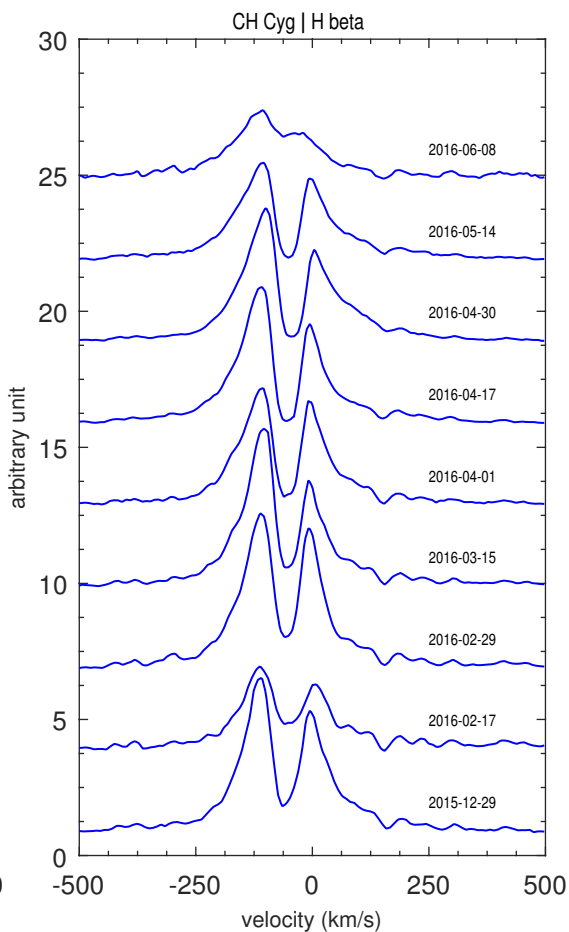
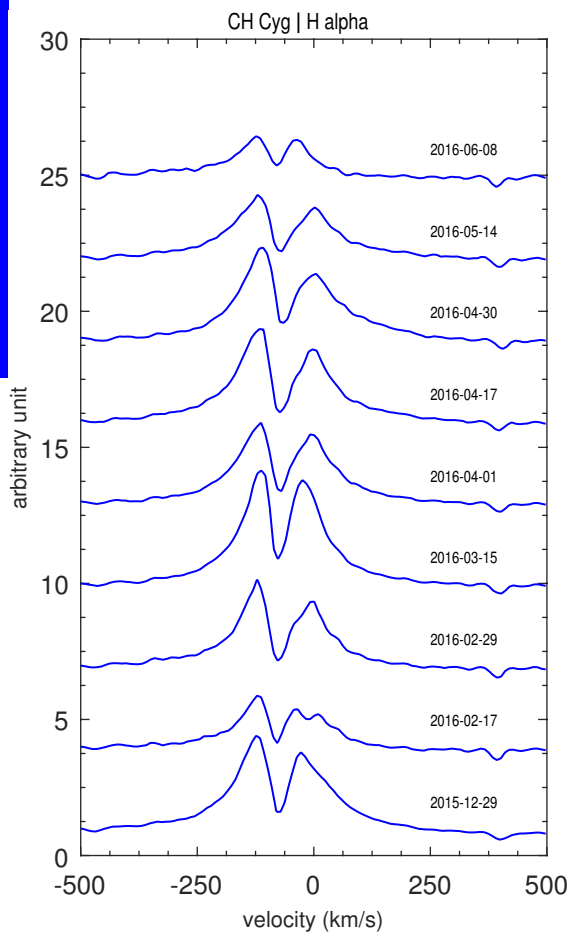
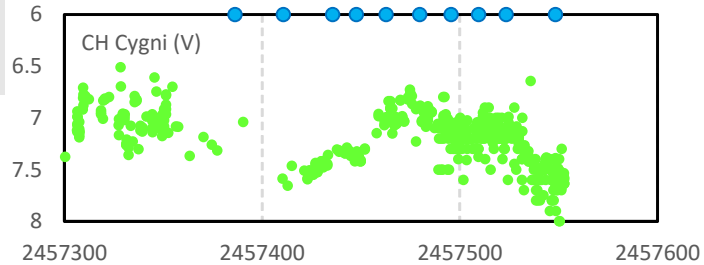


Note that in CH Cyg the [O I] velocities coincide with the Balmer absorption, the [O III] is displaced from both. Toward the blue. The same with the V/R ratio for the Balmer profiles you show. So it would be worth noting that the blueshifted low velocity gas also shows extensions while the red is closer to invariant. This would, one might argue, suggest an expanding ionization front within the RG wind. I don't mean a dynamical interaction, but as the ionization front propagates in an outflow you'd see a change in the mean line velocity.

The advantage is with using forbidden lines as tracers; the neutral gas is optically thin in [O I] (of course, also in [O III]) but that's obvious).

CH Cyg Evolution in 2016

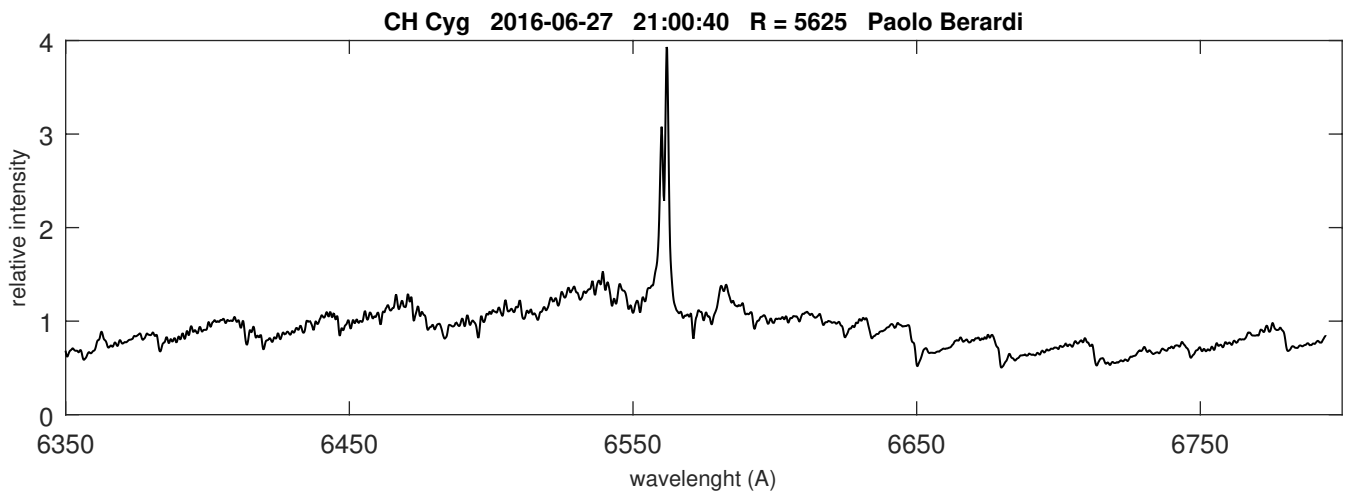
Echel (R = 11000)
F Teyssier



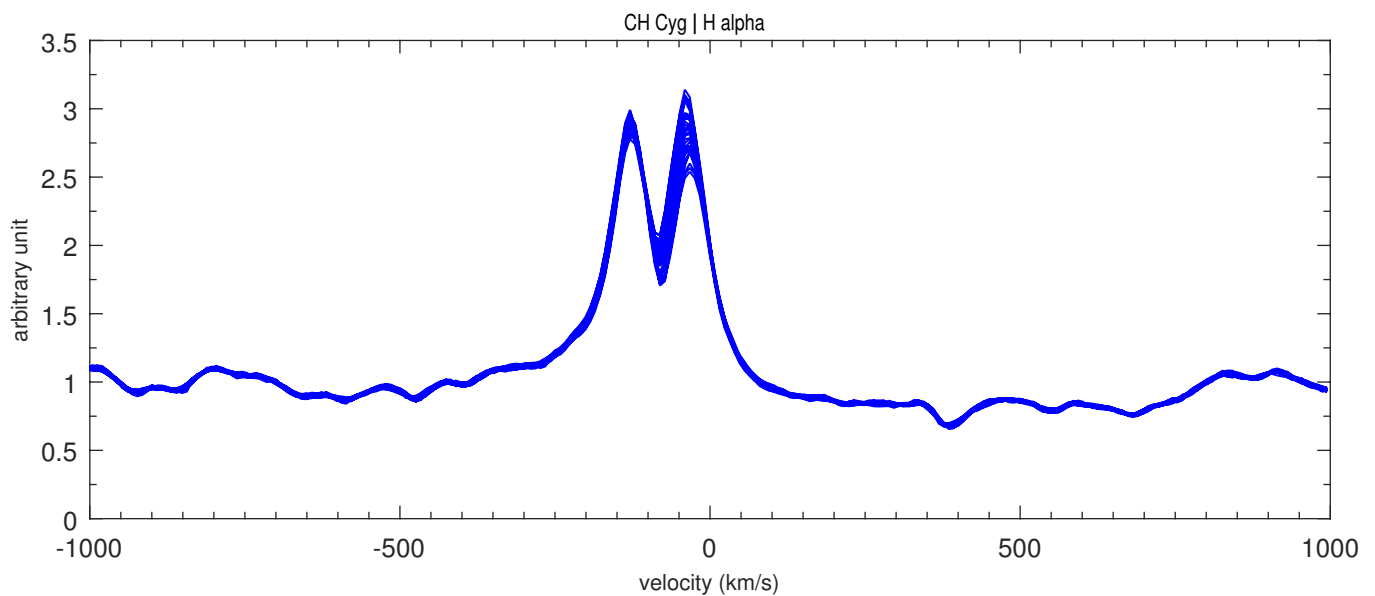
[OIII] 5007 in blue
[OI] 6300 in red

CH Cyg Time-series by Paolo Berardi

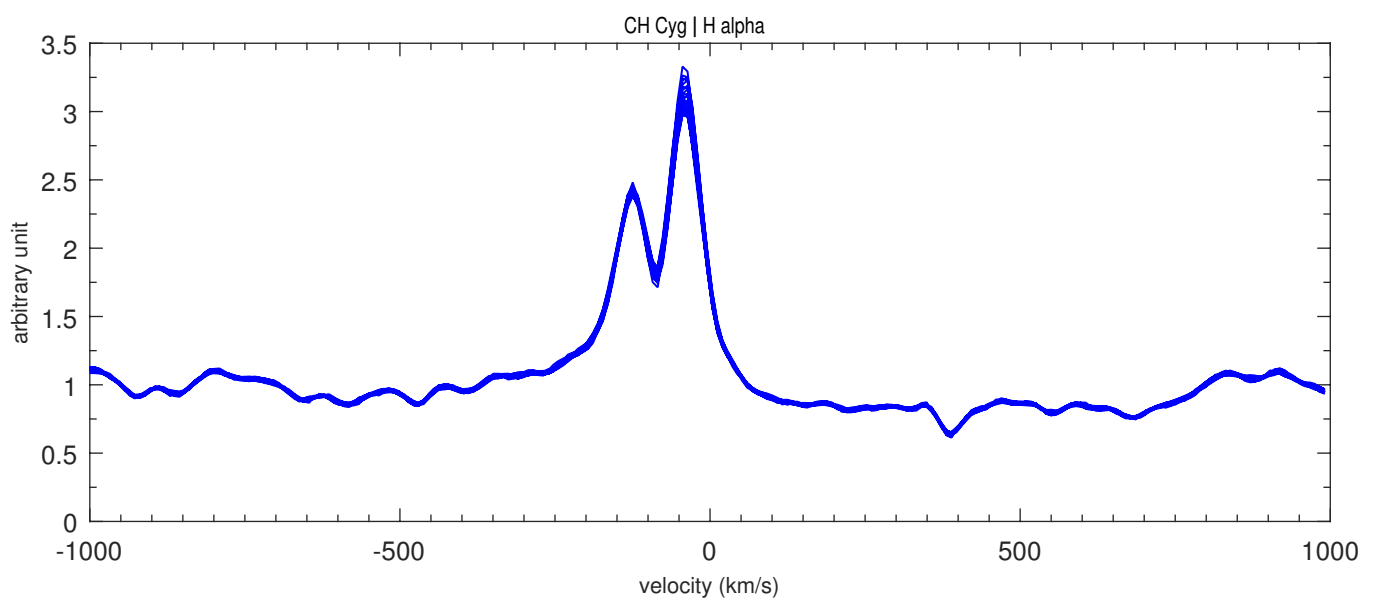
SSC-HO-BMYS



Time series on H α by Paolo Berardi with a Lhires III at R = 6000 (1200 ln/mm)
The spectra can be downloaded from ARAS Database (zip files)



2016-06-21, from 20:32 to 22:55 (27 spectra)

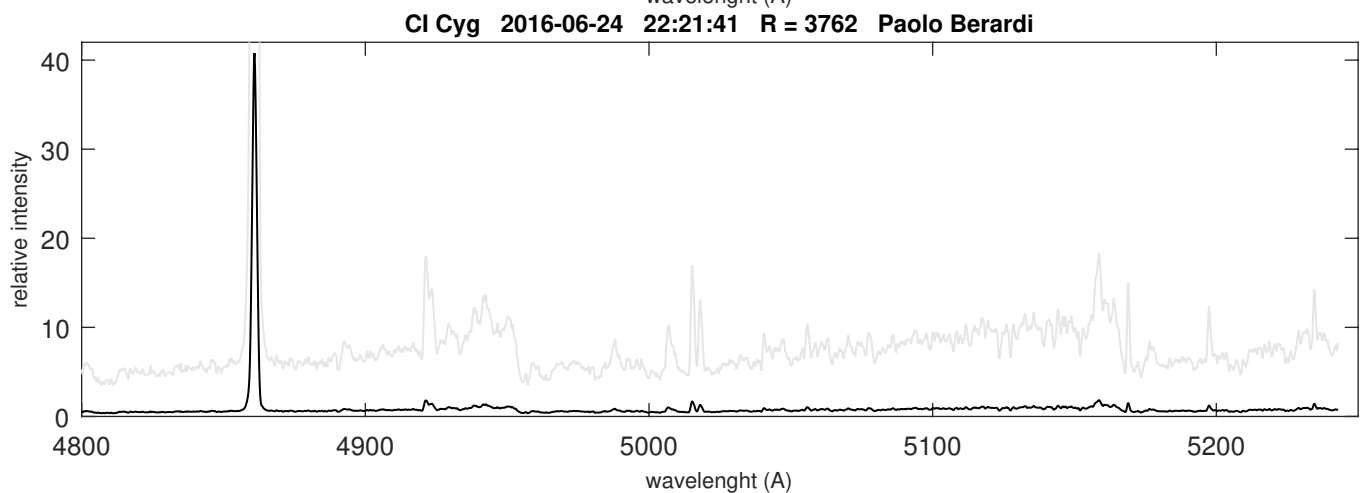
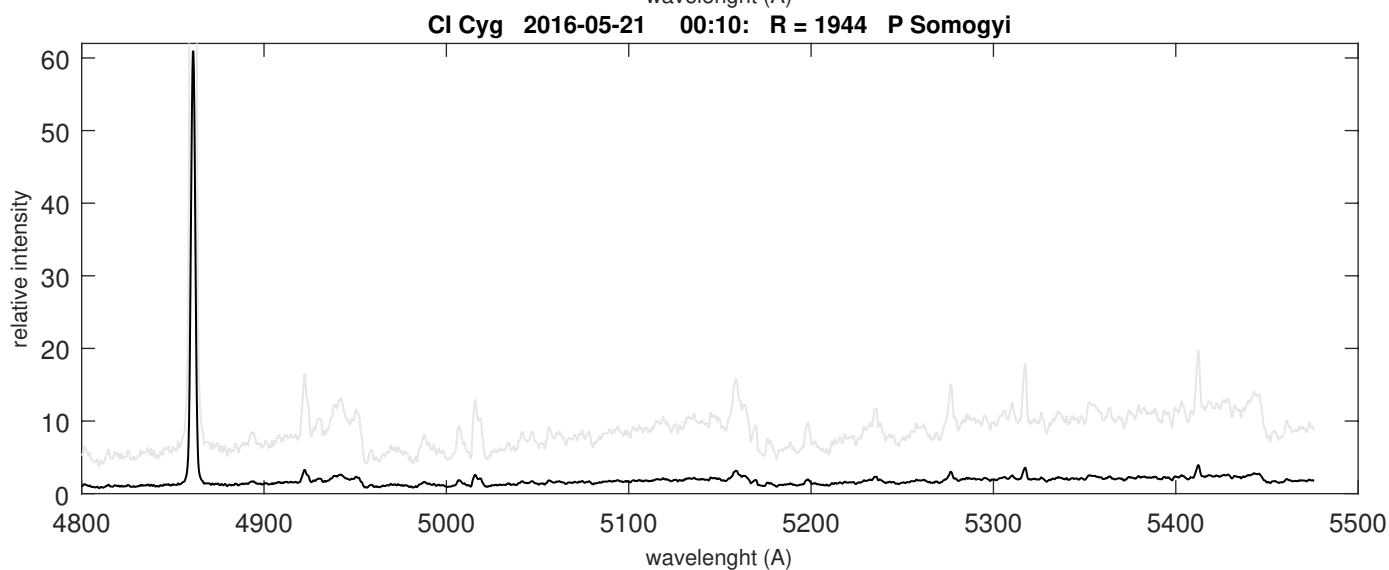
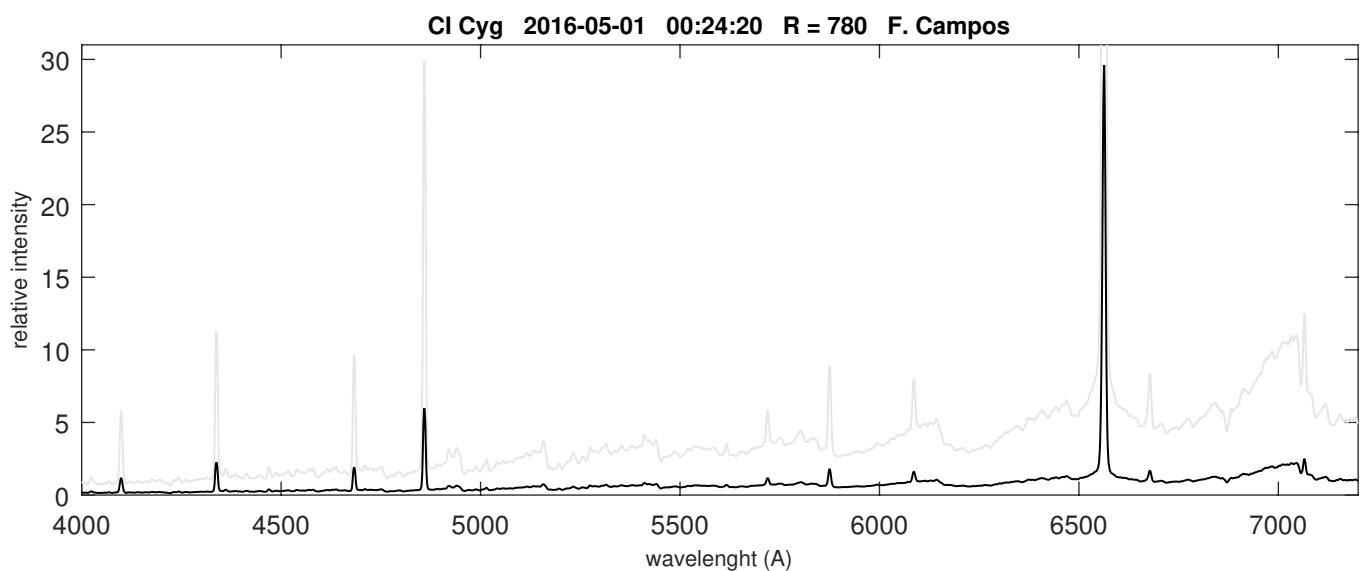
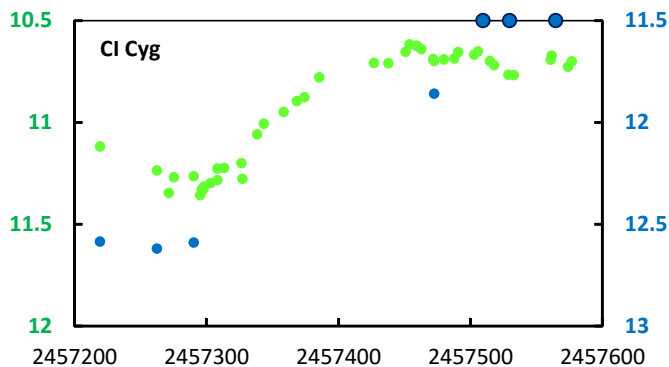


2016-06-27, from 21:00 to 22:51 (35 spectra)

CI Cyg

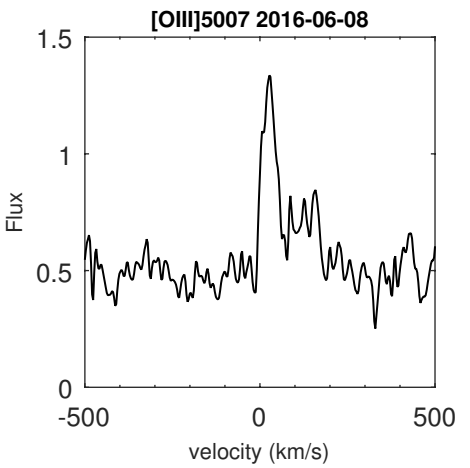
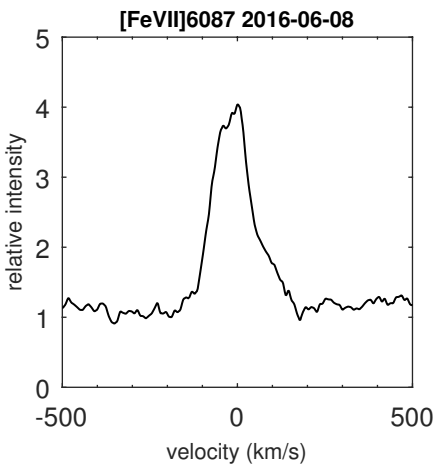
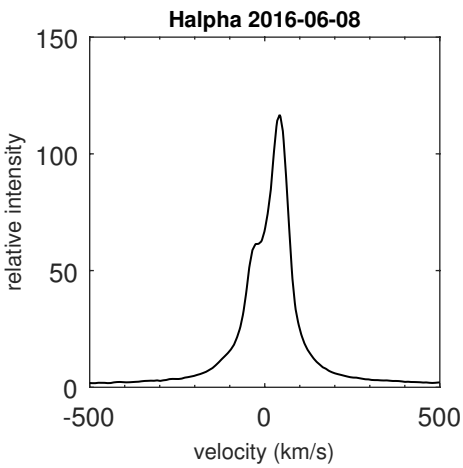
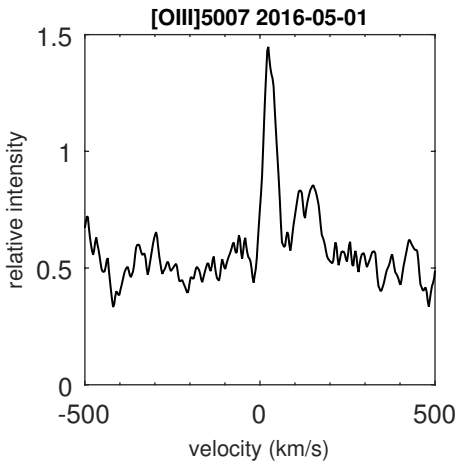
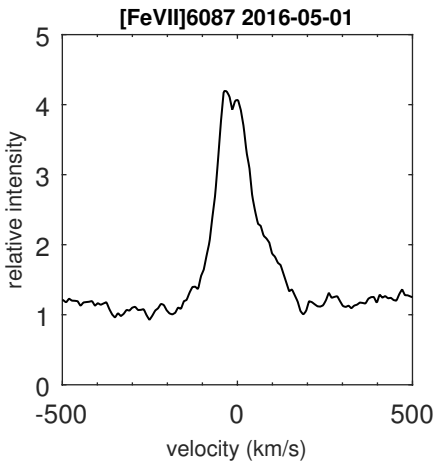
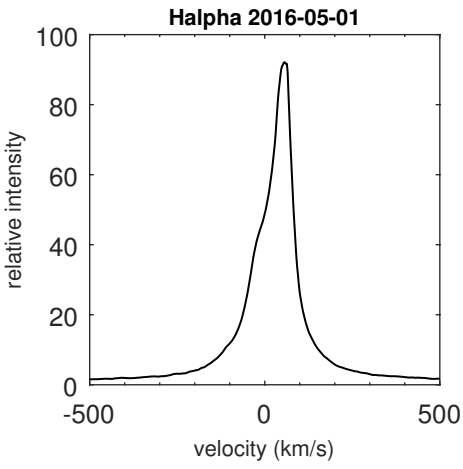
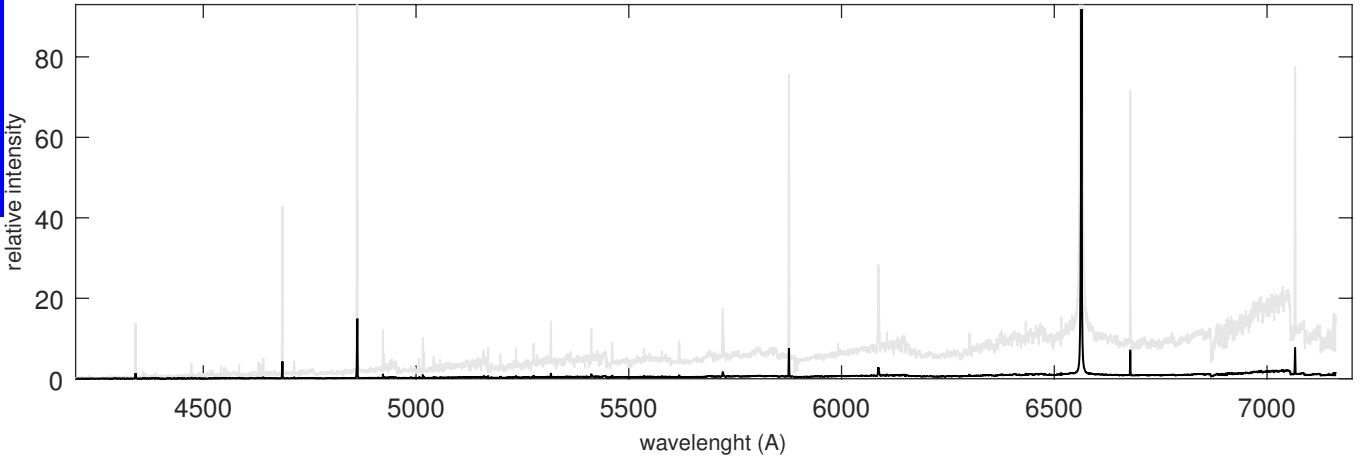
Coordinates (2000.0)	
R.A.	19 50 11.8
Dec	35 41 30
Mag	10.7 (05-2016)

The classical symbiotic CI Cygni remains at high luminosity (10.7)



CI Cyg

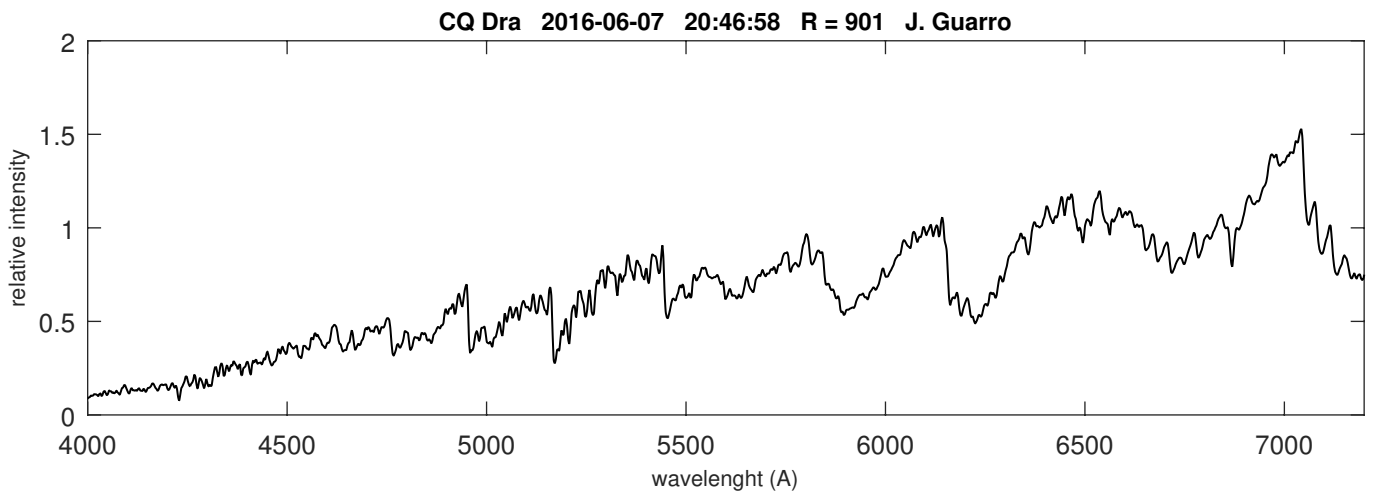
CI Cyg 2016-05-01 00:32:38 R = 11000 FTeyssier



CQ Dra

Coordinates (2000.0)

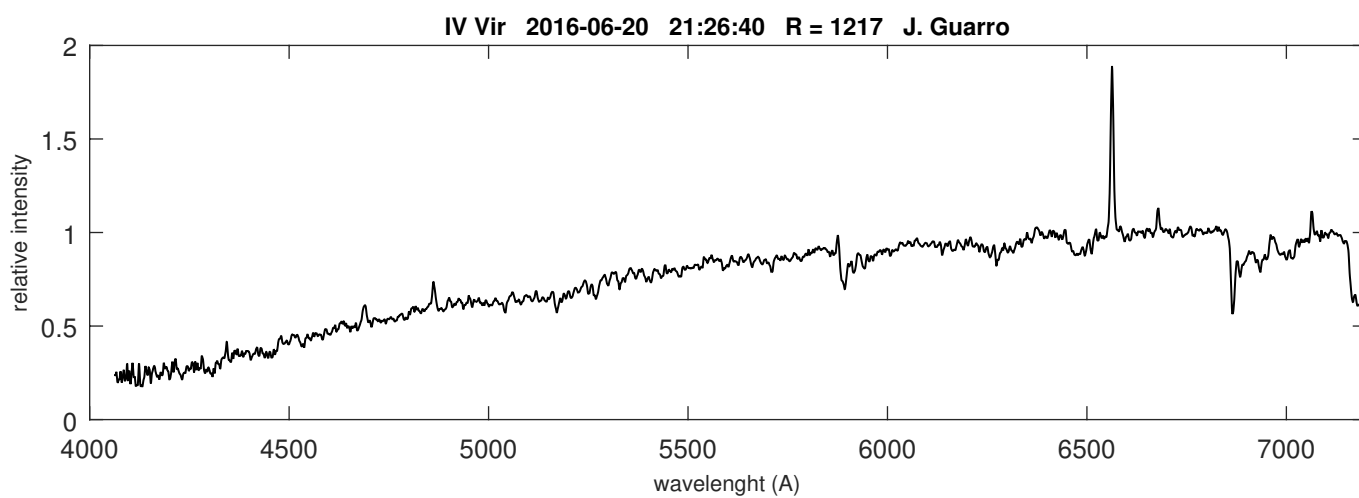
R.A.	12 30 06.6
Dec	+69 12 04.1
Mag	5



IV Vir

Coordinates (2000.0)

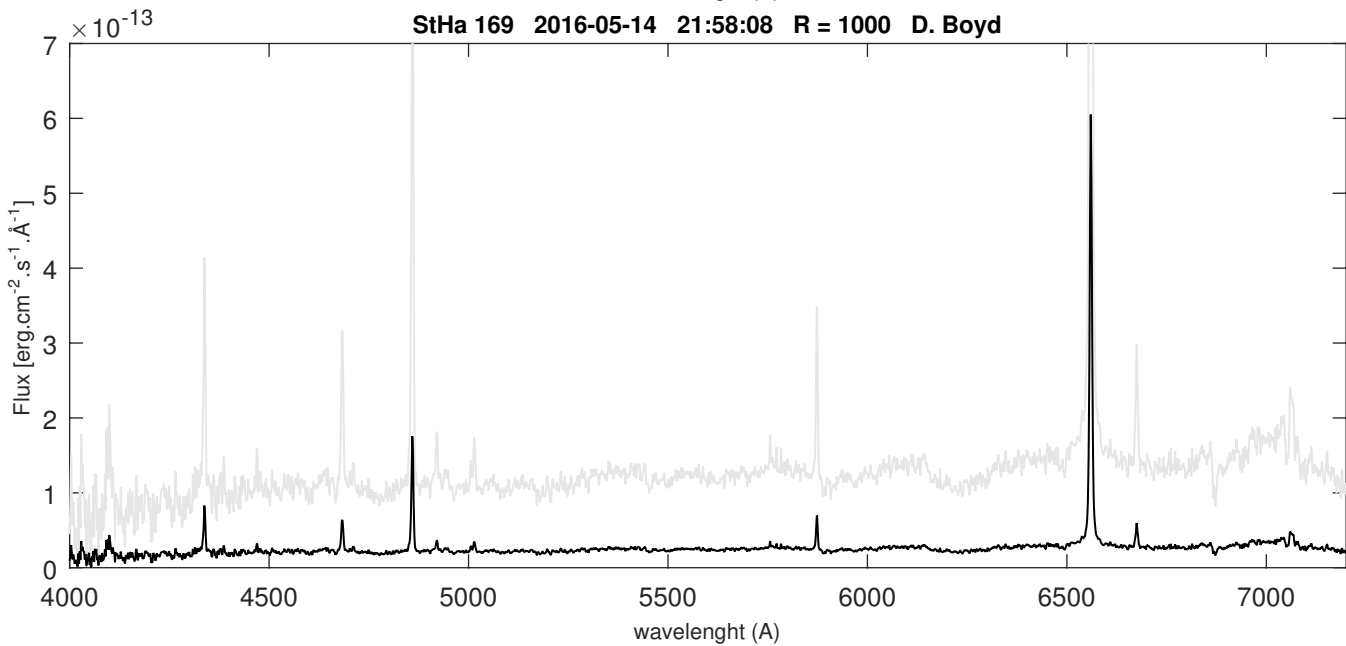
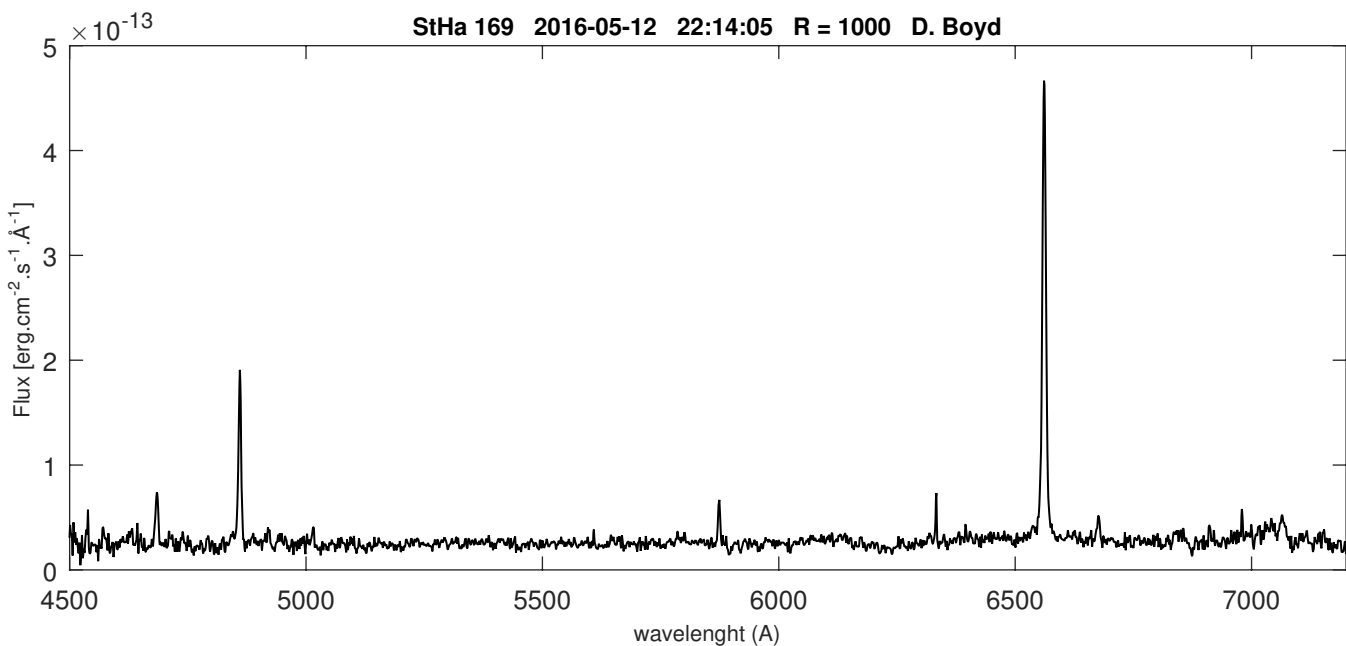
R.A.	14 16 34.3
Dec	-21 45 50.2
Mag	



StHa 169 High state

Coordinates (2000.0)	
R.A.	19 49 57.59
Dec	+46 15 20.58
Mag	12.6 - 13.7

StHa 169 has been detected in outburst by U. Munari & al. (See ATel #9036) at V = 12.8 (25-04-2016)
AAVSO lightcurve shows a point at V = 12.58 (21-03-2016) by Steve O'Connor
David Boyd obtained two spectra at R = 1000 during the decline. The V magnitude is respectively 12.9 and 13.0



more about StHa 169

StHa 169 is a poorly studied star

It has been discovered as an H alpha emission star by Stephenson (1986) and classified as an symbiotic star by Downes & Keyes (1988) - see above. It is included in the catalog of symbiotic stars (Belczynski & al., 2000)

The symbiotic nature of StHa 169 is contested by G. Ramsay & al. (2014). From Swift and Kepler observations, they deduce that StHa 169 is a binary consisting in a relatively main sequence hot star (~10000 K, late B or early A) producing He II emission and a red giant star (~ 3700 K) with a mean period of 34 days.

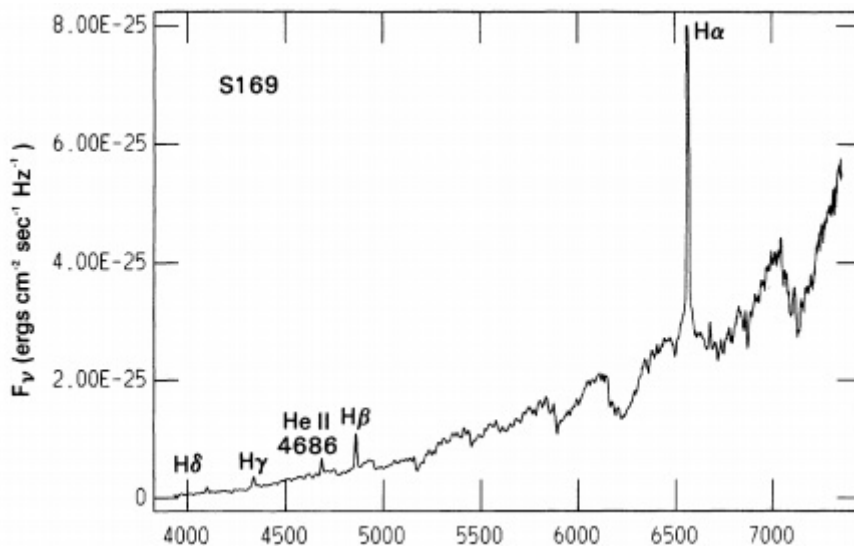
More observations are needed ... both photometry and spectroscopy (a good target for LISA and "large" amateur scopes 14 to 20")

Comments from Steve

Never forget that what we observe in spectroscopy is the atmosphere only as deep as the photosphere. That is, the absorption and emission lines formed within the optically thin strata of the envelope -- that part we call the atmosphere, whether of a star, disk, or even cloud. The deeper layers, that are conventionally called "envelope" is where at *any wavelength* the optical depth exceeds about unity. So imagine you have somehow scooped up a quantity of stuff, with some arbitrary chemical composition, and placed it on top of a gas sphere (in our case, a white dwarf) with consisting of a pure helium or carbon gas. The layer can reach mechanical balance, and look just like an atmosphere, if there isn't any mixing. If the composition is light, and the temperature perhaps higher than the interior, it will not buoyantly mix, and even diffusion won't happen. Even if there's a kind of violence to the accretion, like a boundary layer in an accretion disk, nothing will mix deep enough to alter the mean composition of each portion and for a low enough temperature *you won't see the helium lines*. So if a layer with a column density of hydrogen of around 10^{25} cm⁻² or more is layered on top of a low mass helium WD, you wouldn't know that the underlying star was actually pure He. The higher the molecular weight of the accreted matter the larger the opacity and the more likely the buoyant mixing if it can cool. But if the temperature, as in this case, is only around 10⁴K, there's no reason to expect any signatures of the degenerate star {it unless it is more massive and a CO or ONe star}, as in novae. If no active mass transfer is now occurring, or if there's a low enough luminosity that the RG wind absorbs all of the XRs and UV, you would -- again -- never know what the underlying star is. Keep in mind, these systems are called *symbiotic* because they have combination spectra but, in a more physical sense, they also share common environments.

The only published spectrum of StHa 169 (Downes and Keyes, 1988)

S169. Figure 4 displays the spectrum of this star. The Balmer lines, as well as He I λ 5876, λ 6678 and He II λ 4686 are clearly present, but no λ 6830 feature is seen. The cool continuous spectrum is slightly later than that of S164. Apart from the presence of He II, this spectrum resembles that of the quiescent phase of the symbiotic recurrent nova RS Ophiuchi.



Red giant pulsations from the suspected symbiotic star StHA 169 detected in Kepler data

Ramsay, Gavin; Hakala, Pasi; Howell, Steve B.

Monthly Notices of the Royal Astronomical Society, Volume 442, Issue 1, p.489-494

New H-alpha emission stars found above 10 deg galactic latitude

Stephenson, C. B.

Astrophysical Journal, Part 1, vol. 300, Jan. 15, 1986, p. 779-784

Spectroscopic observations of H-alpha emission stars from the Stephenson and Stephenson-Sanduleak lists

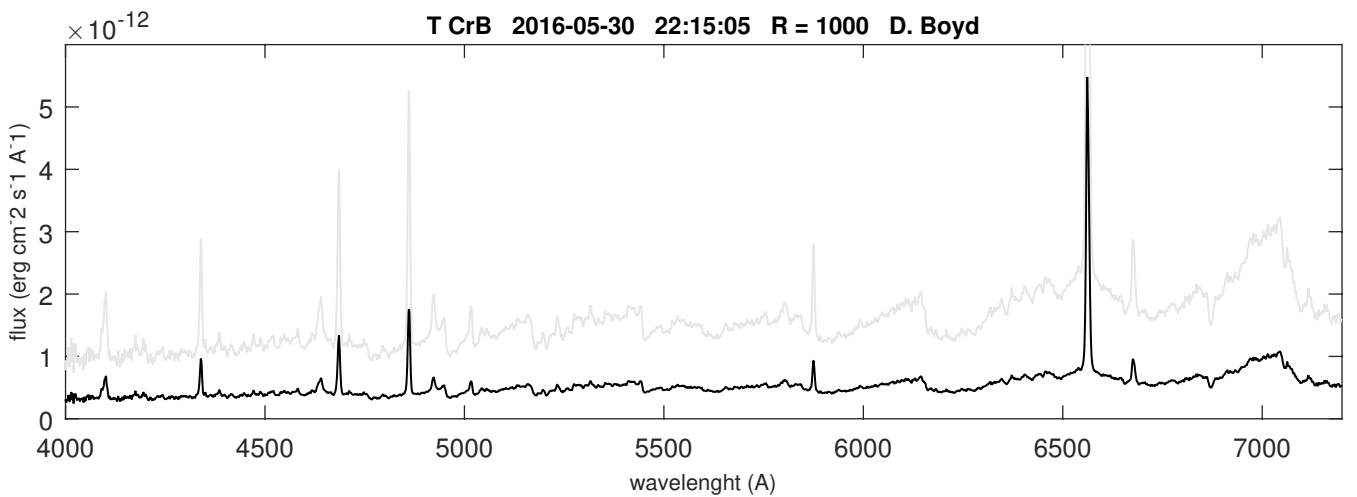
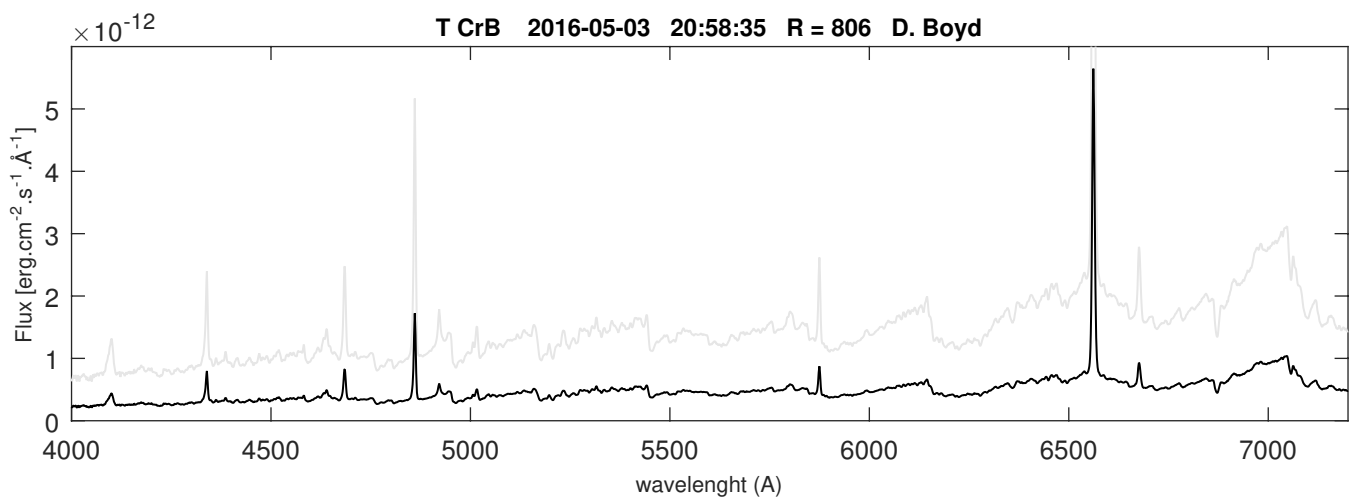
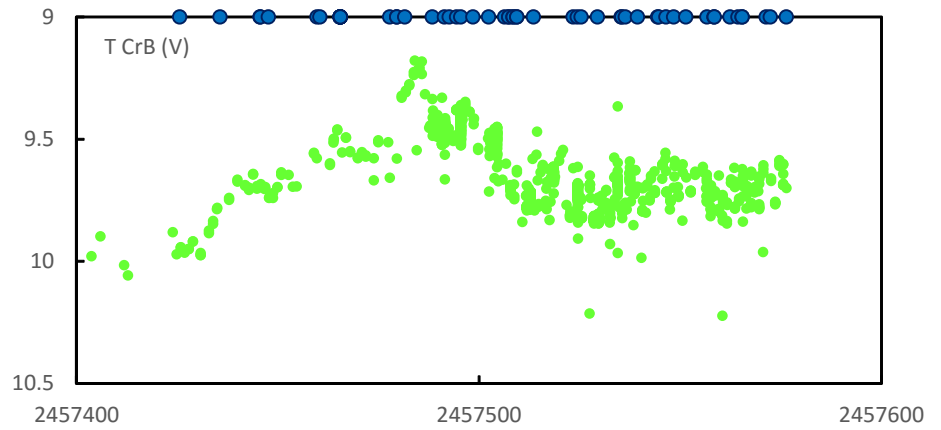
Downes, Ronald A.; Keyes, Charles D.

Astronomical Journal (ISSN 0004-6256), vol. 96, Aug. 1988, p. 777-790

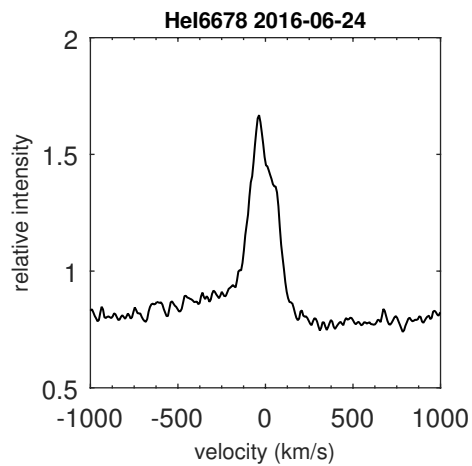
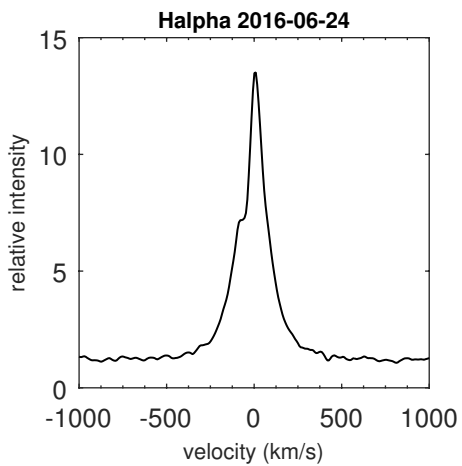
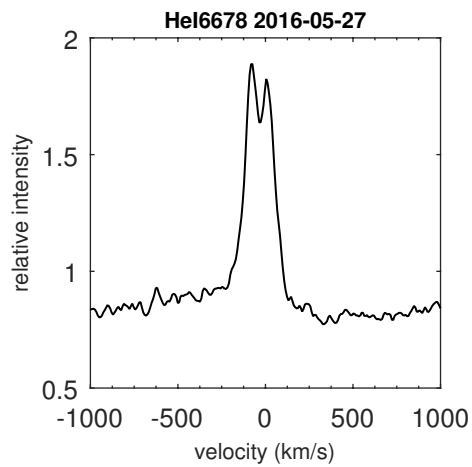
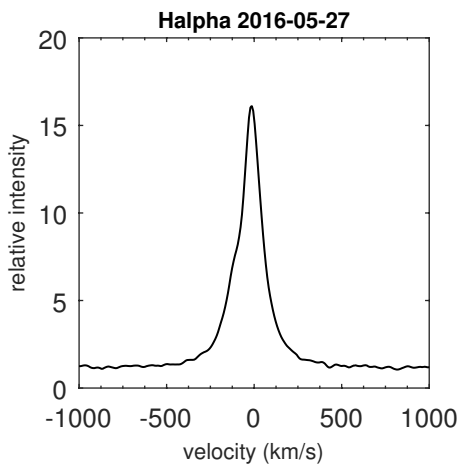
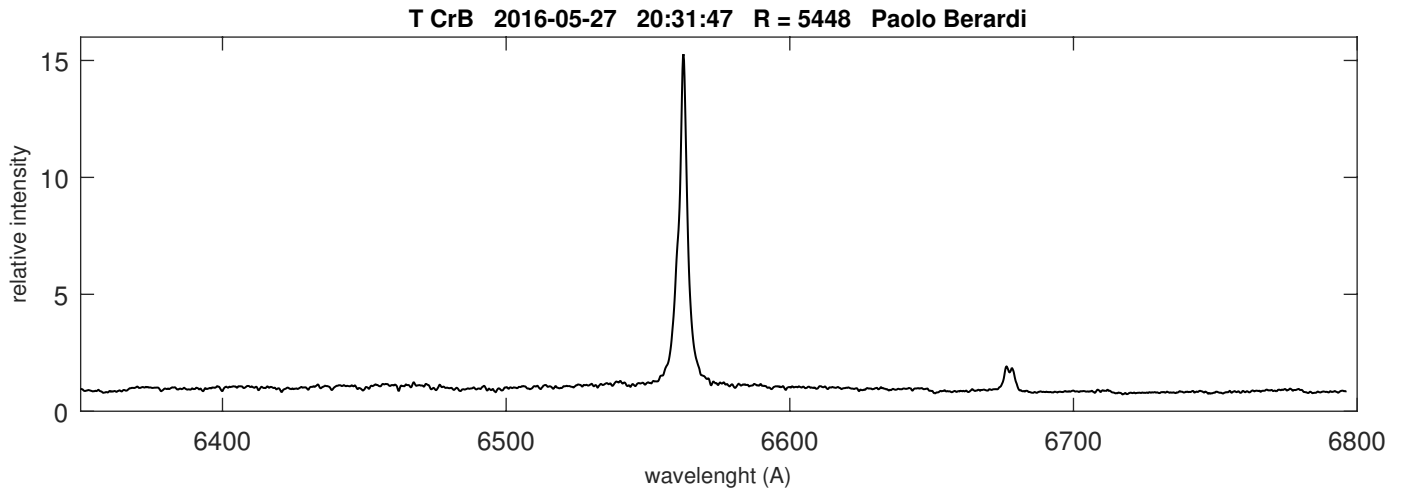
T CrB

Coordinates (2000.0)

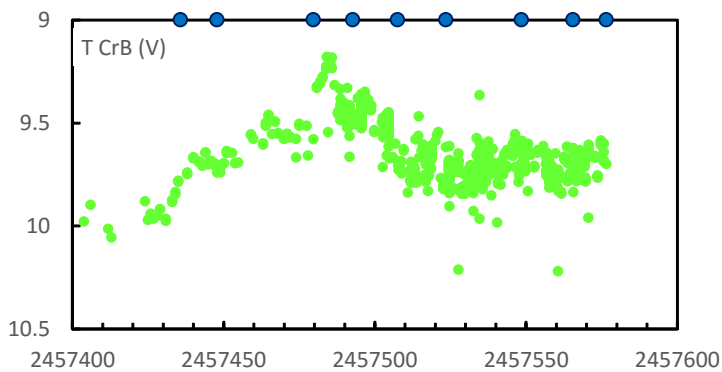
R.A.	15 59 30.2
Dec	+25 55 12.6
Mag	9.7 (V)



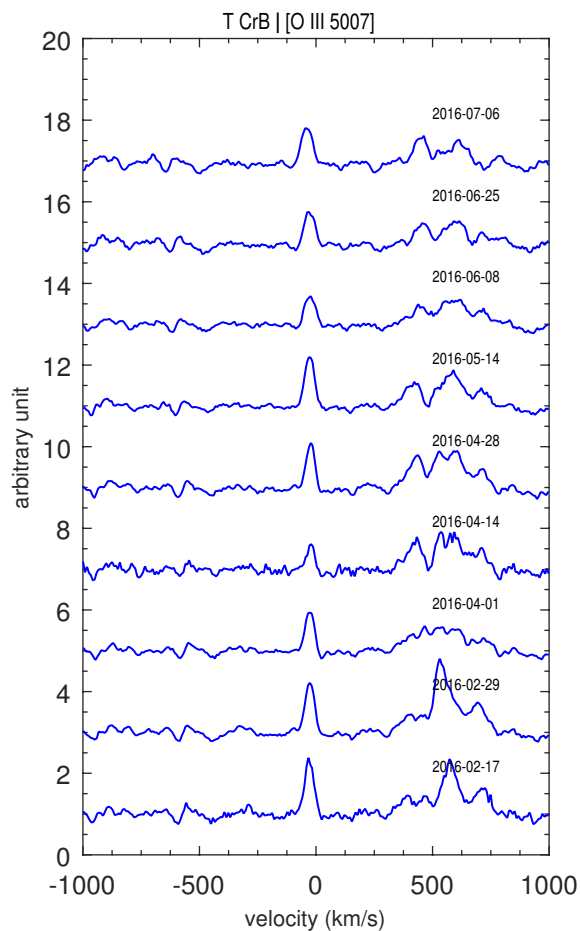
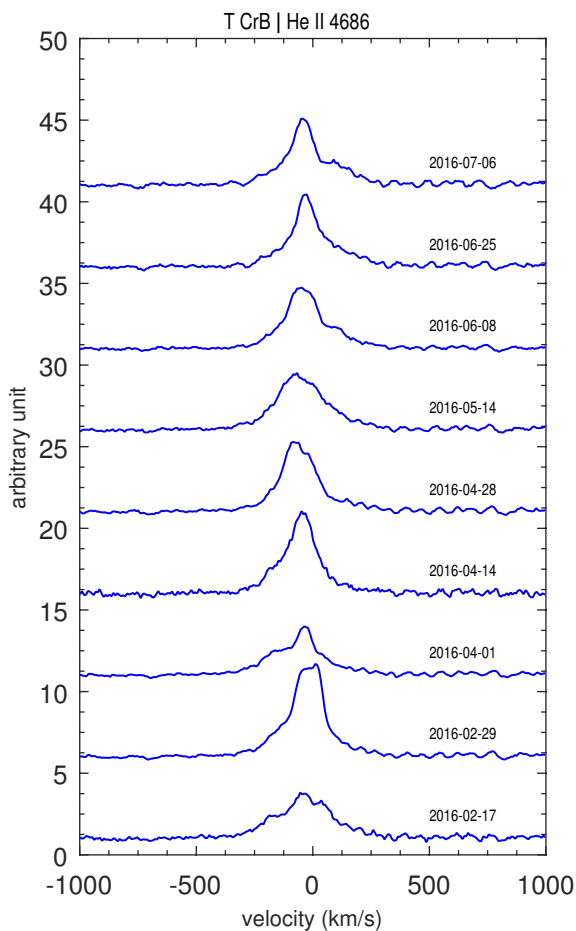
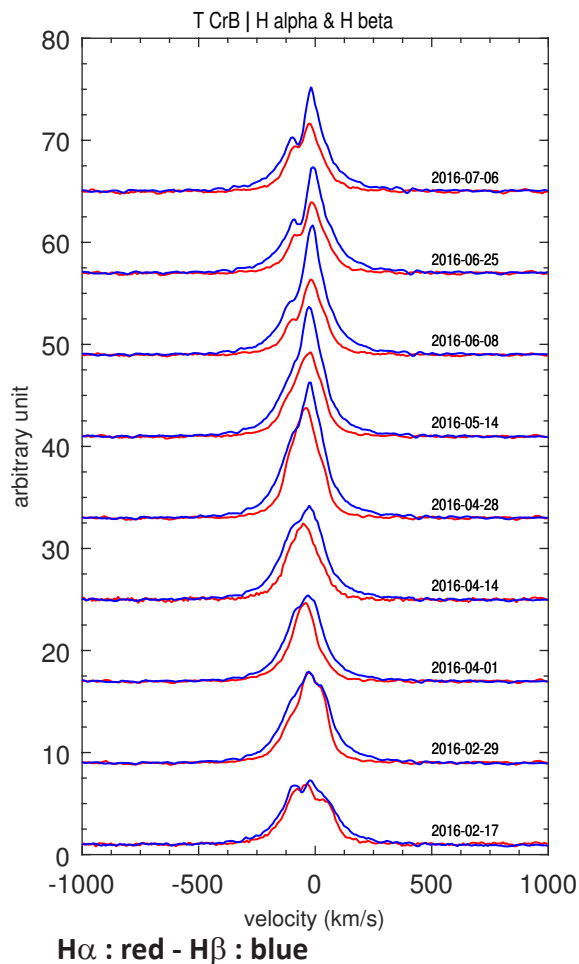
H alpha region by Paolo Berardi with Lhires III at R = 6000 (1200 ln/mm)
in May and June



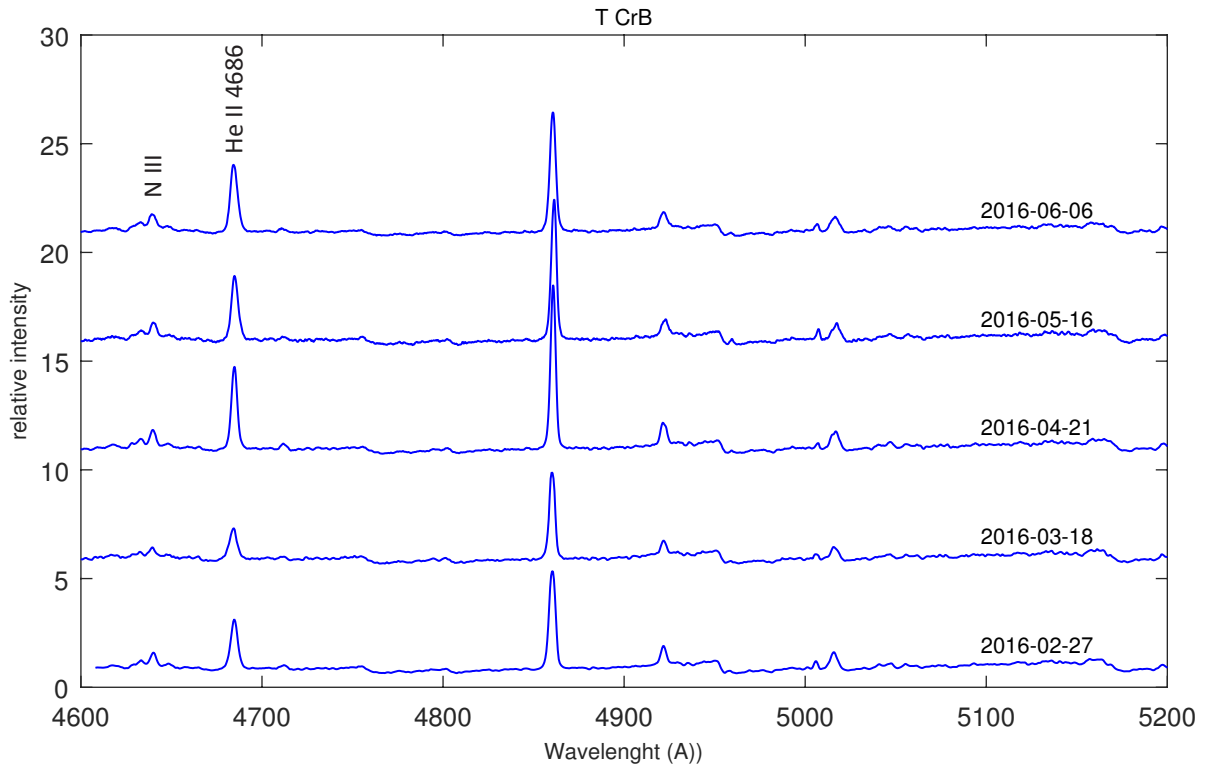
T CrB in 2016



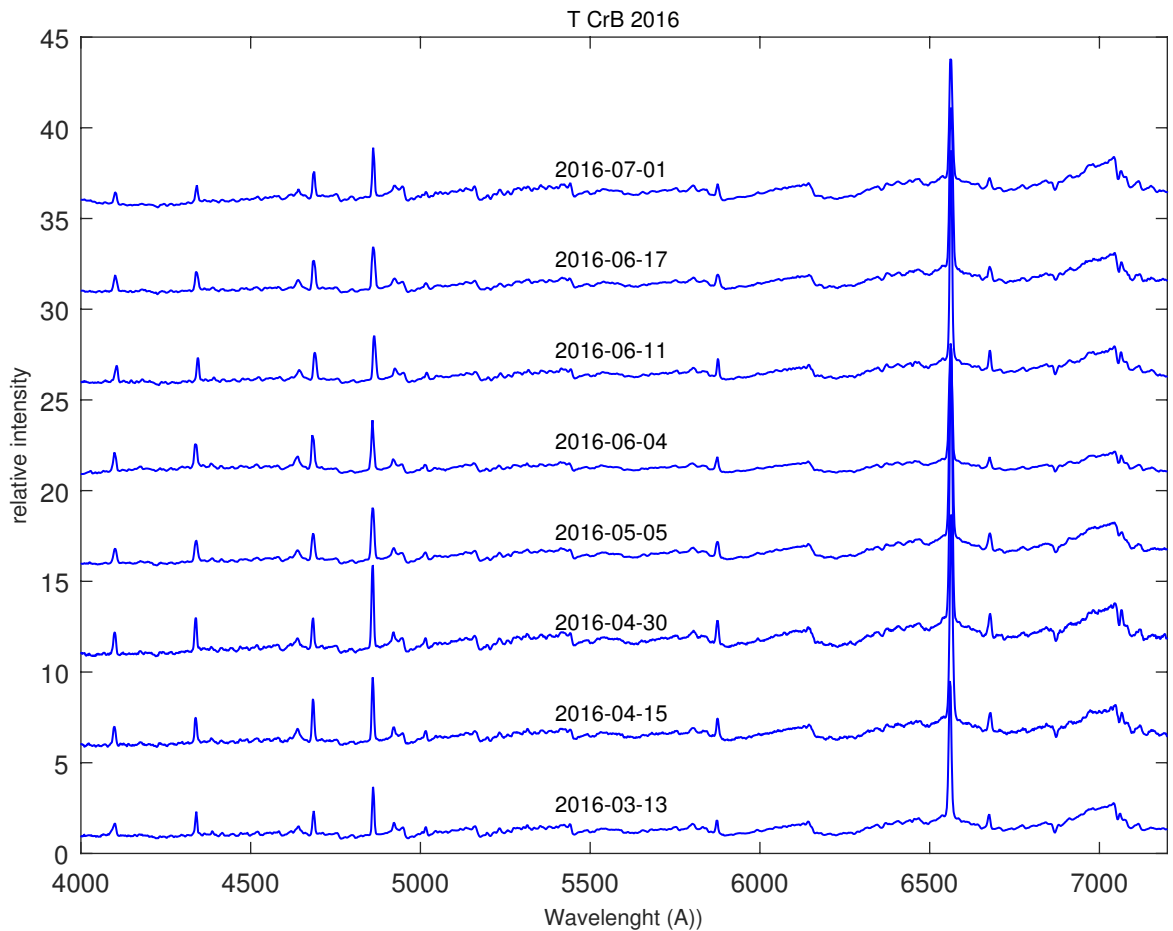
Lines evolution in 2016
Echel spectra (R = 11000)
F. Teysier



T CrB



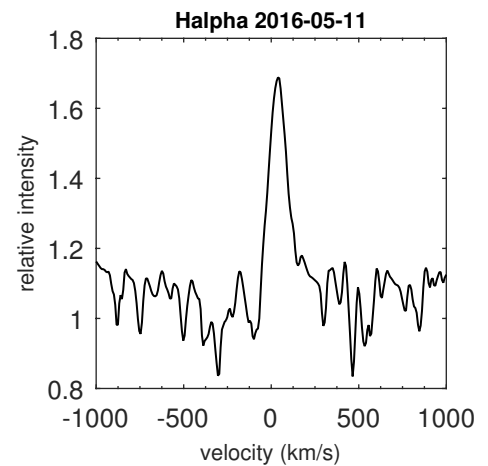
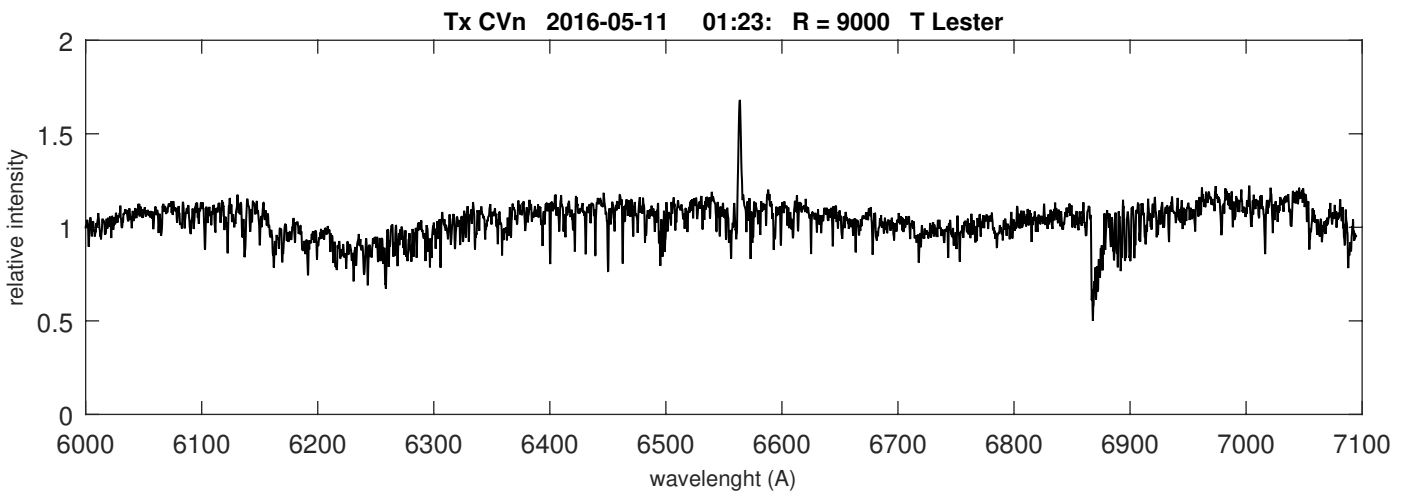
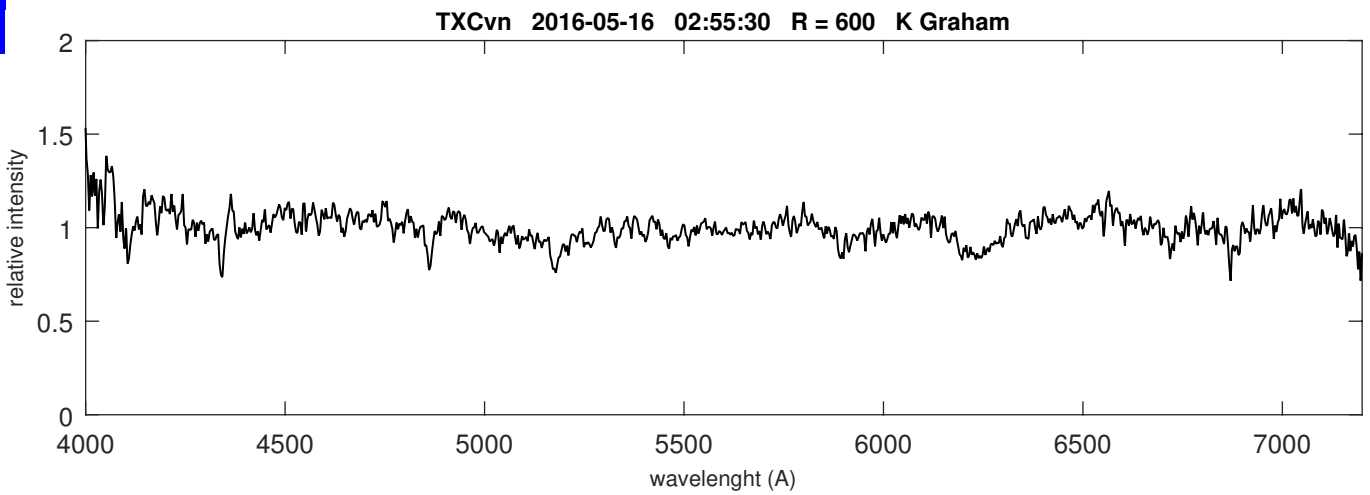
H β region by P. Somogyi - Lhires III 600 ln/mm - R = 2500
NIII blend : NIII 4634 OII 4639 NIII 4640 NIII 4641 (See Munari & al., 2016)



Sample of low resolution spectra (R = 600 to 1000) obtained in 2016 by J. Guarro, F. Campos, J. Montier, L. Franco, K Graham, C. Kreider

TX CVn

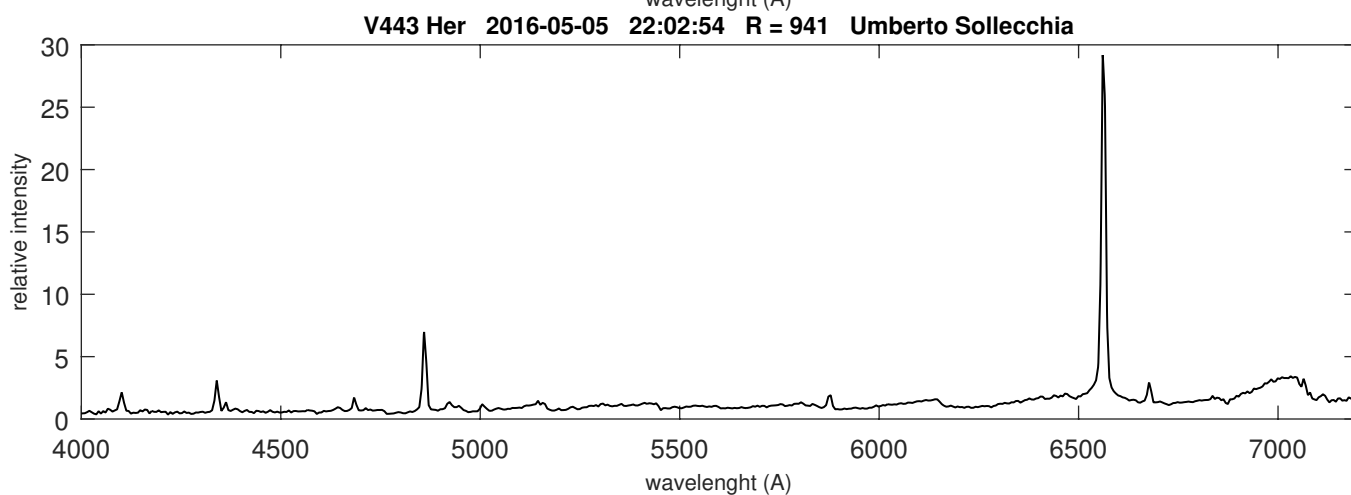
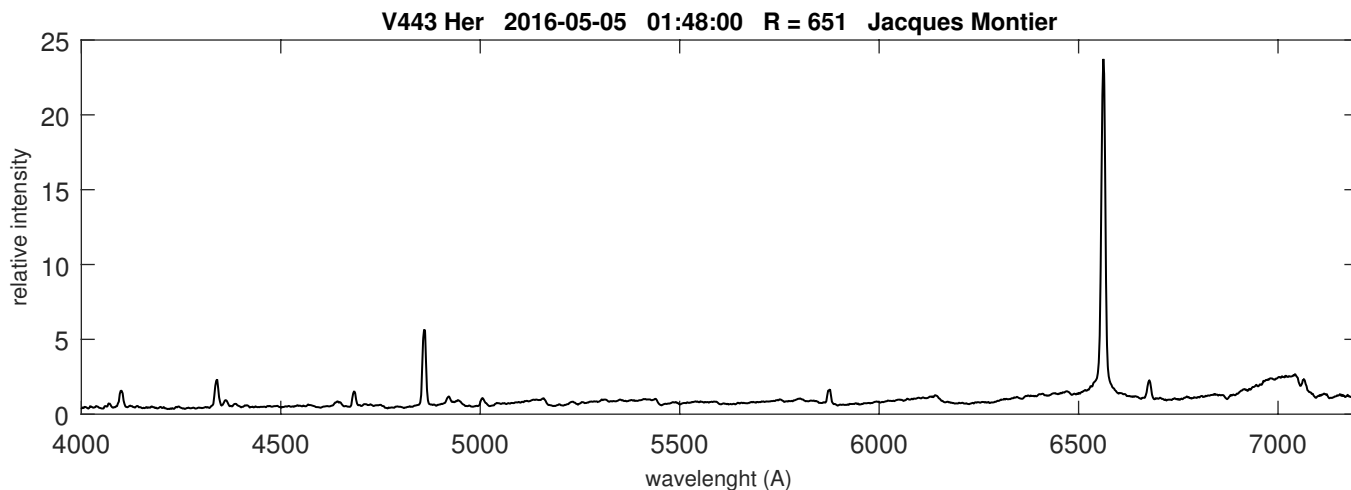
Coordinates (2000.0)	
R.A.	12 44 42.0
Dec	+36 45 50.7
Mag	10 (04-2016)



V443 Her

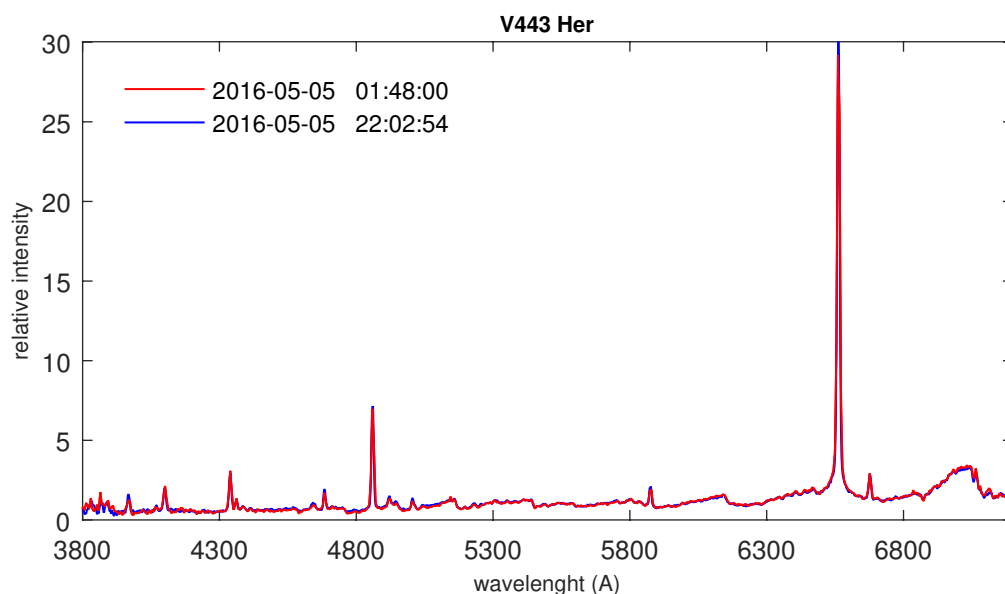
Coordinates (2000.0)

R.A.	18 22 07.8
Dec	+23 27 20.0
Mag	~ 11.5



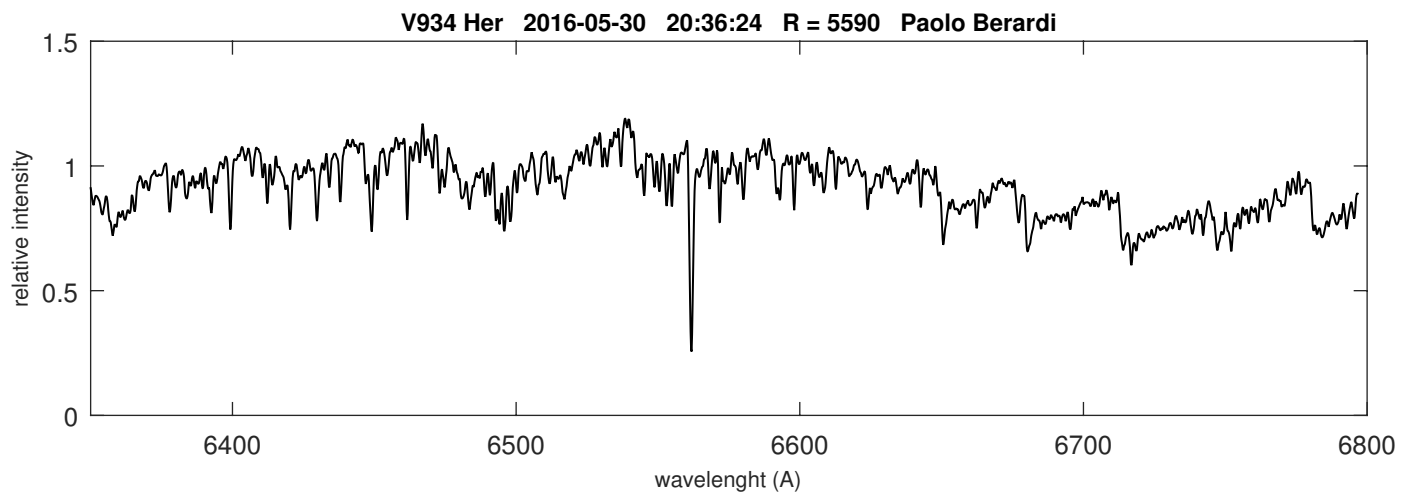
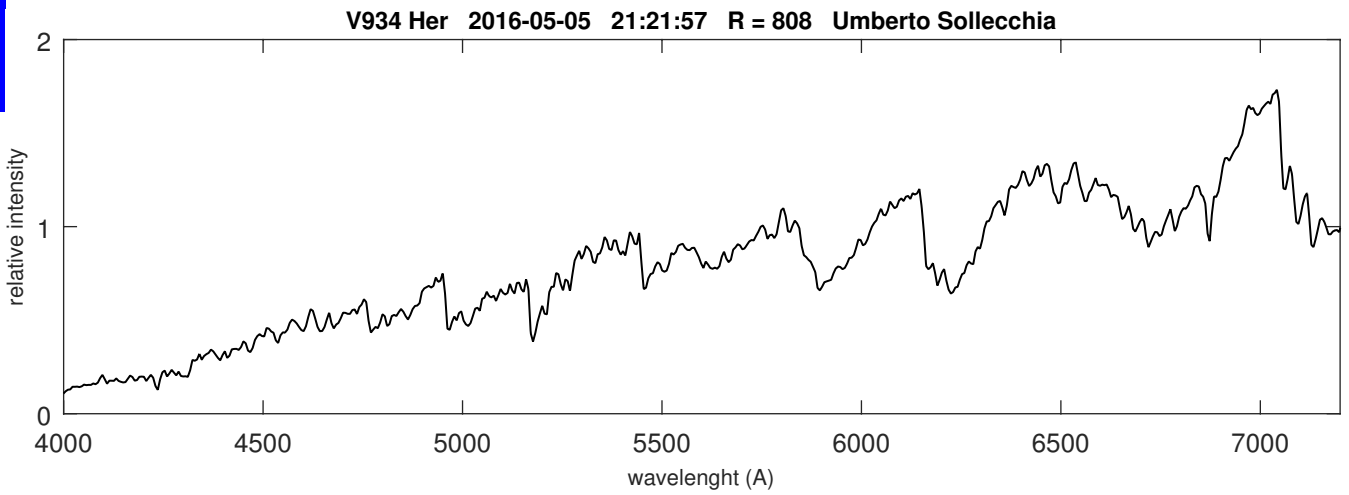
About the quality of spectra in ARAS Database

Comparison of the spectra of V443 Her obtained the same day (20 hours difference) by Umberto and Jacques and processed with ISIS Very good spectral calibration and excellent instrumental/atmospheric correction

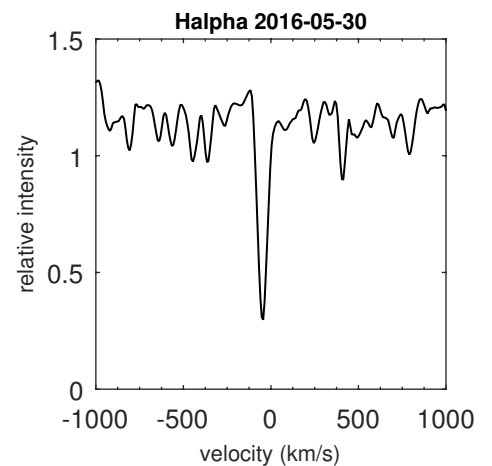


V934 Her

Coordinates (2000.0)	
R.A.	17 06 34.5
Dec	+23 58 18.5
Mag	~ 7.5

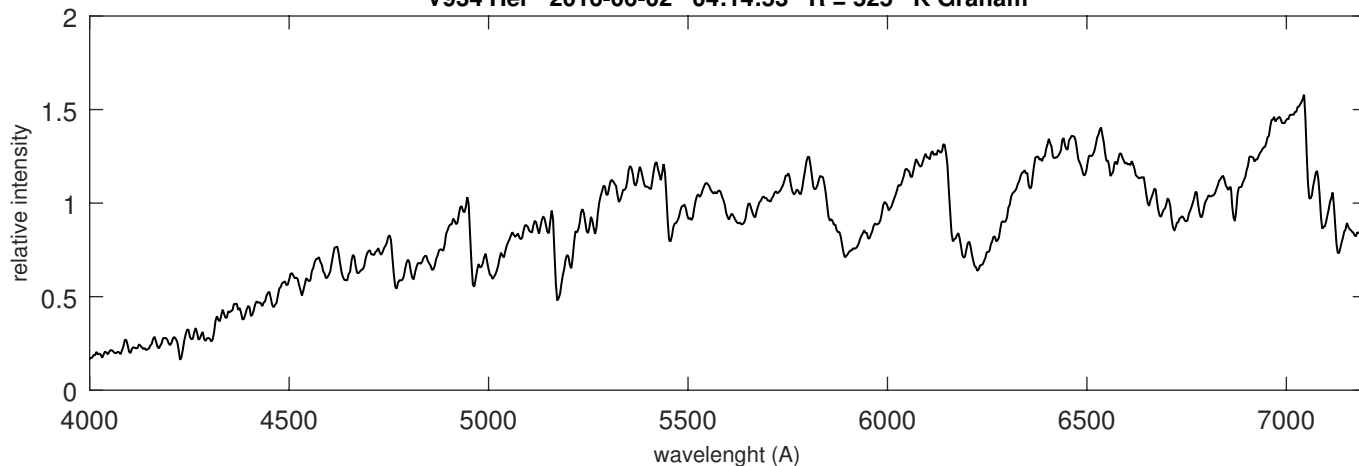


H α region by Paolo Berardi with a Lhires III 1200 l/mm at R = 5500 and crop on H α absorption line

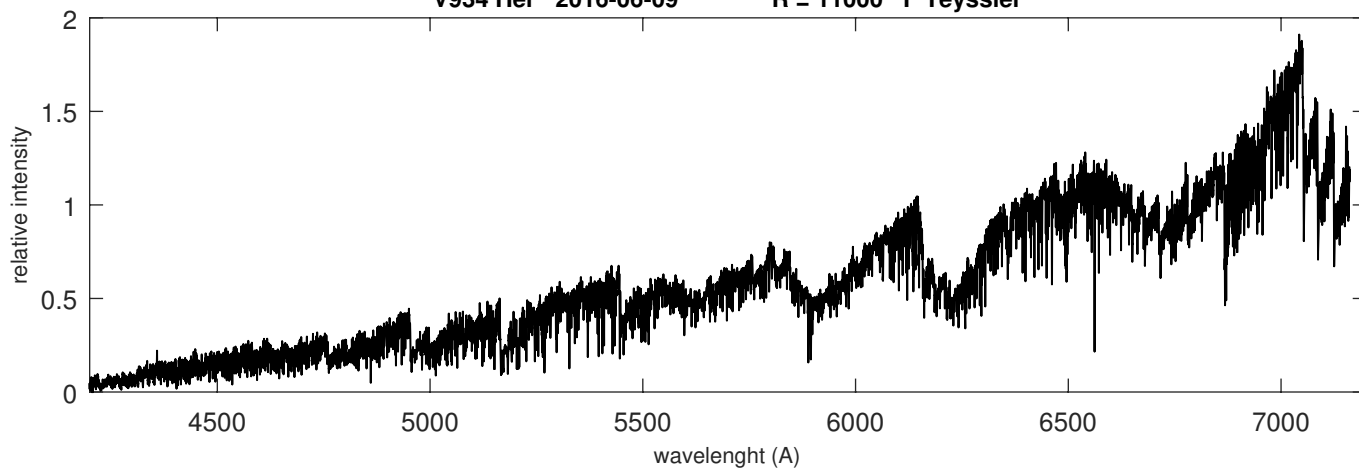


V934 Her

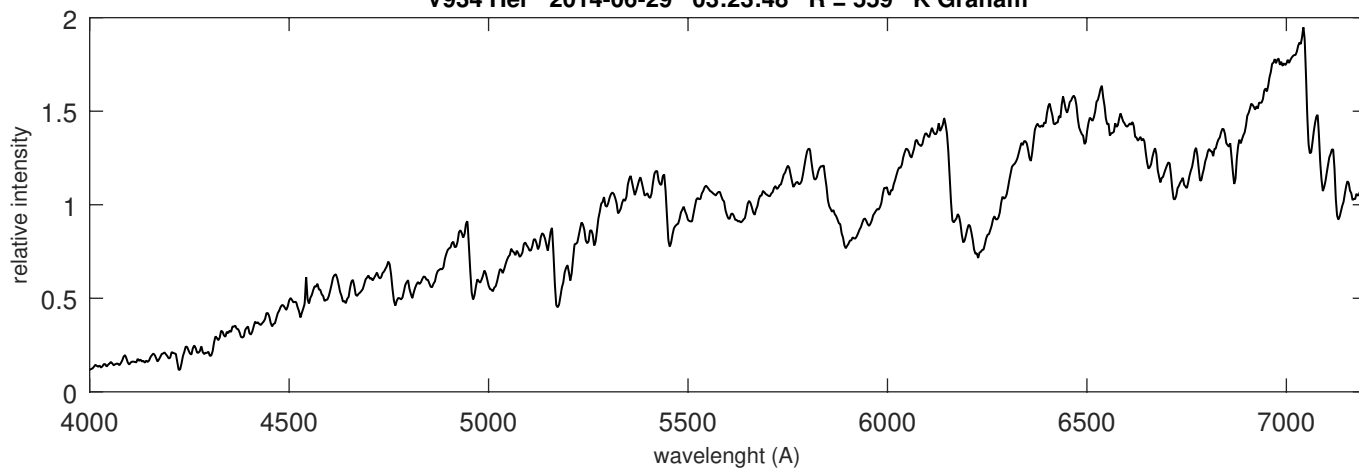
V934 Her 2016-06-02 04:14:53 R = 525 K Graham



V934 Her 2016-06-09 R = 11000 F Teyssier



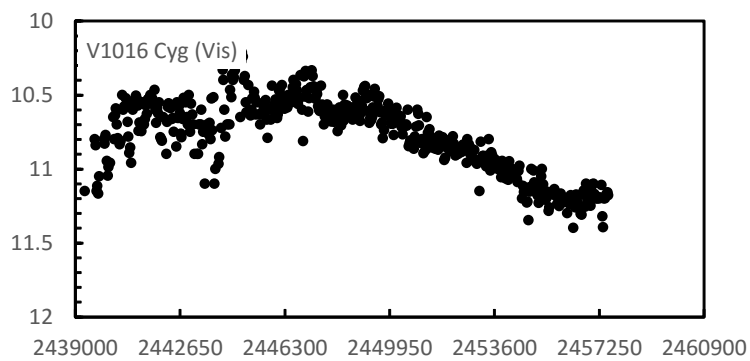
V934 Her 2014-06-29 03:23:48 R = 559 K Graham



V1016 Cyg

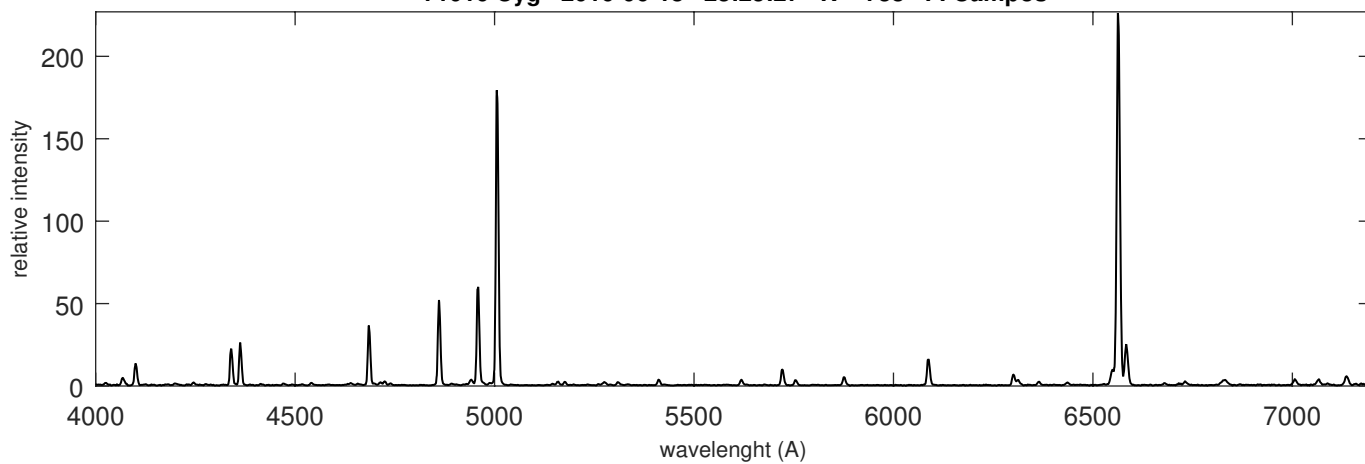
Coordinates (2000.0)

R.A.	19 57 05.0
Dec	+39 49 36.3
Mag	11.7 (V)



AAVSO Visual lightcurve (30 days mean) since 1966 showing the very slow symbiotic nova outburst of V1016 Cyg

V1016 Cyg 2016-06-18 23:25:27 R = 738 F. Campos

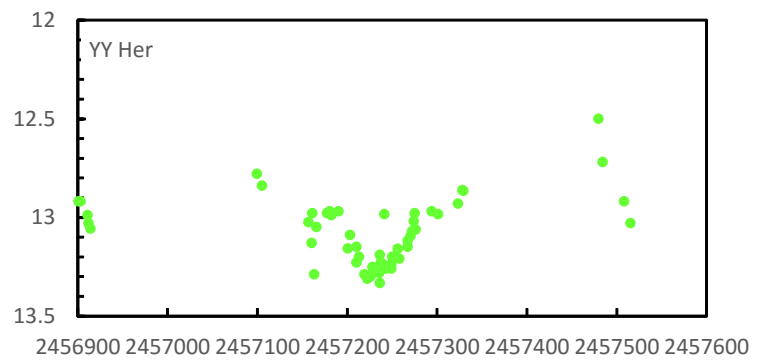


YY Her

Coordinates (2000.0)

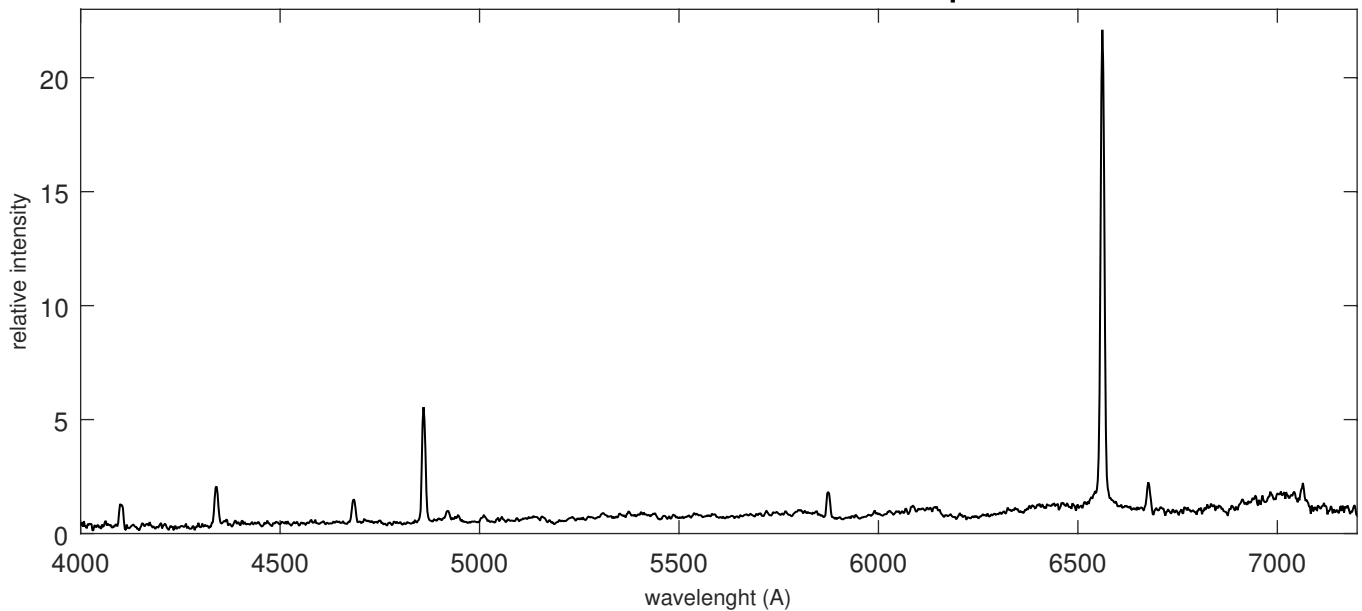
R.A.	18 14 34.19
Dec	+20 59 21.3
Mag	12.5 - 13.3 (V)

The classical symbiotic YY Her returns to quiescence after an outburst
Jacques Montier obtained a spectrum (Alpy R = 600) at mag 13



AAVSO V band - June 2014 to June 2016

YY Her 2016-05-05 02:35:31 R = 641 Jacques Montier



1 Some analysis techniques and ideas

We have discussed the line formation in many astrophysical systems, such as binaries and novae and winds, but perhaps it will help now to suggest some different sorts of physical questions you can ask and processes you can study that will be both interesting and very much scientific research. In this and a few more columns, I'll try to provide some more general things you can do with *any* spectra. Don't worry that there are more details (and equations) than before. For those who might want to program I'm putting in more details. For others, the measurements are simple and the methods are algorithmic so don't be put off by the level. You've been through so much in our years together, you can do it! I want to follow up on Peter Somogyi's excellent comments and procedures. Once you have the data in hand there are a lot of important questions you can ask yourselves and see how the astrophysics comes out of what you're doing. To drive the point home: you are more astrophysicists than *many* of the professionals and it won't take much to go to the next level, if you feel the urge.

1.1 Line profiles

For outflows or ejecta, P Cygni profiles form when there is optically thick material along the line of sight to a deeper part of the line forming region. In ejecta, as we've discussed, there's a maximum but not *terminal* velocity so the absorption decreases monotonically with increasing (negative) radial velocity. In a wind, there's a maximum and terminal velocity, they're the same, and the line saturated if the column density is high enough and forms the sharp terminal edge of the classical picture. If the region that's seen in projection against the deeper layers (or stellar surface) covers only a small fraction of the solid angle available for the line formation, the absorption will be weak and not seen at the highest velocity- the line will be asymmetric but may even lack a discernible absorption component. So you can make some preliminary guesses based only on the visibility of the absorption relative to the emission.

Measuring the absorption velocity, or the wings, does not result in a unique picture. The red wing is often ignored but that is as important as the blue side, the emission is from the whole volume and for ejecta there's important information there. Quote the Full Width Zero Intensity (FWZI) of the line at the continuum *at the point where the signal to noise allows you to say there is emission*. Then give the velocity centroid wavelength. See the next section for what that means based on the profile. Don't assume the peak is the zero velocity. For very optically thick flows or ejecta, it's always redshifted since the absorption component has its own line profile and absorbs against the whole flow (approaching and receding). The asymmetry of the line is measured in the same way as the mean wavelength from the *skews* or "third moment".

If the line is formed from spherically symmetric pure scattering (not likely) the total equivalent width (absorption + emission) will be zero (as much is removed as redistributed into the line). But in general, the line has some real absorption (collisional effects) so the EW will always differ from zero. Note that the EW is a relative measure, how much more flux there is in the line relative to the continuum so you have to normalize the value to the photometry to get a meaningful quantity. This means taking the lines and producing artificial photometry. This is going backwards from how you've calibrated the spec-

trum but it allows you to say how much flux is coming out from the line forming region. If F_i is the flux in pixel i and S_i is the filter profile (normalized to unity at peak transmission) then the flux in the filter is

$$F_{\text{int}} = \sum_{i=0}^{N-1} F_i S_i \Delta\lambda$$

where $\Delta\lambda$ is the pixel wavelength increment (and flux is in wavelength units). Then this integrated flux is compared to the magnitude. If you used filters to get the fluxes, then the EW will tell you the relative contribution of the lines to the measured photometry. In Skopal's discussions this was mentioned but remember that the lines and continuum are not distinguished by filter photometry so be careful using photometric magnitudes to get fluxes. Use standard-calibrated spectra. Then with this information you can get the energy in the lines. The equivalent width is an integrated measure but if you use the profiles you can also indicate asymmetries. We discussed some time ago that the ratio of the line profiles is important for obtaining where different parts of the line are formed. You can interpolate the profiles to the same velocity intervals and then take the ratios digitally. This is really simple but, especially for the forbidden lines, it tells you how inhomogeneous the region is. For planetary nebulae, for instance, it's hard because the lines are narrow and may be unresolved (so use the EW). But at resolutions of 5000 or higher you can get velocity structures in some lines so it's worth the try. Keep this in mind: the density measured by the EW is a mean value over the whole line forming region. The individual parts of the profile, in velocity, can come from regions of very different local density (likely, though, the same excitation temperatures). So – and this is especially true for novae and Be stars – the ratios reveal the inhomogeneities.

1.2 Radial velocities

It seems that the radial velocity is one of the simplest things to measure, once you've obtained a linear set of wavelengths and, in general, that's right. But there are some complications that symbiotics, novae, and other freaks present. So a few thoughts are in order here. First, the lines are often not symmetric so the definition of a mean velocity is uncertain. Normally, you'd expect that taking the mean value of the wavelength (relative to the laboratory line center and denoted by brackets) would suffice,

$$\langle (\lambda - \lambda_0) \rangle = \frac{c}{\lambda_0} \left[\int (\lambda' - \lambda_0) F_{\lambda'} d\lambda' \right] / \left(\int F_{\lambda} d\lambda \right)$$

where the integral is taken over the line. If the data has been set in a linear grid, you can replace the integrals by the sum. Here F_{λ} is the flux (in counts if you haven't absolutely calibrated the spectrum) and the division is just to normalize the flux at each wavelength to the total flux in the interval. Remember that every integral is really a sum when implemented, so as an example, the mean is then:

$$(\text{mean}) = \sum_{i=0}^{N-1} \left[\text{any quantity at wavelength } \lambda_i \right] \times \left[\text{profile}(\lambda_i - \lambda_0) \right] / \sum_{i=0}^{N-1} \left[\text{profile}(\lambda_i - \lambda_0) \right]$$

Defining the line is actually a problem but that should be done examining the spectrum by hand or specifying the interval. Alternatively, if you know the width in velocity, you can integrate between velocity limits of the line. Similarly, $\langle (\Delta\lambda)^2 \rangle$ defines the dispersion without force-fitting a Gaussian profile. Remember, you do not always know the form of the line and, unless it is unresolved and dominated by the line spread function (lsf, the one dimensional analog of the point spread function) of the spectrograph. The skew, the simplest measurement of the line asymmetry, is the third moment. The difficulty arises from the noise. Characterizing the quality of the spectrum where there are no lines requires

measuring the continuum fluctuations in a lineless part of the spectral interval, near the profile you want to study. Since there really isn't such a region, or at least it's difficult to define depending on your resolution, the alternative is to look in the wings of the line and measure the mean fluctuation there. This is your "noise". In fact, if you chose the interval poorly, e.g. it's too broad, you have no net flux but the dispersion (because of the weighting) may be negative. No, that's not possible, so the mean (the integral) is dominated by a part of the line (in the far wing) where there's also no signal. To get around this, be sure to measure the noise after reduction, not from the raw image of the spectrum. A sufficiently high count will suffice, say a maximum of about 1000 counts, which has a S/N ratio of about 30. The signal accumulates linearly in time, the noise (for statistics dominated by the rate of photon arrival within a single time interval and how it lands on a pixel. The rate is a *Poisson* process, meaning all detections are statistically independent. The mean rate of arrival is the number of counts per unit time so for a fixed arrival rate, the expected fluctuation in the counts is

$$S \sim R \cdot \Delta t \text{ and } N = (R \cdot \Delta t)^{1/2} \quad (2)$$

so the S/N ratio increases as $(\Delta t)^{1/2}$. You can check your estimates of the continuum fluctuations relative to any emission line (for which S/N is inevitably higher). So what does this have to do with v_{rad} ? To specify the uncertainty in the velocity, you are not putting a cursor by hand on the line. You're trying to do this automatically, in an unbiased way. But the lower S/N, the more likely an error in the mean. You see, this is what the eye does rather well, averaging over the noise, provided S/N is high enough (S/N \approx 30 is just fine). The essential point is that you must demonstrate that your measurement is statistically real.

1.2.1 Correlation methods

While the method of cross (or self-) correlation works well for late type stars for which there are a gazillion lines, for hot stars it doesn't work quite so well. Take two spectra, (S_1, S_2) that have wavelength vectors λ_1, λ_2 . These may not be the same. So first you need to interpolate them onto the same grid. With this, the cross correlation is the shift in the spectrum. This is written in continuous form as a folding or convolution where you take F_1 and F_2 to be the two spectra:

$$C_\lambda(\Delta\lambda) = \int_{-\infty}^{\infty} F_1(\lambda + \Delta\lambda') F_2(\lambda + \Delta\lambda - \Delta\lambda') d\Delta\lambda' \quad (3)$$

where we can replace the integral by the sum. The most important feature of this correlation is that *it doesn't matter if F_1 is shifted relative to F_2 or the opposite, the result is the same*. This is the convolution theorem, the heart of the method. There's a very (!) good reason for doing this. The spectrum contains a lot more information than a single line and the entire spectrum will shift because of radial velocities. Therefore, unless there are *differential motions* (e.g. from rotation, see the next section), the precision of the measurement improves as $N^{1/2}$ where this is the number of points you have on the profiles. So you get a far higher accuracy than you would either force-fitting a Gaussian or by trying to measure the line center by eye.

1.2.2 Reproducing the measuring machine

The alternative is, of course, to fit the center of the profile. For this, a technique originally developed for the *Grant comparator* is very helpful. This was a screw micrometer, with a reproduction accuracy of about 1-2 microns, that was used for photographic plates. The trace was projected by an oscilloscope (remember what those were?) and a mirror reflected the spectrum so there were

two opposing images that were cross-correlated by eye. This is really the same effect as the numerical method. You can achieve this by taking the two spectra, displacing them by some distance (from line center (that is, from the rest wavelength) and then shifting and multiplying them together recording the product of the spectrum for each shift summed over the interval you're interested in. This is what you're really doing in a convolution but without the reflection. The accuracy is, again, improved because the entire profile is used, not just the peak. The advantage of this method is its simplicity in implementation and its avoidance of an assumed form for the profile. Its main disadvantage is when the line is asymmetric, this produces (with all correlation methods) possibly spurious shifts. Thus a word of warning: **correlation methods should not be used for stellar winds or differentially shifted spectra.**

2 Physical properties from spectra: some ideas of what you can measure without resorting to detailed models

In past issues we've covered winds (everywhere), explosions (novae), and environments (e.g. symbiotics and AGN), and now there are some more subtle bits of astrophysics I hope to introduce. All of these will have broad applications, many are related to things you will have already seen in spectra. They're often left undiscussed when the broader issues of peculiarities (such as emission lines, outflows, long term variations) are covered.

2.1 Rotational velocities

It's hard to find a cosmic object that doesn't rotate but, usually, this is ignored in discussions of the stellar properties. It shouldn't be. I'll give a few examples of things that might make use of all of the techniques you've been developing to work with spectra, including calibrations of fluxes and wavelengths. I hope these will be interesting, they're not just exercises.

2.1.1 Measuring sunlight on planets, how the solar constant is monitored

Start with the planets. This is a good way to get a feel for what rotation does. With a slit planed across, say, Saturn (which is well laced now) you can cover the rings and planet simultaneously. Using a resolution as low as 2000, you'll see two features. The lines are mainly solar, from scattering and reflection of sunlight. After all, that's why the planet is shining, but instead of just measuring the difference between the ring and disk spectra (to bring out the methane band in the red, for instance), you can see in the image before extraction that the lines are tilted and those of the rings (for Saturn) are further displaced discontinuously at the inner boundary of the rings. The tilt is symmetric about the disk center (if the slit is properly aligned), indicating the radial velocity of the planet relative to you and the Sun (well, to your line of sight since the orbit is nearly circular). Integrating over the slit broadens the line because the full spectral shift is summed but measuring the line-by-line shift gives twice the projected rotational velocity. This is the reflected solar spectrum; if there were narrow features in the planetary spectrum you would see a differential shift (observable at the highest resolution) with the planet's lines having 1/2 the displacement. Using the angular velocity (the maximum shift), dividing by two, and using the rotation period you can find the radius of the planet in physical units; then using the angular diameter, you can derive its distance from the Earth. Then using Kepler's law, you know the distance from the Sun in AU so, finally, you can measure the solar constant

at the planet from its magnitude. You'll also get a feel for the effect of the atmospheric structure on the measurements since at the limb, because of scattering, the line profiles will be less distinct. This also serves as a cautionary tale: the integrated spectrum of a star is the sum of all surface contributions.

2.1.2 Stellar rotational velocities

Now for the problem for stars. Since stars are point sources, as you see them, their spectra are produced by integrating over their surfaces. The atmosphere has a temperature gradient and the lines form at different depths and are weighted differently because of their individual sensitivities to temperature and density. This is the general explanation of how limb-darkening effects the appearance of the spectrum. When you say a star has a temperature and spectral type, you're really saying that when viewed from an enormous distance .

If the star is rotating this isn't quite so simple. For slow enough rotation, when the centrifugal acceleration (in the frame of reference corotating with the star) is small relative to the surface gravity, the star is still nearly spherical. But the rotating gas ball isn't necessarily in solid body rotation. Look at any time lapse of Jupiter, for instance, and you'll notice that the equator has a far shorter rotation period than the poles, as does the Sun. This differential rotation can be

If, instead, the rotation period is the same everywhere, so-called solid body rotation, the radial velocity – relative to the observer – is constant on cylinders that are aligned on the rotation axis so the closer you are to the limb the higher the projected radial velocity (toward or away from you). But since the contribution to the line profile depends on the projected area, and that is effectively zero at the limb and maximal at the center, the resulting line profile is neither Lorentzian nor Gaussian nor any simple combination of the two (called a Voigt profile). Instead, each piece of the surface is such a profile but combined with every other part of the photosphere weighted by the area in which the angle (longitude) and wavelength displacement (Doppler shift) are interchangeable. So the result is a sum over all possible angles, producing a profile (derived by Unsöld (1955) and others)

$$P_{rot}(\Delta\lambda) = \frac{3}{(3+2u)\Delta\lambda_{rot}} \left\{ \frac{2}{\pi} \left[1 - (\Delta\lambda/\Delta\lambda_{rot})^2 \right]^{1/2} + u \left[1 - (\Delta\lambda/\Delta\lambda_{rot})^2 \right] \right\}$$

where $\Delta_\lambda = v_{rot}\lambda_0/c$ from the Doppler shift and u is the limb darkening coefficient¹. There is no other broadening here even if the profile is very complicated. It vanishes for $\Delta\lambda \geq \Delta\lambda_{rot}$. The final profile is then formed from the folding or convolution of the rotational profile with the whole spectrum:

$$P_{obs}(\Delta\lambda) = \int_{-\infty}^{\infty} P_{rot}(\Delta\lambda') F(\Delta\lambda - \Delta\lambda') d\Delta\lambda'$$

Again, this is the weighted sum of the flux (the full spectrum, every point is merged with others by this process). You might also think of it as a smoothing process. It is reversible in that, were you to be on the stellar surface, you would see only the emergent spectrum from the photosphere so you can, numerically, undo the effects of the rotation if the spectrum has a high enough S/N ratio.

The importance of this alteration of the spectrum is that the line profiles change in a characteristic way and their FWHM is now not that of a Gaussian but of the rotational profile when $\Delta\lambda_{rot} > \Delta\lambda_D$, where $\Delta\lambda_D$ is the thermal Doppler width of the line. It isn't difficult to satisfy this condition, e.g., almost all early type main sequence stars (A and earlier). One oddball is, sadly, Vega. This is actually a rapidly rotating star but the lines are incredibly narrow (essentially thermal only) but it happens

¹You will have seen this in any discussions of eclipsing binary light curves, it's the parameter (number) that encodes the temperature gradient of the photosphere and lower atmosphere and causes the departure from pure geometric ingresses and egresses.

to have its axis oriented along the line of sight (a nearly zero degree presentation to the observer).

One important thing. It relates to an old discussion on spectral types. The classification system depends on two main sensitivities of spectrum formation: the variation of line strengths and ionization ratios with temperature, and the line widths and ionization stages being sensitive to pressure (hence surface gravity) through the Stark effect on the strongest line wings. But there is another, less obvious contributor. That's rotation. Low mass stars, especially on the main sequence, are slow rotators – their periods of rotation are months, like the Sun. On the upper main sequence, in contrast, they're much more rapid, typically with periods of days. Combined with their larger radii, the photospheric spectra of massive stars are always affected by rotational broadening far more than those of lower mass. But since the classification criteria are calibrated using standards, not models, the spectral types already implicitly include the rotational broadening. This is one reason why models do not exactly reproduce spectra, they have to be appropriately broadened to achieve a match. For stars that are especially narrow lined, for instance because of their axial inclinations, the spectra may appear anomalous, the lines may seem too strong for their spectral type. You will have seen this in any discussions of eclipsing binary light curves, it's the parameter (number) that encodes the temperature gradient of the photosphere and lower atmosphere and causes the departure from pure geometric ingresses and egresses.

A particularly beautiful effect can be observed using even moderate resolution spectra during eclipses for some short period binaries. As the eclipse proceeds, first the blue- and then the redshifted side of the star is occulted. The wavelength of the centroid of the profile therefore shifts from the rest wavelength to the red and then reverses and shifts to the blue, in antiphase with the radial velocity of the eclipser, and the lines become asymmetric in opposite senses. This is the Rossiter-McLaughlin effect and is the best way to directly measure the rotational velocity of a star. The effect is enhanced for systems where the eclipsed star is a rapid rotator, e.g. U Cep (an Algol system with a $>300 \text{ km s}^{-1}$ B star eclipsed by a G giant). You can see this for resolutions >5000 for those systems that have rotational velocities $>150 \text{ km s}^{-1}$ and, depending on the brightness of the star and the duration of the eclipse, it is a way to study the variation of the rotation with latitude by comparing the predictions of a rigid rotator with the amplitude of the eclipse effect.

2.2 Line profile variations and what they mean: first comments

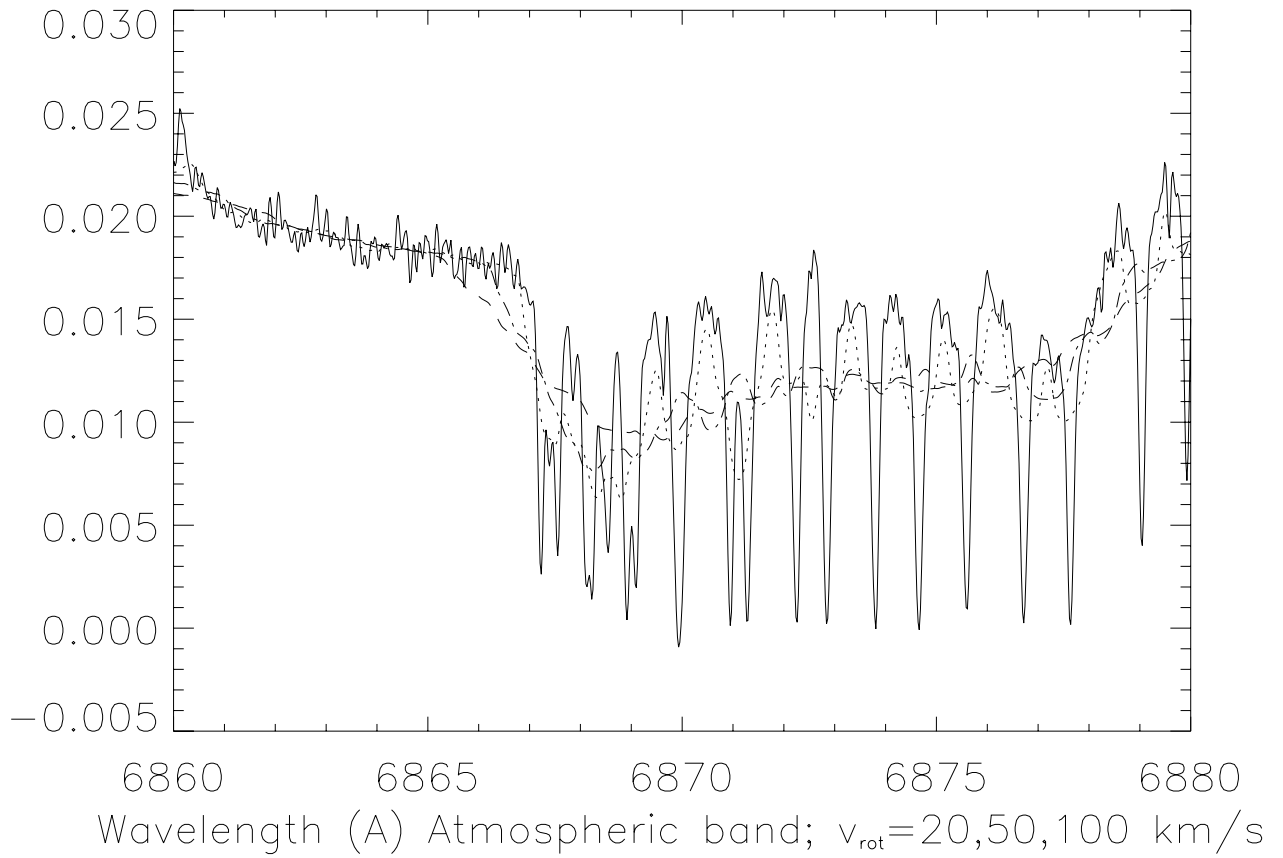
This is rather general because it's the heart of what you've been doing for symbiotics and novae and cataclysmics. But there are several methods that should be remembered. A method for enhancing emission line visibility is to remove the underlying absorption from the photosphere using a standard. This must be done very carefully, especially regarding the rotational velocity if the lines are narrow. You are actually making a physical assumption when subtracting one profile from another: the profile is assumed to be composite from two disconnected regions. For accretion disks or nebular environments (e.g. symbiotic stars) this procedure is physically fine but it doesn't work for winds. Stellar outflows begin in the photosphere and accelerate outward, they are really moving atmospheres and there are not disconnected regions. On the other hand, for disks (without outflows) this is a very good way to see whether weak features might be present. But remember that when you subtract two profiles, both of which are empirical, the S/N of the result is reduced since even if the means subtract, the dispersions add in quadrature ($\sigma_{\text{combined}}^2 = \sigma_1^2 + \sigma_2^2$ even if you take $I_{\text{combined}} = I_1 - I_2$). The match to the wings of a line, for instance the Balmer profiles, doesn't guarantee that the cores will be correctly removed. Magnetic fields can also lead to variations but not because of the Zeeman effect (with a very few exceptions

where the surface fields are so strong that the magnetic broadening of the line can be detected even without polarizers). For example, HD 215441 has a surface field of >30kG, about 105 times the solar value and more than 30 times that observed in sunspots. It is so intense that all the lines are broadened by the intense Zeeman effect although each is differently broadened because of different magnetic splitting terms of the energy levels. It is the same as we discussed for multiplets of atomic energy levels. The individual states are split by the magnetic field, linearly dependent on the field strength, B , by $\Delta\lambda_b \sin B$ but each line (transition) has a different numerical coefficient. The Ap (peculiar A stars) are the best ones to observe if you want to see what happens, especially the star I mentioned and some such as β CrB and α^2 CVn. But what's more important is the line variations, in profile and strength, happen on the rotation period of the star. So you can combine the rotational line measurements with the changes in line strength to get an idea of how the line is distributed over the surface of the star. The same method is used for spots, as in the W Uma stars and the RS CVn stars. Both show evidence for large scale concentrated magnetic spots, like those on the Sun but a factor of 100 larger in area (or more) that are dark and change the photometric properties (in eclipsing systems these cause light curve distortions that change phase relative to the eclipses over time because of spot migration). Since the surface is darker in the spot region (this doesn't seem to be true for the Ap stars but they don't have convective photospheres) then that part of the surface will not be seen in the spectrum and the line profile distorts. As the system revolves, and you see different sides of the star, you can form a picture of the surface. The technique is called Doppler imaging and it is well within the capabilities of your spectrographs. Even if the individual profiles don't change, the spectra do. This means even at low resolution you can obtain spectrophotometry and see how the light is redistributed through the spectrum.

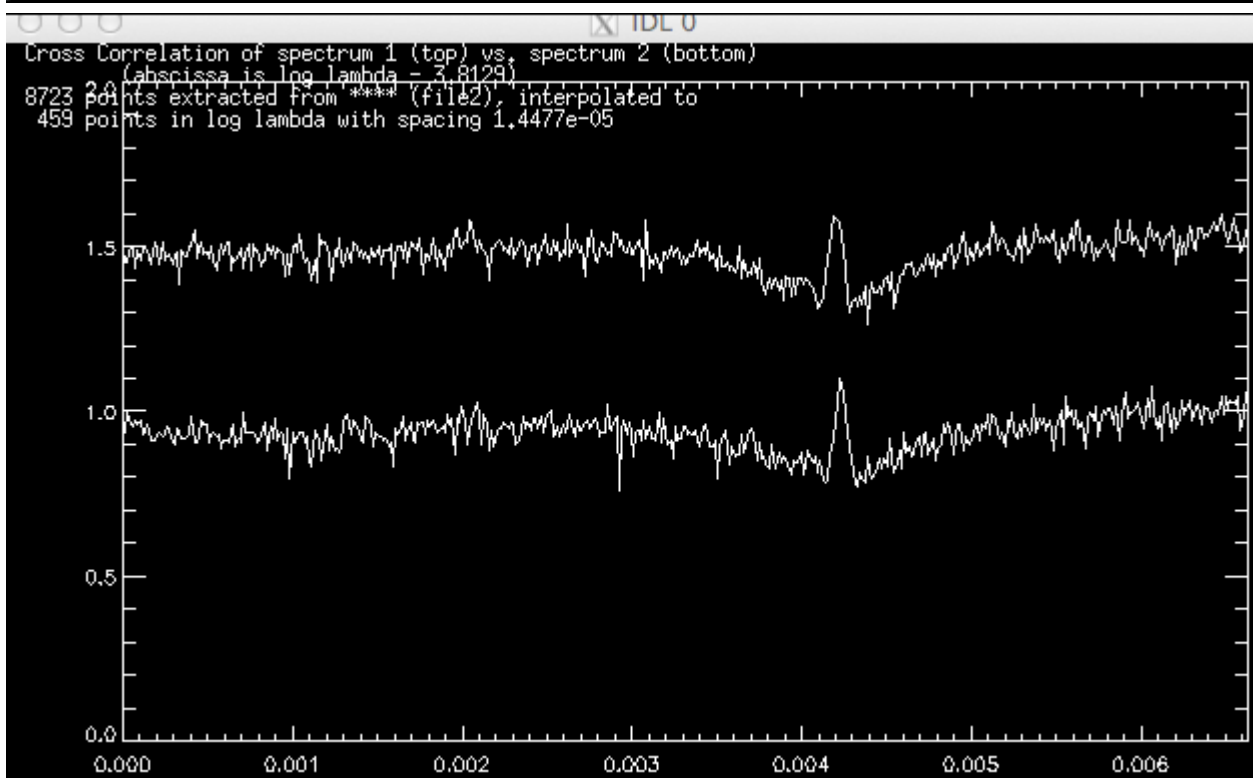
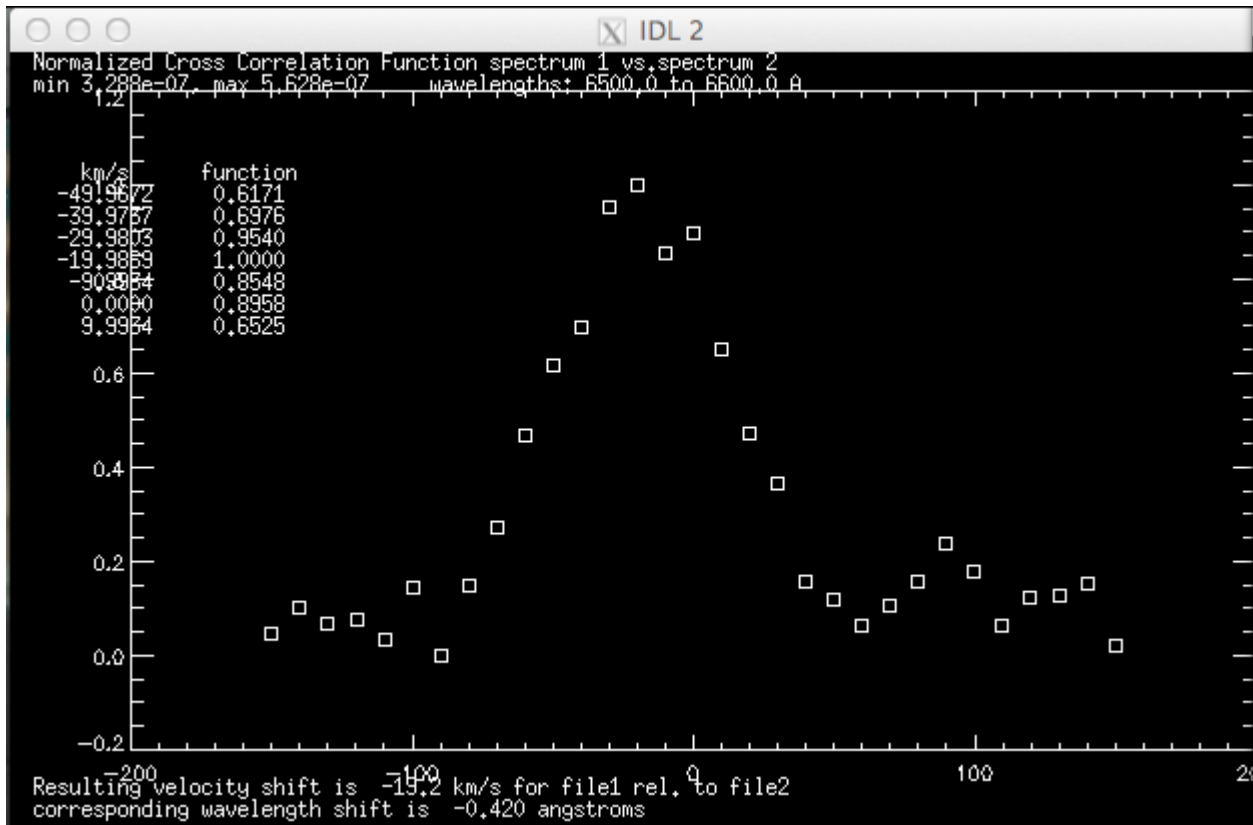
3 ... so ...

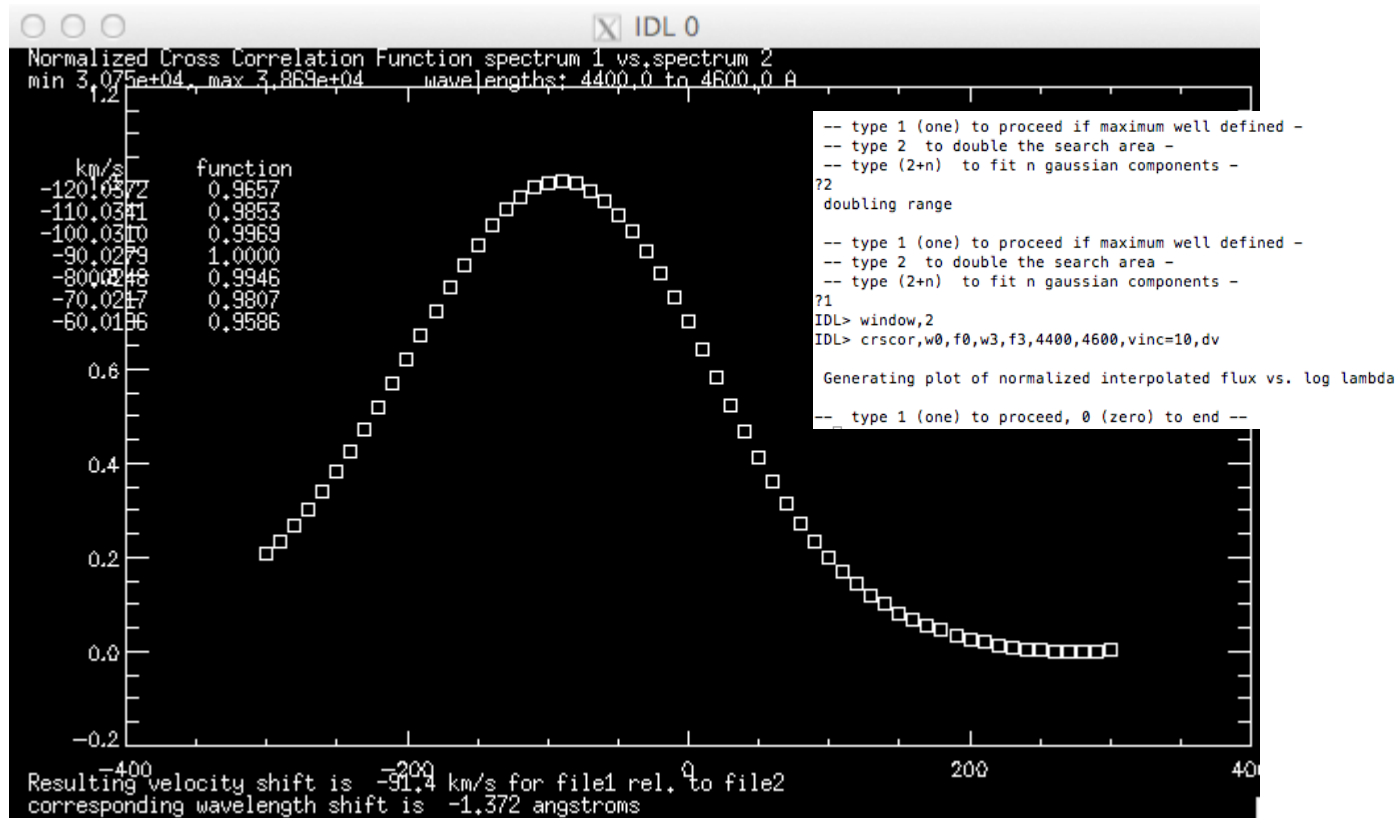
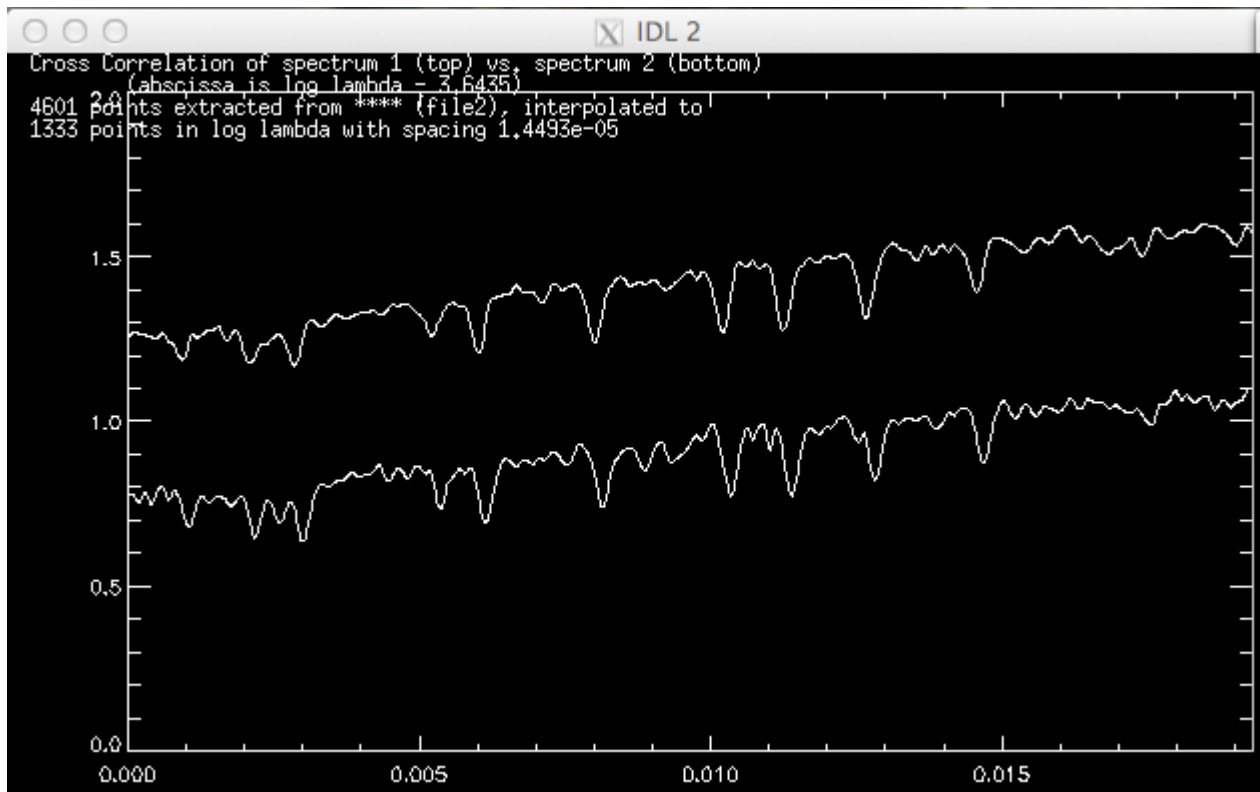
I'm ending here because by now you're going to be exhausted. But I hope you see how many things can come from precisely the data you already have in hand. In the next installment I'll spend much more time on the reasons for profile variations, other than in novae. That is, what orbital modulation means in binaries (especially symbiotics), accretion flows and what is called Doppler imaging and Doppler tomography (neither of which is difficult to understand, really!!). Just bear with this for a little longer. I hope to see many of you at OHP, we'll go over this there and please send whatever questions you might have!

Steve Shore
04-07-2016



Rotation example





For weeks Elena Mason (who some of you have had the pleasure of meeting and know from studies in the literature) and I have been trying to understand a weirdness of early nova spectra. The “anomaly” is that in early nova spectra, like those you observed for V339 Del and V5668 Sgr, there is a strong Na I line, strong Ca II H and K (3933, 3964 Å) -- both of which are resonance lines (hence, from the ground state for the respective ion) and *nothing* at Ca I 4226 Å. I wrote this in quotation marks because, finally, it’s clear: this is the difference between spectra of ejecta and atmospheres.

To explain, because in the end it’s really simple, it has to do with what controls the ionization. In an atmosphere, in LTE (so collisional rates dominate), the radiation and gas have the same temperature and the ionization is controlled by the density and temperature. It’s in equilibrium. Simple: the radiation is locally in thermal balance so the ionization matches that which you would get at a certain gas temperature, recombinations balance ionizations in collisions separately. That’s the whole point of spectral classification for stars (and why those for novae and supernovae are just indicators with no physical backing). Think, for a moment, about the solar spectrum, G2 V. It has strong Ca I and Na I, but also strong Ca II and Fe II, and only weak C I and no C II. So the Ca II/Ca I fraction, the ionization, is governed by the temperature and the density is high enough that you see two states of calcium. Na I has the same ionization potential as Ca I but Ca II has a much lower value than Na II (11 eV compared to 47 eV, respectively) so you have a lot of Ca II but also some Ca I. The same persists to spectral types as early as F2 V. But in ejecta, the energy for ionization, not the number of states available, determines the fractional abundance of the ions. So Ca II disappears if you can ionize C I and Na I, if you have above 11 eV you’ll have ionized much the Ca II to Ca III and will have C I and C II in the spectrum, no Ca I (!), and still see Na I. In other words, the ionization and its variation in time is indicating the properties of the incident radiation, from the central star, and not the local thermal conditions.

This applies to symbiotics, to supergiant atmospheres (especially in post-AGB stars and proto-planetary nebulae (I mean hot gas, not forming solar systems, horrible terminology)). Why I mention this is as an example of things we have discussed in different times and places: the key property of such dilute, dynamical environments as expanding ejecta is the non-locality of the radiation and the locality of the thermal effects. Recombinations depend on the local density, but ionization comes from somewhere else, from a distant hot source. The spectrum of that source is moderated by the intervening gas, but as that thins out the higher energies of the UV get through and the ejecta ionize depending on their local recombination rates. The richness of the ion’s spectrum determines whether it will be visible, hence no Ca I when you still see some Ca II and no Na II when you still see Na I.

Ionization Energy in eV

	0	+	2+	3+	4+	5+	6+
	I	II	III	IV	V	VI	VII
H	13.6						
He	24.6	54.4					
C	11.3	24.4	47.9	64.5			
N	14.5	29.6	47.4	77.5	97.9		
O	13.6	35.1	54.9	77.4	113.9	138.1	
Ne	24.6	41.0	63.4	97.2	126.2		
Na	5.1	47.3	71.6	98.9	138.4		
Mg	7.6	15.0	80.1				
Al	6.0	18.8	28.4				
S	10.4	23.3	34.9				
Ar	15.8	27.6	40.7	59.6	74.8		
Ca	6.1	11.9	50.9	67.3	84.3		
Fe	7.9	16.2	30.7	54.9	75.0	99.0	125.0

NIST Atomic Spectra Database Ionization Energies

<http://physics.nist.gov/PhysRefData/ASD/ionEnergy.html>

In my last comments on symbiotic stars for your informative bulletin (No. 19) I introduced a basic principle on how a complicated absorption/emission profiles in the spectrum of some symbiotic stars (e.g. CH Cyg) can be created. Using a template for creation of the P Cygni type of the profile, it was possible to get at least an imagination on the nature of a complex mass-outflow from active component in CH Cyg. A high-velocity pulsing mass-outflow of blobs of material, probably driven more into specific directions, seems to be a possible interpretation of the observed profiles during that raging 2015 period of CH Cyg evolution. However, during September 2015 the hydrogen Balmer lines became to be relatively stable, showing a typical double-peaked profile with a sharp central absorption and broad emission wings. It is very interesting that such the change happened during a relatively short period of around or less than 1 month (September 2015) and at the same optical brightness. Although some details of the H-alpha and H-beta profiles still remain rather puzzling (e.g. variations in the ratio of emission peaks and/or the origin of the central absorption), the broad and symmetrical emission wings suggest that the mass-outflow has now a form of more or less (spherically) symmetrical ionized wind. Therefore, it could be advantageous to describe basic principle on how such the wind is driven by a star. The first question is:

What is the stellar wind?

Apart from electromagnetic radiation, i.e. photons, stars emit also particles. Flux of emitted particles that are continuously outflowing from stars is called the stellar wind. The most important parameters of the stellar wind, we can determine from observations, is the mass-loss rate, dM/dt (denoted also as \dot{M} , reading as “M-dot”) and the so-called terminal velocity of the wind denoted as v_∞ . Parameter \dot{M} is the amount of mass lost by the star per unit of time, and v_∞ is the velocity of the stellar wind at a large distance from the star (terminal, and also maximal velocity). Usually, \dot{M} is expressed in units of solar masses per year ($1 M_\odot/\text{yr} = 6.3 \times 10^{25} \text{ g/s}$). For example, a star losing the mass at the rate of $\dot{M} = 10^{-6} M_\odot/\text{yr}$ loses an amount of mass equal to the mass of

our Earth during three years. The terminal velocity v_∞ of a stellar wind ranges typically from about 10 km/s for cool supergiants to about 3000 km/s for luminous hot stars. For a star with a stationary spherically symmetric wind, the mass-loss rate is given by its density $\rho(r)$ and the velocity $v(r)$ at any distance „ r “ from the center of the star via the continuity equation

$$\dot{M} = 4\pi r^2 \rho(r) v(r) \quad (= \text{constant}) \quad (1)$$

This equation expresses the fact that no material is destroyed nor created in the stellar wind, i.e. the amount of material flowing per second through a sphere with radius „ r “ around the central star is constant. The relation (1) is easy to derive. If we imagine a spherical layer with the radius r and a thickness dr around the star, its volume is $dV = 4\pi r^2 dr$, and thus its mass is $dM = dV \times \rho(r) = 4\pi r^2 dr \times \rho(r)$. Finally, dividing it by the time interval dt , we obtain the continuity equation (1) (knowing that $dM/dt = \dot{M}$ and $dr/dt = v(r)$). The gas which escapes from the outer layers of the star is accelerated outwards from small velocities at the star's surface ($v \leq 1 \text{ km/s}$) to high velocity at large distance from the star, where the wind particles are asymptotically reaching the terminal velocity v_∞ (when $r \rightarrow \infty$). The distribution of velocities in the wind with the radial distance „ r “ is called the velocity law, $v(r)$. Observations and models of stellar winds suggest that the velocity law can often be approximated by the so-called β -law as

$$v(r) = v_\infty (1 - R^*/r)^\beta \quad (2)$$

This function describes how the velocity of wind particles increases from its beginning at the star's photosphere, R^* , ($v(R^*) = 0$) to the terminal velocity v_∞ . The parameter β describes how steep the velocity law is. Figure 1. illustrates the velocity law (2) for very hot and luminous stars, whose wind can be characterized with small values of β (around 0.5 – 1.5) and for cool giants, whose slow wind can be described by larger value of β (a typical value is 2.5).

In your „Information letter No. 19“ I briefly described how the stellar wind can be identified in the star's spectra. We now know that most convincing indicator of stellar wind is the P-Cygni type of profile. Its ab-

A note on stellar winds in symbiotic binaries

Augustin Skopal

sorption component reflects the optically thick part of the wind that is projected on the star's photosphere, whereas the broad emission wing is generated within the optically thin hemisphere around the star and its width at the continuum level (HWZI) corresponds to the terminal velocity of the wind. In the following, I will try to explain how stellar winds can be driven.

What drives the stellar winds?

The most important and also most natural mechanism accelerating stellar wind is the pressure of radiation that comes outwards from the star's photosphere. Going throughout the expanding medium of the wind, photons interact with the wind particles and transfer some of their energy to them. In this way the wind particles are accelerated in the radial direction from the star. As this interaction causes mainly discrete (i.e. absorption) transitions in the atoms of the wind, we say about acceleration of stellar wind by radiative pressure in lines; the so-called line-driven winds. Basic principle of this mechanism can be described as follows.

Large amount of absorption lines is created in the bottom layers of hot star's atmosphere. This implies that the photospheric radiation will be in certain lines absorbed (or scattered) already at bottom layers of the atmosphere, and thus its outer parts will not be illuminated directly from the photosphere by photons of corresponding transitions. However, this would lead to damping of acceleration of the outer parts of the star's atmosphere, because of less and less photospheric photons of the given transition would be available at larger distances. So, how does this mechanism work? The force of radiation onto atoms (ions) due to their spectral lines would not be effective in accelerating stellar wind, if the Doppler effect would not exist. Each atmosphere has a certain gradient of velocities (i.e. the velocity difference in the radial direction), for example, the gas pressure increases with density ($P=NkT$). Thus, the large pressure of the gas at the photosphere will drive atmosphere outside. As a result, the outer layers, which move in the radial direction faster than the lower layers (i.e. become more distant from the

photosphere), will, due to the Doppler effect, „see“ photospheric photons shifted more to the red part of the spectrum than the lower layers, which move from the photosphere at a lower velocity. This means that atoms from the outer atmosphere will be capable to absorb photons (in the given transition) emitted directly by the photosphere, because they are not attenuated by layers between the photosphere and the outer layers of the star's atmosphere. In the case of hot stars, which produce a large amount of high-energy photons, the accelerating mechanism in spectral lines is very effective. However, the wind is often ionized; it is plasma. Therefore, although the accelerating process is most efficient in resonance lines of C, N, O and kinds of Fe elements, their ions will interact with free electrons and other ions, mainly of hydrogen and helium, transferring them a fraction of their additional momentum from photons, and thus drive outside all particles of the star's atmosphere in the form of stellar wind. In summary, the stellar wind of hot (super)giants of spectral types O and B reaches very high terminal velocity around of 3000 km/s already at a small distance from the star's surface, whereas cool giants of spectral types M to K accelerate their wind much more slowly, to terminal velocity around 10 to 100 km/s (Figs. 2 and 3).

On the stellar wind from cool giant in symbiotic binaries

The presence of the wind in symbiotic stars represents fundamental condition for arising the symbiotic phenomenon. In other words, if there is no wind from the giant, no symbiotic stars would exist. However, a direct indication of the giant wind in the spectrum of symbiotic stars is difficult, because the giant's radiation at low effective temperatures around 3500 K is practically not capable to ionize the wind and, in addition, maximum velocity dispersion of the giant's wind runs to 50 – 100 km/s. This means that emission lines will be narrow and their creation will be connected only with the part of the giant wind that is ionized by the hot component. The fact that the symbiotic nebula during quiescent phases represents only the ionized fraction of the giant wind was independently confirmed by the

A note on stellar winds in symbiotic binaries

Augustin Skopal

diagnosis of the nebular line spectrum. Already in the 90's decade of the last century, Nussbaumer with collaborators revealed that the abundances of C, N and O is very close to that usually observed for normal red giants. In the red part of the spectrum (approximately within VRI passbands and far), we observe a large amount of absorption lines. However, most of them (mainly from metals) has origin in the densest parts of the giant's atmosphere, and thus with practically no information about the kinematic of the wind. They reflect only the orbital motion of the star. Some information is, however, provided by the H-alpha line, which belongs to the strongest lines in the optical spectrum of symbiotic stars. We often observe an absorption component at/around the center of the main emission core, which position is rather stable irrespectively to the orbital phase, and always shifted bluewards with respect to its reference wavelength (Fig. 2). These properties suggest that this absorption component can be created in the neutral wind of the giant that is located between the observer and the stellar disk – the source of the wind. The effect is more pronounced in eclipsing systems around the inferior spectroscopic conjunction of the giant (i.e. during eclipses), because at these positions of the binary, there is the largest amount of the neutral hydrogen between the observer and the giant's photosphere. The shift of the absorption component in the spectrum, i.e. the radial velocity after subtracting the systemic velocity, is near to the terminal velocity of the wind from the giant. This absorption is usually weak, so that its superposition with the emission core does not look like a typical P Cyg profile. Fig. 2 shows examples for systems with high orbital inclination, YY Her, CI Cyg, Z And and RW Hya during their quiescent phases. The figure suggests that terminal velocities are around 50 km/s or less.

Also values of mass-loss rates can be determined on the basis of the knowledge that the symbiotic nebula during quiescent phases represents its ionized part. In principle, we determine a theoretical value of the total nebular emission in the continuum and compare it to that obtained from observations (e.g. from modelling the SED as I showed in my previous contributions No. 16 and 23 – the green line in models SED). It is assumed that the wind is spherically symmetric and the distribution of the wind density

and velocity at any distance from the giant surface is given by the above mentioned relations (1) and (2). As the theoretical value of the total nebular emission depends on \dot{M} , then having the observed emission measure of the nebula and assuming some parameters of the wind (e.g., $\beta=2.5$, $v=20$ km/s), we can estimate the value of the mass-loss rate. In this way it was found that cool giants in symbiotic binaries lose their mass at rates around of 10^{-7} solar masses per year. These values of \dot{M} are in agreement with those obtained from radio observations. Nebular radiation is relatively strong in the radio wavelengths (from a few times 0.1 mm to tens of cm) and represents here the only source of radiation in symbiotic stars – radiation from the giant's photosphere and that from the hot component are negligible in the radio. Therefore, the radio emission is well measurable, and thus useful to determine properties of symbiotic nebulae.

Finally, I note that there is also an emission contribution from the hot component wind, however, its value is more than one order of magnitude smaller during quiescent phases. During active phases, the mass-loss rate via the wind from hot components significantly increases. However, this is a story for a future commenting on.

Augustin Skopal
17-07-2016

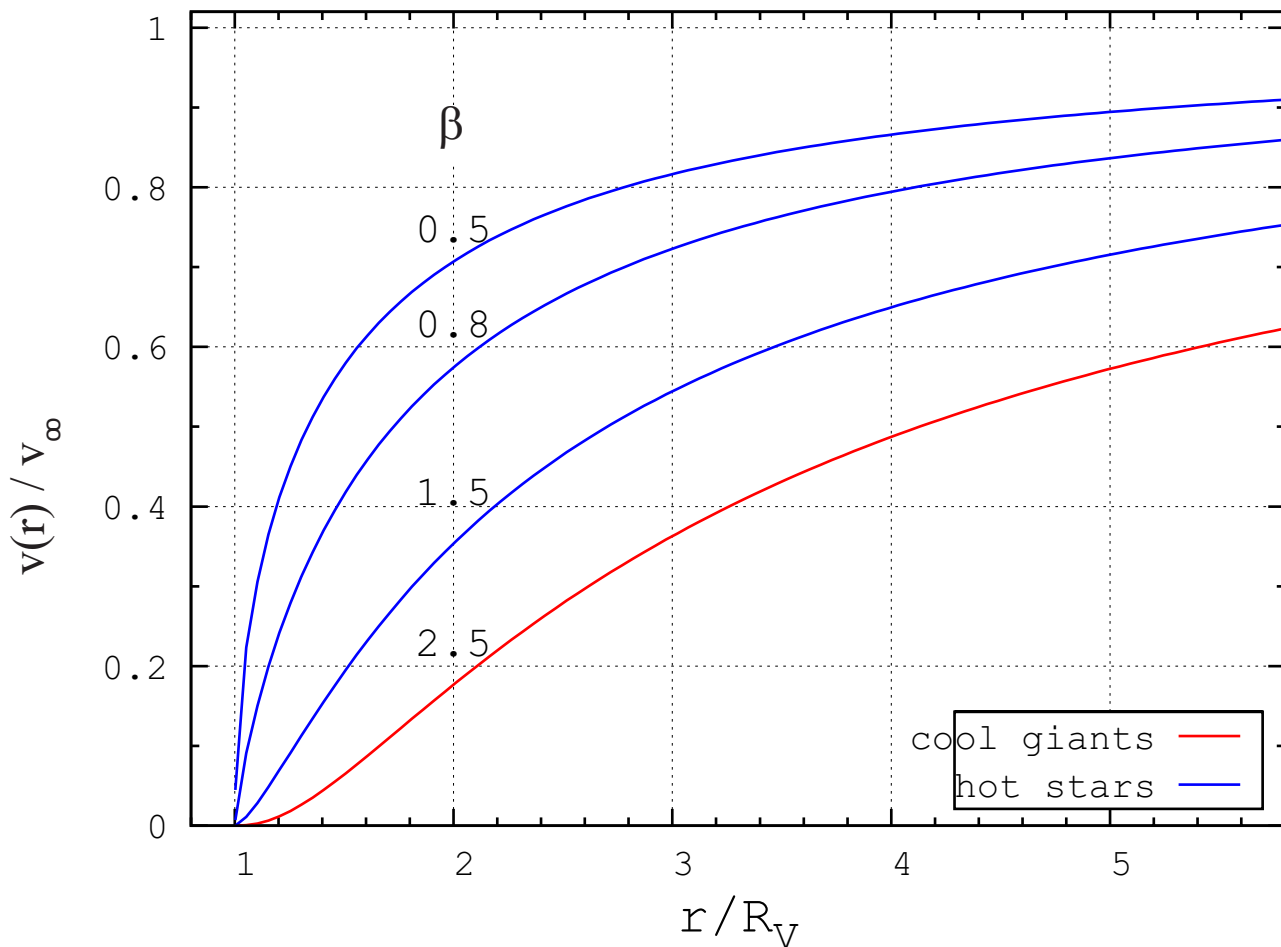


Figure 1. Acceleration of the stellar wind from the star's photosphere outward according to the β -law wind (2). For cool giants (red line) the acceleration is slower, the parameter $\beta = 2.5$, whereas hot stars drive their wind significantly faster (blue curves), the parameter $\beta = 0.5 - 1.5$

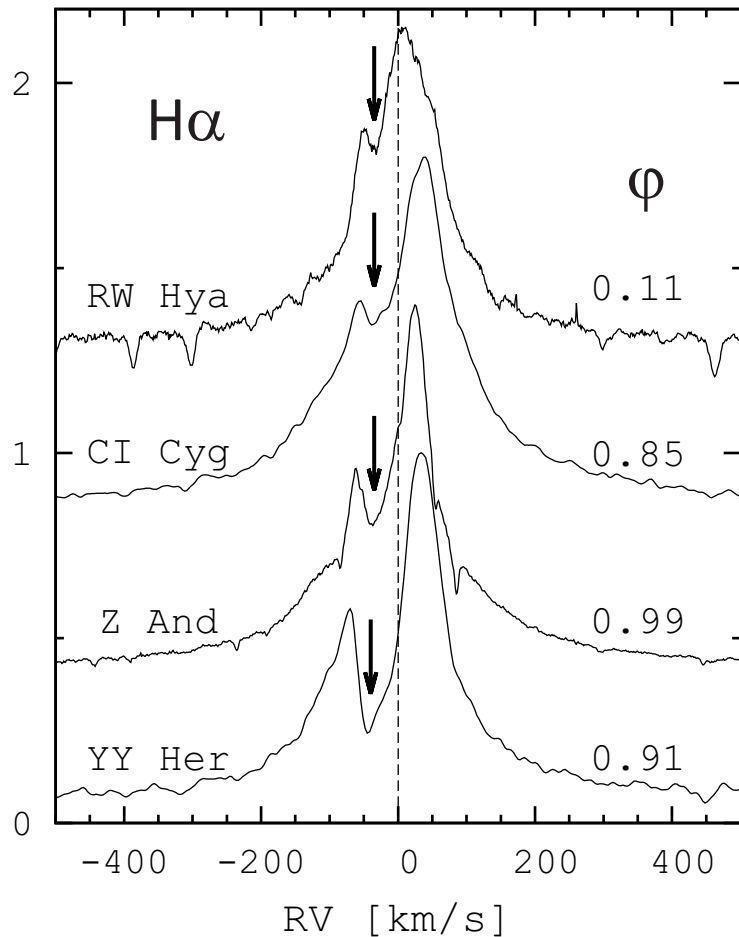


Figure 2. Examples of H-alpha line profiles for some symbiotic stars with high orbital inclination as observed around the inferior conjunction of the giant. The absorption component (denoted by arrows) arises in the stellar wind of the cool giant. Its position is always shifted blueward, and is near to the terminal velocity of the wind (30 – 50 km/s). Fluxes are in relative units. Observations are from the survey of H-alpha line profiles as published by Ivson et al. (1994, A&AS, 103, 201).

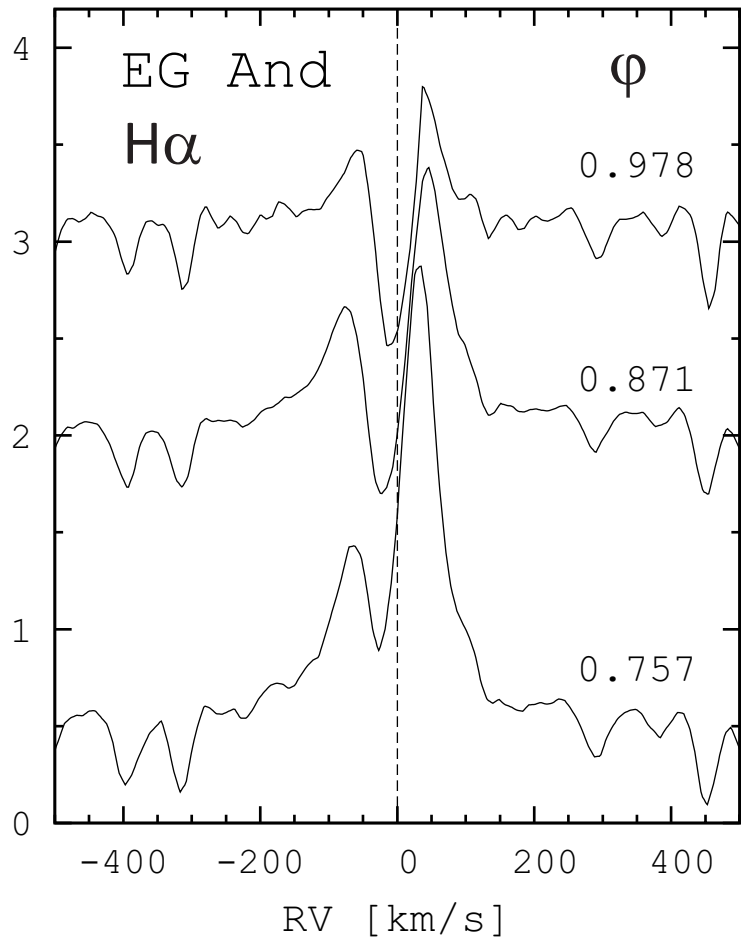


Figure 3. Example of H-alpha line profiles of EG And. Systemic velocity of -95 km/s was subtracted. At the conjunction (top), the absorption component is the strongest, because the line of sight goes throughout the largest column density of neutral hydrogen. Its larger shift in radial velocity at the quadrature (bottom, orbital phase 0.76) is partly caused by orbital motion of the giant that moves towards the observer. Fluxes are in relative units and offset for a better visualization. The spectra were obtained by Francois Teysier.

Novae

V5852 Sgr: An Unusual Nova Possibly Associated with the Sagittarius Stream

E. Aydi, P. Mróz, P. A. Whitelock, S. Mohamed, Ł. Wyrzykowski, A. Udalski, P. Vaisanen, T. Nagayama, M. Dominik, A. Scholz, H. Onozato, R. E. Williams, S. T. Hodgkin, S. Nishiyama, M. Yamagishi, A. M. S. Smith, T. Ryu, A. Iwamatsu, I. Kawamata

We report spectroscopic and photometric follow-up of the peculiar nova V5852 Sgr (discovered as OGLE-2015-NOVA-01), which exhibits a combination of features from different nova classes. The photometry shows a flat-topped light curve with quasi-periodic oscillations, then a smooth decline followed by two fainter recoveries in brightness. Spectroscopy with the Southern African Large Telescope shows first a classical nova with an Fe II or Fe IIb spectral type. In the later spectrum, broad emissions from helium, nitrogen and oxygen are prominent and the iron has faded which could be an indication to the start of the nebular phase. The line widths suggest ejection velocities around 1000 km s⁻¹. The nova is in the direction of the Galactic bulge and is heavily reddened by an uncertain amount. The V magnitude 16 days after maximum enables a distance to be estimated and this suggests that the nova may be in the extreme trailing stream of the Sagittarius dwarf spheroidal galaxy. If so it is the first nova to be detected from that, or from any dwarf spheroidal galaxy. Given the uncertainty of the method and the unusual light curve we cannot rule out the possibility that it is in the bulge or even the Galactic disk behind the bulge.

Symbiotic stars in X-rays III: Suzaku observations
<http://arxiv.org/abs/1606.02755>

The Galactic Nova Rate Revisited

A. W. Shafter

(Submitted on 7 Jun 2016)

Despite its fundamental importance, a reliable estimate of the Galactic nova rate has remained elusive. Here, the overall Galactic nova rate is estimated by extrapolating the observed rate for novae reaching $m \leq 2$ to include the entire Galaxy using a two component disk plus bulge model for the distribution of stars in the Milky Way. The present analysis improves on previous work by considering important corrections for incompleteness in the observed rate of bright novae. Several models are considered to account for differences in the assumed properties of bulge and disk nova populations. The simplest models, which assume uniform properties between bulge and disk novae, predict Galactic nova rates between 50 to as many as 100 per year, depending on the assumed incompleteness at bright magnitudes. Models where the disk novae are assumed to be more luminous than bulge novae are explored, and predict nova rates up to 30% lower, in the range of 35 to 70 per year. An average of the most plausible models yields a rate of 50 ± 19 yr⁻¹, which is arguably the best estimate currently available for the nova rate in the Galaxy. All plausible models produce rates that represent significant increases over recent estimates, and bring the Galactic nova rate into better agreement with that expected based on comparison with the latest results from extragalactic surveys.

tion from these boundary layers. Given the time between previous observations and these observations, we find that the intrinsic X-ray flux and the intervening absorbing column can vary by factors of three or more on a time scale of years. However, the location of the absorber and the relationship between changes in accretion rate and absorption are still elusive.

<http://arxiv.org/abs/1606.02358>

The Thermonuclear Runaway and the Classical Nova Outburst

S. Starrfield (1), C. Iliadis (2), W. R. Hix (3 and 4) ((1) ASU, (2) UNC, (3) ORNL, (4) UTK)

Nova explosions occur on the white dwarf component of a Cataclysmic Variable binary stellar system that is accreting matter lost by its companion. When sufficient material has been accreted by the white dwarf, a thermonuclear runaway occurs and ejects material in what is observed as a Classical Nova explosion. We describe both the recent advances in our understanding of the progress of the outburst and outline some of the puzzles that are still outstanding. We report on the effects of improving both the nuclear reaction rate library and including a modern nuclear reaction network in our one-dimensional, fully implicit, hydrodynamic computer code. In addition, there has been progress in observational studies of Supernovae Ia with implications about the progenitors and we discuss that in this review.

<http://arxiv.org/abs/1605.04294>

The panchromatic spectroscopic evolution of the classical CO nova V339 Del (Nova Del 2013) until X-ray turnoff

S. N. Shore, E. Mason, G. J. Schwarz, F. M. Teysier, C. Buil, I. De Gennaro Aquino, K. L. Page, J. P. Osborne, S. Scaringi, S. Starrfield, H. van Winckel, R. E. Williams, C. E. Woodward

Classical novae are the product of thermonuclear runaway-initiated explosions occurring on accreting white dwarfs. V339 Del (Nova Delphinus 2013) was one of the brightest classical novae of the last hundred years. Spectroscopy and photometry are available from γ -rays through infrared at stages that have frequently not been well observed. The complete data set is intended to provide a benchmark for comparison with modeling and for understanding more sparsely monitored historical classical and recurrent novae. This paper is the first in the series of reports on the development of the nova. We report here on the early stages of the outburst, through the X-ray active stage. A time sequence of optical, flux calibrated high resolution spectra was obtained with the Nordic Optical Telescope (NOT) using FIES simultaneously, or contemporaneously, with the Space Telescope Imaging Spectrograph (STIS) aboard the Hubble Space Telescope during the early stages of the outburst. These were supplemented with MERCATOR/HERMES optical spectra. High resolution IUE ultraviolet spectra of OS And 1986, taken during the Fe curtain phase, served as a template for the distance determination. We used standard plasma diagnostics (e.g., [O III] and [N II] line ratios, and the H β line flux) to constrain electron densities and temperatures of the ejecta. Using Monte Carlo modeling of the ejecta, we derived the structure, filling factor, and mass from comparisons of the optical and ultraviolet line profiles. <http://arxiv.org/abs/1606.01777>

We thank our collaborators in the ARAS group for their remarkable diligence, skill, and persistence in obtaining spectroscopy of this and other novae and for the resulting archival treasures. The program described here was planned during a workshop in Pisa in July 2013, fortuitously just before the announcement of V339 Del, and we thank the participants or their insights, especially A. Caleo, C-C. Cheung, J. Jose, J-U Ness, and B. Warner. We also thank D. Gies, P. Hauschildt, D. Korcakova, P. Kuin, P. Selvelli, F. Walter, and P. Woudt for discussions and exchanges.

Swift observations of the 2015 outburst of AG Peg -- from slow nova to classical symbiotic outburst

Ramsay, Gavin; Sokoloski, J. L.; Luna, G. J. M.; Nunez, N. E.

Classical novae are the product of thermonuclear runaway-initiated explosions occurring on accreting white dwarfs. V339 Del Symbiotic stars often contain white dwarfs with quasi-steady shell burning on their surfaces. However, in most symbiotics, the origin of this burning is unclear. In symbiotic slow novae, however, it is linked to a past thermonuclear runaway. In June 2015, the symbiotic slow nova AG Peg was seen in only its second optical outburst since 1850. This recent outburst was of much shorter duration and lower amplitude than the earlier eruption, and it contained multiple peaks -- like outbursts in classical symbiotic stars such as Z And. We report Swift X-ray and UV observations of AG Peg made between June 2015 and January 2016. The X-ray flux was markedly variable on a time scale of days, particularly during four days near optical maximum, when the X-rays became bright and soft. This strong X-ray variability continued for another month, after which the X-rays hardened as the optical flux declined. The UV flux was high throughout the outburst, consistent with quasi-steady shell burning on the white dwarf. Given that accretion disks around white dwarfs with shell burning do not generally produce detectable X-rays (due to Compton-cooling of the boundary layer), the X-rays probably originated via shocks in the ejecta. As the X-ray photo-electric absorption did not vary significantly, the X-ray variability may directly link to the properties of the shocked material. AG Peg's transition from a slow symbiotic nova (which drove the 1850 outburst) to a classical symbiotic star suggests that shell burning in at least some symbiotic stars is residual burning from prior novae. <http://adsabs.harvard.edu/abs/2016arXiv160607397R>

We also thank François Teyssier for altering us to the many amateur spectroscopic observations which have been made and we acknowledge and thank François Teyssier, Umberto Sollecchia, Joan Guarro Flo, Jacques Montier, Peter Somogyi, Keith Graham and V Bouttard for use of their spectra.

Recent X-ray observations of the symbiotic star AG Peg: do they signify Colliding Stellar Winds?

Svetozar A. Zhekov, Toma Tomov

We present an analysis of recent X-ray observations of the symbiotic star AG Peg. The X-ray emission of AG Peg as observed with Swift in 2015 shows considerable variability on time scale of days as variability on shorter time scales might be present as well. Analysis of the X-ray spectra obtained in 2013 and 2015 confirms that AG Peg is an X-ray source of class β of the X-ray sources amongst the symbiotic stars. The X-ray emission of AG Peg as observed with ROSAT (1993 June) might well originate from colliding stellar winds (CSW) in binary system. On the other hand, the characteristics of the X-ray emission of AG Peg in 2013 and 2015 (Swift) are hard to accommodate in the framework of the CSW picture. Analysis of the light curves in 2015 shows that the power spectrum of the X-ray variability in AG Peg resembles that of the flicker noise (or flickering) being typical for accretion processes in astronomical objects. This is a sign that CSWs did not play a key role for the X-ray emission from AG Peg in 2013-2015 and a different mechanism (probably accretion) is also getting into play. <http://arxiv.org/abs/1606.01777>



About ARAS initiative

Astronomical Ring for Access to Spectroscopy (ARAS) is an informal group of volunteers who aim to promote cooperation between professional and amateur astronomers in the field of spectroscopy.

To this end, ARAS has prepared the following roadmap:

- Identify centers of interest for spectroscopic observation which could lead to useful, effective and motivating cooperation between professional and amateur astronomers.
- Help develop the tools required to transform this cooperation into action (i.e. by publishing spectrograph building plans, organizing group purchasing to reduce costs, developing and validating observation protocols, managing a data base, identifying available resources in professional observatories (hardware, observation time), etc.
- Develop an awareness and education policy for amateur astronomers through training sessions, the organization of pro/am seminars, by publishing documents (web pages), managing a forum, etc.
- Encourage observers to use the spectrographs available in mission observatories and promote collaboration between experts, particularly variable star experts.
- Create a global observation network.

By decoding what light says to us, spectroscopy is the most productive field in astronomy. It is now entering the amateur world, enabling amateurs to open the doors of astrophysics. Why not join us and be one of the pioneers!

Be Monthly report

Previous issues :

<http://www.astrosurf.com/aras/surveys/beactu/index.htm>

VV Cep campaign

<http://www.spectro-aras.com/forum/viewforum.php?f=19>

Submit your spectra

Please :

- respect the procedure
- check your spectra BEFORE sending them

Resolution should be at least $R = 500$

For new transients, supernovae and poorly observed objects,

SA spectra at $R = 100$ are welcome

1/ reduce your data into BeSS file format

2/ name your file with:

`_ObjectName_yyyymmdd_hhh_Observer`

Exemple: `_chcyg_20130802_886_toto.fit`

3/ send you spectra to

Novae, Symbiotics : François Teyssier

Supernovae : Christian Buil

VV Cep Stars : Olivier Thizy